An Examination of Brain Network Organization and the Analgesic Mechanisms of a Non-Pharmacological Treatment in Chronic Centralized Pain

by

Chelsea M. Kaplan

A dissertation submitted in partial fulfillment
of the requirements for the degree of
Doctor of Philosophy
(Neuroscience)
in The University of Michigan
2018

Doctoral Committee:

Associate Professor Richard E. Harris, Co-Chair
Professor George A. Mashour, Co-Chair
Associate Professor Alexandre F. DaSilva
Professor Anthony G. Hudetz
Professor Rachael D. Seidler

Chelsea M. Kaplan

chelsmar@umich.edu

ORCID iD: 0000-0001-9324-655X

Dedication

For Steve, Asher and Baby Kaplan #2

Acknowledgements

I would like to express my overwhelming gratitude to the many mentors, colleagues, friends and family that have supported me throughout my graduate training at the University of Michigan.

I won the mentor jackpot. The scientific expertise and brilliance of all the mentors I'm about to thank is obvious and well known. Instead, I would like to acknowledge the kindness and care they have shown me, which have gone well beyond anything I ever expected when I started graduate school.

First to my co-mentors, Rick Harris and George Mashour, I am thankful for their unwavering support and encouragement of both my professional and personal goals. Any grad student would have been privileged to have had just one of them as a mentor. Rick, I aspire to be as Zen-like as you are, as both as a scientist and a parent. George, your razor sharp focus and discipline paired with big-picture creativity and curiosity is what I always hoped science would be.

Thank you to Dan Clauw, who manages to be a world-class scientist and a remarkably kind and generous human being at the same time. Your guidance, candor and humor I appreciate more than I can say. Thank you for adopting me into the CPFRC family… and for all the ribs.

To all of the faculty, staff and colleagues at the CPFRC - especially Steve Harte, Afton Hassett, Dave Williams, Suzie Zick, Daniel Harper, Andrew Schrepf, Eric Ichesco, and Tony Larkin - thank you for so much support and inspiration. I feel lucky to work with you all and look forward to many more years of hilarious lunchtime conversations. A special thank you to Kathy Scott and all of the study coordinators at the CPFRC – without you, this dissertation would not exist. Karen Brown, thank you for making my working life run like a Swiss watch.

Deniz Vatansever – thank you for your guidance during the very early days of network analyses and steadfastly offering your time and knowledge to further this dissertation.

Thank you to all the Mashour lab members, especially UnCheol Lee, Joon-Moon Young, and Hyoungkyu Kim for their patience and kindness in explaining graph theoretical equations in ways that didn't make my eyes cross.

I am incredibly grateful to my committee members, Alex DaSilva, Tony Hudetz and Rachael Seidler, for their encouragement, insights and questions, which pushed me to think critically and become a better scientist.

Thank you to Ed Stuenkel, Valerie Smith, Rachel Harbach and the Neuroscience Graduate Program. I am so appreciative of my training, and for the opportunities and support you have given me.

My early scientific mentors, Ilana Hairston, Tiffany Love and Jon-Kar Zubieta, gave me a chance and changed the course of my life.

Phil Saccone showed incredible kindness to a total stranger and spent a huge amount of time helping me with my grad school application (all while tackling coursework for his first year of a pharmacology Ph.D., no less). I don't think I'd be here without you.

Thank you to my family – my parents Dale and Kay, my in-laws Daniel and Yvonne, my brother Aaron, my sisters Leah and Katie and my nieces Shae, Paige and Haley - and my second family – David & Holly, Derek, Dave & Niki, David O, and Ray – for their unwavering confidence and presence during every up and down.

Finally, I have immeasurable gratitude for my husband, Steve. Detailing all the ways you have supported me during this process would be longer than the dissertation itself. Without your optimism and sense of humor, these last five years wouldn't have been nearly so sunny.
And thank you to my son, Asher, for so much joy.

I have enjoyed my graduate training perhaps more than any student should. One last thank you to all those involved.

Table of Contents

List of Tables

List of Figures

List of Appendices

List of Abbreviations

ACC: anterior cingulate cortex
CNS: central nervous system
DMN: default mode network
FC: functional connectivity
FM: fibromyalgia
fMRI: functional magnetic resonance imaging
GABA: γ-aminobutyric acid
Glx: glutamate + glutamine
HC: healthy controls
^{1}H-MRS: proton magnetic resonance spectroscopy
IPL: inferior parietal lobule
M1: primary motor cortex
MCS: motor cortex stimulation
mPFC: medial prefrontal cortex
NMDA: N-methyl-D-aspartate
PAG: periaqueductal gray
PANAS: positive and negative affect schedule
PET: positron emission tomography
S1: primary somatosensory cortex
SFG: superior frontal gyrus
SMA: supplementary motor area
STG: superior temporal gyrus
SVC: small volume correction
tDCS: transcranial direct current stimulation
V1: primary visual cortex
V2: secondary visual cortex
V3: visual association cortex
VAS: visual analog scale
VL: ventral lateral
VPL: ventral posterior lateral

Abstract

Chronic pain is a global public health challenge, affecting nearly one third of adults worldwide. Current treatments are inadequate, especially since some of the mainstay therapies (e.g. opioids, NSAIDs) are often ineffective and/or associated with significant toxicity. The solution to these problems requires an improved understanding of chronic pain pathology, particularly the role that the brain plays in causing or amplifying pain perception, and how analgesic intervention might target these brain-based mechanisms. This dissertation aims to identify brain network alterations in fibromyalgia (FM), a common and canonical chronic pain condition with presumed CNS pathology, and determine how non-invasive brain stimulation may target aberrant brain network connectivity to promote analgesia.

Across a wide range of diverse neurological disorders, hubs (i.e. highly connected brain regions) appear to be disrupted and the character of this disruption can yield insights into the pathophysiology of these disorders. In Chapter 2, we describe the application of a brain network based approach to examine hub topology in FM patients compared to healthy volunteers. We identified significant disruptions in hub rank order in FM patients. In FM, but not controls, the anterior insula was a hub with significantly higher inter-modular connectivity and membership in the rich club (a functional backbone of connectivity formed by highly interconnected hubs). Among FM patients, rich club membership varied with the intensity of clinical pain: the posterior insula, primary somatosensory and motor cortices belonged to the rich club only in FM patients with the highest pain. Further, we found that the eigenvector centrality (a measure of how connected a brain region is to other highly connected regions) of the posterior insula

positively correlated with clinical pain, and mediated the relationship between levels of glutamate + glutamine within this structure and the patient's subjective clinical pain report. Together, these findings demonstrate an altered hub topology in FM and are the first to suggest that disruptions in the excitatory tone within the insula could alter the strength of the insula as a hub and subsequently lead to increased clinical pain.

Transcranial direct current stimulation (tDCS) has emerged as an attractive noninvasive treatment for pain, given its ability to target specific cortical regions with relatively few side effects. Motor cortex (M1) tDCS relieves pain in FM, but the analgesic mechanism remains unknown. In Chapter 3, we measured changes in resting state functional connectivity after sham and real M1 tDCS in twelve FM patients and examined if these changes were related to subsequent analgesia. M1 tDCS (compared to sham) reduced pro-nociceptive functional connectivity, specifically between the motor and sensory nuclei of the thalamus and multiple cortical regions, including primary motor and somatosensory areas. Interestingly, decreased connectivity between the thalamus and posterior insula, M1 and somatosensory cortices correlated with reductions in clinical pain after *both* sham and active treatment. These results suggest that while there may be a placebo response common to both sham and real tDCS, repetitive M1 tDCS causes distinct changes in functional connectivity that last beyond the stimulation period and may produce analgesia by inhibiting pro-nociceptive thalamic connectivity.

This research offers new insight into the neurobiology of chronic centralized pain conditions and contributes to the understanding of how non-invasive brain stimulation causes analgesia. This knowledge could lead to more informed stimulation sites and personalized treatment based on network connectivity in each individual patient.

Chapter 1 : Introduction

Chronic pain is a global public health challenge. Nearly one third of adults worldwide suffer from a chronic pain condition (Elzahaf et al., 2012). In the United States, 116 million Americans suffer from chronic pain, which is more than heart disease, cancer and diabetes combined. At a cost of $560-635 billion annually, chronic pain is arguably the most prevalent and costly public health crisis in America today (Institute of Medicine (US) Committee on Advancing Pain Research, Care, and Education, 2011).

Pain is a multidimensional, conscious experience that is shaped by environmental, psychological and biological factors unique to an individual. Nociception is an unconscious physiological process reflecting the activity of specialized sensory receptors (nociceptors) in the periphery that respond to a noxious stimulus and transmit this information to the central nervous system (CNS). Nociception is neither a necessary, nor sufficient, cause of pain. Pain, on the other hand, is a complex emotional and cognitive experience primarily generated by the brain, and may or may not be correlated with actual tissue damage (Merskey H, 1994; Tracey, 2005).

The transition from acute to chronic pain (defined as persistent symptoms for more than three months) is not well understood but functional, structural and neurochemical abnormalities observed in the CNS of chronic pain patients point to central mechanisms in some individuals. Centralized pain, in this context, refers to dysfunction in CNS processing that causes, amplifies or sustains the perception of pain (Sluka and Clauw, 2016) in a way that is distinct or even disconnected from peripheral nociceptive events. Fibromyalgia (FM) is a common chronic centralized pain condition, affecting 2-8% of the population (Wolfe et al., 1995; McBeth and

Jones, 2007; Vincent et al., 2013). It is considered the canonical centralized pain disorder, although other chronic pain disorders (i.e. irritable bowel syndrome, temporomandibular joint syndrome, chronic lower back pain) may share underlying pathophysiology (Clauw, 2009; Maixner et al., 2016). FM is characterized by widespread musculoskeletal pain without accompanying tissue inflammation or damage (Clauw, 2014). FM patients also have diffuse hyperalgesia (elevated pain responses to painful stimuli) and allodynia (perception of pain for normally non-painful stimuli). Additional markers of centralized pain are comorbid CNS-mediated symptoms such as fatigue, insomnia, and mood disorders. Finally, FM patients are hypersensitive to a variety of non-noxious sensory stimuli (such as light, noise, and odors) (Petzke et al., 2003; Geisser et al., 2008; Wilbarger and Cook, 2011; López-Solà et al., 2014; Harte et al., 2016; Martenson et al., 2016), which suggests a more global dysfunction in sensory processing. The widespread nature of the pain, lack of conclusive peripheral abnormalities, and accumulating neuroimaging evidence point to the CNS as the primary driver in the amplification and persistence of pain in FM.

Central Nervous System Alterations in Fibromyalgia

The CNS plays an active role in pain processing and can either enhance or diminish the perception of pain. The perception of pain is a product of the activity in a diverse network of brain regions, including the somatosensory cortex (S1), insula, anterior cingulate cortex (ACC), prefrontal cortex, thalamus, hypothalamus, amygdala, hippocampus, cerebellum, periaqueductal gray (PAG) and other brainstem nuclei (Lee and Tracey, 2013).

Studies of chronic pain patients using noninvasive techniques to study human brain function, such as functional magnetic resonance imaging (fMRI), proton magnetic resonance spectroscopy (^{1}H-MRS), and positron emission tomography (PET), have confirmed alterations in

the functional, chemical and structural brain networks responsible for sensory processing. These alterations fall into two broad categories: increased pro-nociceptive processing and/or decreased descending anti-nociceptive transmission, both of which may be driven by imbalances in excitatory and inhibitory neurotransmitters.

In various chronic pain conditions, there is increased activity in "normal" pain processing regions, which may reflect the subjective magnitude or salience of the pain (Apkarian et al., 2011). Gracely and colleagues demonstrated that FM patients rated the intensity of an equal pressure stimulus as significantly more painful than controls. Using fMRI, they also showed that FM patients had increased activation in a distributed network of pain processing regions, including S1, insula and ACC, during the application of this equal pressure stimulus compared to healthy controls (Gracely et al., 2002). Other studies have confirmed the leftward shift in the stimulus response function and increased activation in pro-nociceptive pain processing regions during painful stimuli in chronic pain patients relative to healthy volunteers (Cook et al., 2004; Giesecke et al., 2004; Gracely, 2004; Pujol et al., 2009; López-Solà et al., 2016).

One method of assessing the brain-based changes related to FM involves functional interactions between regions thought to be involved in pain. Functional connectivity is defined as the statistical covariation between activities in different brain regions and has been used as a surrogate for network-based activity (for a review on functional connectivity methods and interpretations, see van den Heuvel and Pol, 2010). The brain is organized into large-scale networks, wherein the neural activities of the component brain regions are highly correlated over time and spontaneously active even during the resting state. The most commonly reported networks include: sensorimotor network, visual network, salience network, fronto-parietal network, and the default mode network (DMN). The DMN is thought to be involved in self-

referential processing and includes the posterior cingulate, precuneus, lateral parietal lobes and the medial prefrontal cortex.

FM patients, relative to healthy controls, also have increased functional connectivity between pro-nociceptive brain regions, specifically between the DMN and the insula (Napadow et al., 2010). Further, the magnitude of this connectivity is positively correlated with clinical pain intensity (Napadow et al., 2010; Flodin et al., 2014). Reductions in DMN – insula connectivity correlate with decreases in clinical pain intensity after a non-pharmacological treatment (Napadow et al., 2012). FM patients also have increased functional connectivity between the DMN and secondary somatosensory cortex, ACC and insula, and M1 with supplementary motor areas (Cifre et al., 2012; Pujol et al., 2014). More recently, our laboratory reported increases in resting state functional connectivity after an experimental pain task between the insula and ACC, and between the thalamus and precuneus/posterior cingulate cortex (key regions of the DMN). These connectivity changes were positively correlated with increases in clinical pain intensity over the course of the scan (Ichesco et al., 2016). The functional and structural changes observed in FM may be common across other pain conditions. In a large study, patients with chronic pelvic pain (a condition that shares the centralized pain phenotype) displayed increased gray matter volume in S1/M1 and increased functional connectivity between these regions and the insular cortex (Kutch et al., 2017). These findings were confirmed in FM patients, but were absent in pain-free healthy controls.

FM patients also have deficits in descending analgesia. During a pressure pain paradigm, FM patients had decreased activation in anti-nociceptive brain regions, including the rostral ACC and brainstem (Jensen et al., 2009). FM patients had decreased functional connectivity in descending pain inhibitory pathways during this pain task, specifically between the ACC,

amygdala, hippocampus and brainstem, and between the thalamus and orbitofrontal cortex (Jensen et al., 2012). The decreases in functional connectivity between anti-nociceptive structures (ACC, thalamus and insula to PAG) are also present during the resting state (Cifre et al., 2012; Pujol et al., 2014). A recent meta-analysis found that FM patients have decreased gray matter volume in anti-nociceptive regions such as the ACC (Shi et al., 2016). In summary, FM patients have increases in activity, connectivity and gray matter volume in pro-nociceptive brain regions and decreases in activity, connectivity and gray matter volume in anti-nociceptive areas (summarized in Figure 1.1).

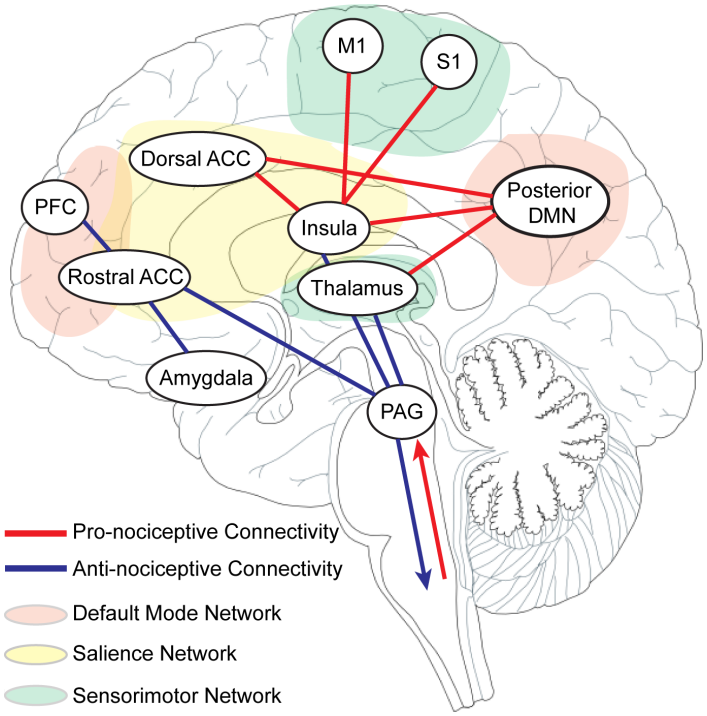

Figure 1.1. Summary of Alterations in Pro- and Anti-Nociceptive Brain Activity. FM patients have increased activation during experimental pain tasks in pro-nociceptive brain regions such as the insula, M1, S1, dorsal ACC and thalamus. Patients also have increased functional connectivity at rest between pro-nociceptive brain regions and the DMN. Moreover, FM patients have decreased descending analgesic activity in anti-nociceptive brain regions such as the rostral ACC and PAG. Further there is evidence of decreased functional connectivity to these anti-nociceptive structures. FM, fibromyalgia; M1, primary Motor Cortex; S1, primary somatosensory cortex; ACC, anterior cingulate cortex; PFC, prefrontal cortex; DMN, default mode network; PAG, periaqueductal gray

The altered activation and connectivity patterns observed in FM may be due to imbalances in the excitatory and inhibitory neurotransmitters that play a role in pain perception. FM patients have increased cerebrospinal fluid levels of the pro-nociceptive neurotransmitters substance P, nerve growth factor and glutamate (Russell et al., 1994; Giovengo et al., 1999; Sarchielli et al., 2007), and decreased levels of the anti-nociceptive neurotransmitters serotonin, norepinephrine and dopamine (Russell et al., 1992). ^{1}H-MRS is a non-invasive MRI technique that measures the relative concentration of brain metabolites in vivo. Using this technique, our laboratory has shown that FM patients have decreased levels of γ-aminobutyric acid (GABA), the brain's major inhibitory neurotransmitter, in the anterior insula and increased levels of glutamine + glutamate (Glx; the latter being the brain's major excitatory neurotransmitter) in the posterior insula (Harris et al., 2009; Foerster et al., 2012). These alterations in GABA and Glx were associated with increased experimental pain sensitivity. Other studies have found higher concentrations of Glx in the posterior cingulate, a key node of the DMN, of FM patients relative to healthy volunteers (Fayed et al., 2010).

Numerous studies have found alterations in baseline opioidergic activity in FM (see Goldenberg et al., 2016 for a recent review). Briefly, FM patients have reduced μ-opioid receptor availability (as measured with the PET radiotracer [^{11}C]-carfentanil) in several pain processing regions, including the ACC, amygdala and nucleus accumbens, and this reduction was associated with clinical pain intensity (Harris et al., 2007). These data can be interpreted in two ways that are not mutually exclusive: FM patients may have increased endogenous opioid levels or fewer opioid receptors. Opioid analgesics do not effectively treat FM pain and low dose naltrexone, an opioid receptor antagonist, improves FM symptoms, which supports the

hypothesis that FM patients have excess endogenous opioid activity (Younger and Mackey, 2009; Younger et al., 2013; Goldenberg et al., 2016).

As briefly outlined, FM patients have alterations in the function, structure and neurochemistry of brain regions involved in pain processing. Importantly, none of the brain regions or networks mentioned above is uniquely associated with the perception of pain. They contribute to many other sensory, cognitive and emotional processes, which may explain the presence of a wide variety of symptoms in addition to the widespread pain seen in centralized pain states. Since there is most likely not a 'primary nociception cortex,' it may be that coordinated activity within a network of regions modulates the perception of pain (Lee and Tracey, 2013). As such, studying the brain as a complex network of interconnected regions might provide unique insights to the underlying pathophysiology of chronic centralized pain conditions.

The Brain as a Complex Network: Introduction to Graph Theory

Graph theory is a set of mathematical tools to examine the structure and function of networks. The organization, or topology, of a network is critical to its function because it influences the efficiency and content of information transfer (Bullmore and Sporns, 2012; Moon et al., 2015; 2017). The brain is a network that shares an optimal pattern of organization with many other physical and biological systems (e.g., the Internet or social networks). Many of these networks have a "small-world" organization, which strikes a balance between the need for segregated processing and rapid information integration (Sporns and Zwi, 2004).

For an intuitive description of network concepts, consider an analogy: network structure and information flow can be thought of in terms of airport organization and travel. The air transportation network is a collection of nodes (airports) and edges (flight routes between

airports). Small regional airports, with few connections, represent peripheral nodes. Large, highly trafficked airports are called hubs. States could be considered modules, usually containing many regional airports and one large hub. Hub nodes occupy a highly-connected and functionally-central role in the network. They create short-cuts and long-distance connections, keeping the path length between airports in different modules short. Hub airports are also highly interconnected to one another and this organizational structure, termed the "rich-club," serves as a core backbone of the network and makes long-distance travel extremely efficient.

In the case of the brain, nodes represent neurons and/or brain regions and edges are the structural or functional connections between nodes. Hub brain regions, just like hub airports, facilitate communication and information integration across distinct modules (i.e. functional systems) of the brain. A strong hub structure is an important characteristic of the small-world architecture of the brain, ensuring a short average path length and high global efficiency, while maintaining functional modularity (Sporns and Zwi, 2004). Brain networks also have a rich-club organization, in which hubs are more likely to be connected to each other than to peripheral nodes (Colizza et al., 2006; Gorka Zamora-López, 2010; van den Heuvel and Sporns, 2011). The rich club forms a densely connected network core wherein hubs are thought to act in concert and link different functional systems in the brain (van den Heuvel and Sporns, 2011; van den Heuvel et al., 2012). In the healthy human brain, the precuneus/posterior cingulate, ACC, and medial prefrontal cortex have been identified as multimodal functional hubs that participate in numerous functional networks (van den Heuvel and Sporns, 2013). Importantly, while hubs create efficiency, they also create network vulnerability wherein disruption of hub organization can have widespread consequences for information transfer.

Alterations in optimal network structure have been reported in chronic pain disorders (Balenzuela et al., 2010; Liu et al., 2012; Mansour et al., 2017). Balenzuela and colleagues analyzed the community membership across the whole brain network and found that in healthy controls, the insula belonged to a community that included the sensorimotor cortices and cingulate gyrus. However, in chronic pain patients, the insula was abnormally integrated into the auditory and visual networks (Balenzuela et al., 2010). A recent study including patients from three chronic pain conditions confirmed and extended these findings – in healthy controls, the insula was consistently a member of the sensorimotor community, while in patients the insula was more often a member of the DMN, subcortical, salience or attention networks (Mansour et al., 2017).

Beyond pain conditions, work in other clinical populations has shown that hubs may be disproportionately affected in neurological disorders (Crossley et al., 2014; Stam, 2014). A recent meta-analysis of 26 diverse brain disorders found that gray matter alterations were more likely to be in hubs and rich club hubs in particular (Crossley et al., 2014). These studies demonstrate that graph theory can be a useful tool to probe the underlying network architecture associated with chronic pain. However, how brain hub topology is altered in FM, and its relationship to underlying neurochemistry and patient self-reported clinical pain is largely unknown. More broadly, it remains unknown how alterations in neurotransmitter levels (which are major factors influencing neural activity) in a clinical population may relate to changes in hub strength and rich club membership. Characterizing hub topology in chronic pain could provide insight into the pathology of these disorders.

Treatments for Fibromyalgia

Chronic pain conditions with a primarily nociceptive, inflammatory or neuropathic cause are generally well understood and effectively treated by health care providers (Arnold et al., 2016). However, conditions where the CNS is the primary driver in pain perception, such as FM, are often misunderstood and current treatments inadequate. Centralized pain disorders are notoriously unresponsive to treatments that target the periphery and that work well for nociceptive pain (e.g. injections, surgery). Moreover, oral analgesics that work well for peripherally driven pain, such as non-steroidal anti-inflammatory drugs and opioids, do not effectively treat FM pain and emerging evidence suggests that opioids may worsen hyperalgesia in these patients (Brummett et al., 2013; Clauw, 2014; Goldenberg et al., 2016). Instead, most effective treatments target the neurotransmitter systems and brain networks involved in the perception of pain.

Effective pharmacological therapies for FM include drugs that either raise levels of serotonin and norepinephrine (tricyclics such as amitriptyline, and serotonin norepinephrine reuptake inhibitors such as duloxetine and milnacipran), or those that decrease glutamate (gabapentinoids such as pregabalin; see Schmidt-Wilcke and Clauw, 2010; Clauw, 2014 for reviews on drug therapy and their neurobiological mechanisms in FM). In a recent randomized, placebo-controlled trial of milnacipran in FM, our laboratory found that FM patients who had the greatest reduction in clinical pain after treatment had altered connectivity at baseline between pro- and anti-nociceptive regions (Schmidt-Wilcke et al., 2014). This finding is supported by another trial in which milnacipran was found to increase activity in anti-nociceptive brain regions during an evoked pain task (Jensen et al., 2014). In another placebo-controlled trial, pregabalin reduced Glx in the posterior insula and decreased experimental pressure pain

sensitivity in FM (Harris et al., 2013). After treatment these patients also had decreased connectivity between the insula and DMN, and this change in connectivity was associated with a reduction in clinical pain.

Only a subset of chronic pain patients respond to current pharmacological therapies (Häuser et al., 2014), hence there is a critical need for new treatments that target the CNS alterations seen in these individuals. Noninvasive brain stimulation has emerged as an attractive treatment, given its ability to target specific cortical regions with relatively few side effects. Transcranial direct current stimulation (tDCS) of M1 significantly increases experimental pain thresholds in healthy controls (Reidler et al., 2012) and causes lasting clinical pain reduction in FM (Fregni et al., 2006; Valle et al., 2009; Fagerlund et al., 2015). M1 tDCS may also improve other symptoms in FM such as sleep disturbances and depression (Roizenblatt et al., 2007; Khedr et al., 2017). Other stimulation sites, such as the dorsolateral prefrontal cortex, have been explored in FM, but in a comparison trial, M1 stimulation produced the most robust analgesic response (Valle et al., 2009). Although these studies are encouraging, the effect sizes are small and a large review concluded that there is only low-quality evidence for M1 tDCS as an effective treatment for chronic pain (O'Connell et al., 2014). The mixed results may be due in part to variation in stimulation parameters, the duration of treatment and inclusion of many chronic pain conditions. A more recent review of high quality tDCS studies found probable efficacy for pain reduction in FM (Lefaucheur et al., 2017). Some of the variation in analgesic efficacy may also be explained by the underlying neurobiology augmenting the perception of pain in each condition and, indeed, each patient. By combining an understanding of the CNS alteration driving pain perception with the knowledge of analgesic mechanisms of action of treatments, personalized treatment for chronic pain may become a reality.

Analgesic Mechanisms of Motor Cortex tDCS

During a typical tDCS session, the stimulating electrode (anode) is placed over M1 and a reference electrode (cathode) is placed over the contralateral supraorbital area. A weak electrical current (between 1 – 2 mA) is applied to the scalp and passed between the electrodes for durations of 5 to 30 minutes. tDCS effects are often examined in comparison to a sham (placebo) procedure. During the sham condition, electrodes are applied and positioned exactly as in the active condition but the current is applied for only 30 seconds and then discontinued. The sensations on the scalp during an active session can only be felt during the early phase of treatment, hence the sham condition is an effective placebo (DaSilva et al., 2011).

The electrical current applied in tDCS modifies resting membrane potential, thereby modulating the excitability and firing rates of cortical neurons. As a general rule, anodal stimulation increases cortical excitability by depolarizing neurons, an effect that persists after the stimulation period depending on the intensity and duration of stimulation (Stagg and Nitsche, 2011). Conversely, cathodal stimulation has an inhibitory effect by hyperpolarizing neurons (Rosen et al., 2009). Unlike other invasive and non-invasive brain stimulation methods (e.g., invasive motor cortex stimulation and transcranial magnetic stimulation), tDCS does not generate action potentials (Zaghi et al., 2010). Although this general observation provides some guidance, it is likely too simplistic. tDCS may also reduce membrane resistance (or increase conductance), and the size of this effect depends on the baseline state of the neuron. Moreover, tDCS effects depend on the relationship between the stimulated area and structurally connected regions, and any pathological alterations of neurotransmitter systems (Lefaucheur et al., 2017). Finally, stimulation intensity, duration, number of repetitions and electrode size, shape and

placement can also impact the strength, diffusion and excitability of the electrical current (Lefaucheur et al., 2017).

Axons are more susceptible to the electrical current applied during brain stimulation compared to cell bodies, so mechanisms should be examined in terms of the impact on networks rather than on any individual brain region (Lefaucheur, 2016). Computational models of M1 tDCS depict current flow reaching areas under the stimulating electrode in addition to more distal cortical and subcortical regions (DaSilva et al., 2012). These models have been borne out by in vivo studies of tDCS effects; anodal M1 tDCS increases activity and connectivity in the underlying M1 cortex (Kwon et al., 2008; Polanía et al., 2012a; Sehm et al., 2013) and has a sustained impact on the neural activity of distant cortical and subcortical regions (Lang et al., 2005). Using graph-theoretical techniques, Polania and colleagues examined network connectivity before and immediately after anodal M1 tDCS in healthy participants. They found that M1 tDCS (compared to sham) increased the number of functional connections in the posterior cingulate and the dorsolateral prefrontal cortex (Polanía et al., 2011). Specifically, there was increased connectivity between the posterior cingulate and other DMN regions and between the dorsolateral prefrontal cortex and the anterior insula. They also found decreased long-distance connectivity in S1, and a concomitant increase in short-range connections between S1 and M1. Sehm and colleagues found that M1 tDCS altered connectivity in prefrontal, parietal and cerebellar regions during stimulation and the effects persisted for at least 15 minutes in healthy volunteers (Sehm et al., 2012).

There has not been substantial research on the neurobiology of M1 tDCS analgesia. However, studies from invasive motor cortex stimulation, other types of non-invasive brain stimulation and animal models can provide insight into potential mechanisms of action.

Importantly, the hypotheses outlined below are not mutually exclusive and could occur synergistically to produce analgesia.

Thalamocortical Hypothesis

The ventral lateral and ventral posterior lateral thalamic nuclei have direct connections to the motor and somatosensory cortices, and are involved in motor functions and the sensory-discriminative aspect of pain (Zhang et al., 2010). One influential hypothesis states that M1 stimulation causes analgesia by decreasing thalamic hyperactivity (Tsubokawa et al., 1991; 1993; Nguyen et al., 2011). In studies of healthy rats and rats with neuropathic pain, researchers performed a paw pressure noxious stimulus test and found that following invasive M1 stimulation, the withdrawal threshold was increased compared to sham (meaning that it takes more pressure to induce the withdrawal response, which is interpreted as anti-nociception). Furthermore, neuronal firing rates in the ventral posterior lateral thalamus decreased during M1 stimulation, while the firing rate of neurons in the PAG increased (Pagano et al., 2011; 2012). Garcia-Larrea and colleagues demonstrated that invasive M1 stimulation in patients with neuropathic pain caused an increase in cerebral blood flow in the ventral lateral thalamus, ACC, anterior insula and upper brainstem (García-Larrea et al., 1999). Together, these data suggest that M1 stimulation may activate inhibitory corticothalamic fibers, which results in thalamic inhibition (Zaghi et al., 2009).

tDCS also increases pain and sensory thresholds in healthy volunteers and causes lasting pain relief in chronic pain conditions (Vaseghi et al., 2014), perhaps due to the modulation of thalamic sensory pathways. In a study of healthy volunteers measuring regional cerebral blood flow with PET, researchers found increased blood flow in M1, S1 and the ventral posterior lateral thalamus immediately after anodal M1 tDCS compared to sham, which is similar to the

findings using invasive M1 stimulation (Lang et al., 2005). In another study using healthy controls, M1 tDCS increased functional connectivity between M1 and thalamus relative to the sham condition (Polanía et al., 2012b). It is important to note that these studies were done during or immediately after tDCS and that thalamic activity may either increase or decrease depending on the timing of measurement (Peyron et al., 2007). Our laboratory has shown that after five days of M1 tDCS in FM patients there was trend towards decreased Glx in the bilateral thalami compared to sham, although this did not meet statistical significance (Foerster et al., 2014). This was a small study that needs to be replicated, but it suggests that M1 tDCS may also act via corticothalamic pathways in chronic centralized pain.

Endogenous Opioid Hypothesis

Another hypothesis states that M1 stimulation may cause analgesia via activation of the endogenous opioid system, a major pain modulatory system. In a PET study of cerebral blood flow in neuropathic pain patients there was an increase in blood flow in the ACC, orbitofrontal cortex, putamen, and PAG that persisted 75 minutes after the cessation of invasive M1 stimulation (Peyron et al., 2007). Most of these changes in blood flow were associated with analgesia. Additionally, the authors found a significant increase in functional connectivity between the ACC and PAG, leading to the hypothesis that M1 stimulation activates descending anti-nociceptive systems. The ACC and PAG contain a high density of opioid receptors, and are important players in opioid analgesia (Jones et al., 1991; Petrovic, 2002). Relative to a preoperative PET scan, Maarrawi and colleagues found a reduction in binding potential with the non-selective opioid antagonist [^{11}C]diprenorphine in the ACC and PAG after seven months of invasive M1 stimulation for the treatment of neuropathic pain (Maarrawi et al., 2007). A later

study showed that the density of opioid receptors in these regions - in addition to the thalamus, insula and orbitofrontal cortex - predicted postoperative pain relief (Maarrawi et al., 2013).

Naloxone, an opioid receptor antagonist, blocks the analgesic effects of M1 tDCS in healthy controls (de Andrade et al., 2011). Research combining PET and tDCS confirms that tDCS may also act on the endogenous opioid system. In a neuropathic pain patient, M1 tDCS (compared to sham) caused a release of endogenous opioids in the nucleus accumbens, ACC, insula and thalamus (DosSantos et al., 2012). A later study confirmed these results, in addition to increased release in the PAG, in healthy controls during M1 tDCS (DosSantos et al., 2014). Since the sham tDCS condition also caused endogenous opioid release in many of the same regions, placebo effects cannot be ruled out.

As stated above, chronic centralized pain patients have alterations in the endogenous opioid system (either increased levels of circulating endogenous opioids or fewer opioid receptors). It is unclear if the findings from healthy volunteers and neuropathic pain patients would extend into chronic pain conditions. It is also unknown how tDCS alters endogenous opioid tone or receptor density after repeated tDCS sessions, as an FM patient would be treated in a clinical setting. This is beyond the scope of the current dissertation, but should be examined in future studies.

Neuronal Plasticity Hypothesis

The analgesic effects of tDCS can last well beyond the end of a treatment session and outcomes are generally improved with repeated sessions (Monte-Silva et al., 2013). Antagonists at the glutamate N-methyl-D-aspartate (NMDA) receptor, a key regulator of synaptic plasticity, can abolish the analgesic effects of M1 stimulation (Liebetanz et al., 2002; Ciampi de Andrade et al., 2014). Anodal tDCS to the parietal cortex increased Glx in the same region (Clark et al.,

2011). After repetitive S1 transcranial magnetic stimulation in chronic visceral pain patients, there was a significant increase in S1 Glx and this change was associated with a reduction in clinical pain (Fregni et al., 2011). Anodal tDCS can also reduce GABA near the stimulating electrode, which may impact glutamatergic plasticity as well (Stagg et al., 2009; Lefaucheur et al., 2017). tDCS also alters functional connectivity below the stimulating electrode as well as distant cortical regions (Polanía et al., 2011; Sehm et al., 2012; Polanía et al., 2012a; 2012b; Sehm et al., 2013). The baseline activity of the neural network can determine the effect of tDCS and 'priming' the network by having participants perform a task during stimulation can potentiate behavioral effects (Lefaucheur et al., 2017). For example, when M1 tDCS is applied during a motor learning task, performance is better and improvements are longer lasting compared to tDCS alone (Reis et al., 2009; Reis and Fritsch, 2011; Zimerman et al., 2013). This principle also applies to other cognitive domains and stimulation sites (Cohen Kadosh et al., 2010; Meinzer et al., 2014). All together, these facts strongly suggest that the long term changes seen after noninvasive brain stimulation involve neural plasticity, possibly via long-term potentiation or long-term depression-like mechanisms (Monte-Silva et al., 2013; DosSantos et al., 2016).

Placebo Hypothesis

The placebo response is attributable to the psychobiological effects of the treatment process itself, rather than any active component of a drug or non-drug treatment (Wager and Fields, 2013). Neuroimaging studies have revealed an overlap between brain networks involved in pain processing and those implicated in the placebo response (Tracey, 2010; Meissner et al., 2011). Placebo analgesia is associated with activity in descending anti-nociceptive systems, including the release of endogenous opioids, and the inhibition of ascending pro-nociceptive

activity (Zubieta and Stohler, 2009; Wager and Fields, 2013). Placebo responses are clearly present in tDCS and may account for a portion of the analgesic effect. One study found that sham tDCS causes the release of endogenous opioids in the PAG, precuneus and thalamus (DosSantos et al., 2014). These findings led to the suggestion that the placebo response to tDCS could be leveraged to provide a larger analgesic response when real tDCS is subsequently applied. Active tDCS may be reinforcing brain networks that are activated by the expectation of pain relief (similar to the enhanced effects when tDCS is combined with a motor or cognitive task outlined above). This idea can be summarized as "functional targeting" and may shed light on how tDCS targets specific networks when the electrical current itself is rather widespread and diffuse (Schambra et al., 2014).

To summarize, tDCS is an emerging technology that may hold promise for relieving pain symptoms through network-level changes. It is clear that tDCS can alter functional connectivity and the neurochemistry of regions underneath and distant to the stimulating electrode. Importantly, most of the studies outlined above in healthy controls or neuropathic pain patients examined the neurobiological effects of M1 stimulation during or immediately after stimulation had ended. It is unclear if these results translate to chronic centralized pain conditions. There have not been any studies measuring changes in functional connectivity after repetitive treatments of tDCS in chronic pain patients, as they would be treated in clinical practice.

Aims and Hypotheses of this Dissertation

The goals of this dissertation are to (1) elucidate changes in brain network topology, specifically within regions fundamental to information flow and integration (i.e. hubs), in a common chronic centralized pain condition and (2) determine how a non-pharmacological treatment may alter network connectivity to cause analgesia. The overarching hypothesis is that

there is a reorganization of hub regions in chronic pain, which may contribute to amplifying or sustaining the perception of pain independently of peripheral nociceptive input. Further, we hypothesize that disordered hub regions are prospective targets for non-invasive brain stimulation therapy and that tDCS cause analgesia by disrupting functional connectivity between regions involved in pain perception.

In Chapter 2, we apply a brain network based approach to examine hub topology in 40 FM patients compared to 27 healthy volunteers using graph theoretical techniques. Given the widespread nature of pain and hypersensitivity to other sensory modalities in FM, we hypothesize that the FM brain network will have altered hub organization and rich-club membership of pain and sensory processing regions (such as the insula and S1). We further hypothesize that these differences will be related to neurochemistry and clinical pain intensity.

In Chapter 3, we examine resting state functional connectivity in 12 FM patients at baseline, after five days of sham tDCS, and after five days of anodal M1 tDCS treatment. We sought to answer three questions: (1) Can functional connectivity at baseline predict subsequent analgesia after M1 tDCS? (2) How does M1 tDCS (compared to sham) alter functional connectivity? and (3) Do changes in connectivity relate to treatment response? Previous studies have shown that structural connectivity between M1 and the thalamus may be important for analgesia after a similar noninvasive brain stimulation technique (Goto et al., 2008; Ohn et al., 2012). Therefore, we hypothesize that FM patients with stronger M1-thalamus connectivity at baseline will predict a better clinical response. Additionally, since we found a trend towards decreased Glx in the thalamus after M1 tDCS in the same patients studied here (Foerster et al., 2014), we expect that M1 tDCS will decrease functional connectivity between the thalamus and brain regions involved in pain perception and that these changes will relate to analgesia.

In total, this research may offer new insight into the pathophysiology of chronic centralized pain conditions, may be a clinically useful diagnostic marker of chronic pain, and may contribute to the understanding of how noninvasive brain stimulation treatments cause analgesia. This knowledge could lead to more informed stimulation sites and personalized treatment based on the brain network connectivity in an individual patient. Finally, an understanding of how alterations in the excitatory-inhibitory balance in one brain region might affect information transfer in the whole brain network would be of foundational neuroscientific importance.

References

Apkarian AV, Hashmi JA, Baliki MN (2011) Pain and the brain: Specificity and plasticity of the brain in clinical chronic pain. PAIN 152:S49–S64.

Balenzuela P, Chernomoretz A, Fraiman D, Cifre I, Sitges C, Montoya P, Chialvo DR (2010) Modular Organization of Brain Resting State Networks in Chronic Back Pain Patients. Frontiers in Neuroinformatics 4.

Brummett CM, Janda AM, Schueller CM, Tsodikov A, Morris M, Williams DA, Clauw DJ (2013) Survey criteria for fibromyalgia independently predict increased postoperative opioid consumption after lower-extremity joint arthroplasty: a prospective, observational cohort study. Anesthesiology 119:1434–1443.

Bullmore E, Sporns O (2012) The economy of brain network organization. Nat Rev Neurosci:1–14.

Ciampi de Andrade D, Mhalla A, Adam F, Texeira MJ, Bouhassira D (2014) Repetitive transcranial magnetic stimulation induced analgesia depends on N-methyl-D-aspartate glutamate receptors. PAIN 155:598–605.

Cifre I, Sitges C, Fraiman D, Muñoz MÁ, Balenzuela P, González-Roldán A, Martínez-Jauand M, Birbaumer N, Chialvo DR, Montoya P (2012) Disrupted functional connectivity of the pain network in fibromyalgia. Psychosom Med 74:55–62.

Clark VP, Coffman BA, Trumbo MC, Gasparovic C (2011) Transcranial direct current stimulation (tDCS) produces localized and specific alterations in neurochemistry: a ^{1}H magnetic resonance spectroscopy study. Neuroscience Letters 500:67–71.

Clauw DJ (2009) Fibromyalgia: An Overview. The American Journal of Medicine 122:S3–S13.

Clauw DJ (2014) Fibromyalgia: a clinical review. In, pp 1547–1555.

Cohen Kadosh R, Soskic S, Iuculano T, Kanai R, Walsh V (2010) Modulating neuronal activity produces specific and long-lasting changes in numerical competence. Curr Biol 20:2016–2020.

Colizza V, Flammini A, Serrano MA, Vespignani A (2006) Detecting rich-club ordering in complex networks. Nat Phys 2:110–115.

Cook DB, Lange G, Ciccone DS, Liu W-C, Steffener J, Natelson BH (2004) Functional imaging of pain in patients with primary fibromyalgia. J Rheumatol 31:364–378.

Crossley NA, Mechelli A, Scott J, Carletti F, Fox PT, McGuire P, Bullmore ET (2014) The hubs of the human connectome are generally implicated in the anatomy of brain disorders. Brain 137:2382–2395.

DaSilva AF, Mendonca ME, Zaghi S, Lopes M, DosSantos MF, Spierings EL, Bajwa Z, Datta A, Bikson M, Fregni F (2012) tDCS-Induced Analgesia and Electrical Fields in Pain-Related Neural Networks in Chronic Migraine. Headache: The Journal of Head and Face Pain 52:1283–1295.

DaSilva AF, Volz MS, Bikson M, Fregni F (2011) Electrode positioning and montage in transcranial direct current stimulation. J Vis Exp.

de Andrade DC, Mhalla A, Adam F, Texeira MJ, Bouhassira D (2011) Neuropharmacological basis of rTMS-induced analgesia: the role of endogenous opioids. PAIN 152:320–326.

DosSantos MF, Ferreira N, Toback RL, Carvalho AC, DaSilva AF (2016) Potential Mechanisms Supporting the Value of Motor Cortex Stimulation to Treat Chronic Pain Syndromes. Front Neurosci 10:18.

DosSantos MF, Love TM, Martikainen IK, Nascimento TD, Fregni F, Cummiford C, Deboer MD, Zubieta J-K, Dasilva AFM (2012) Immediate effects of tDCS on the μ-opioid system of a chronic pain patient. Front Psychiatry 3:93.

DosSantos MF, Martikainen IK, Nascimento TD, Love TM, DeBoer MD, Schambra HM, Bikson M, Zubieta J-K, DaSilva AF (2014) Building up analgesia in humans via the endogenous μ-opioid system by combining placebo and active tDCS: a preliminary report. PLoS ONE 9:e102350.

Elzahaf RA, Tashani OA, Unsworth BA, Johnson MI (2012) The prevalence of chronic pain with an analysis of countries with a Human Development Index less than 0.9: a systematic review without meta-analysis. Curr Med Res Opin 28:1221–1229.

Fagerlund AJ, Hansen OA, Aslaksen PM (2015) Transcranial direct current stimulation as a treatment for patients with fibromyalgia. PAIN 156:62–71.

Fayed N, Garcia-Campayo J, Magallón R, Andrés-Bergareche H, Luciano JV, Andres E, Beltrán

J (2010) Localized 1H-NMR spectroscopy in patients with fibromyalgia: a controlled study of changes in cerebral glutamate/glutamine, inositol, choline, and N-acetylaspartate. Arthritis Res Ther 12:R134.

Flodin P, Martinsen S, Löfgren M, Bileviciute-Ljungar I, Kosek E, Fransson P (2014) Fibromyalgia is associated with decreased connectivity between pain- and sensorimotor brain areas. Brain Connectivity 4:587–594.

Foerster BR, Nascimento TD, DeBoer M, Bender MA, Rice IC, Truong DQ, Bikson M, Clauw DJ, Zubieta J-K, Harris RE, DaSilva AF (2014) Excitatory and Inhibitory Brain Metabolites as Targets and Predictors of Effective Motor Cortex tDCS Therapy in Fibromyalgia. Arthritis Rheumatol.

Foerster BR, Petrou M, Edden RAE, Sundgren PC, Schmidt-Wilcke T, Lowe SE, Harte SE, Clauw DJ, Harris RE (2012) Reduced insular γ-aminobutyric acid in fibromyalgia. Arthritis Rheum 64:579–583.

Fregni F, Gimenes R, Valle AC, Ferreira MJL, Rocha RR, Natalle L, Bravo R, Rigonatti SP, Freedman SD, Nitsche MA, Pascual-Leone A, Boggio PS (2006) A randomized, sham-controlled, proof of principle study of transcranial direct current stimulation for the treatment of pain in fibromyalgia. Arthritis Rheum 54:3988–3998.

Fregni F, Potvin K, Dasilva D, Wang X, Lenkinski RE, Freedman SD, Pascual-Leone A (2011) Clinical effects and brain metabolic correlates in non-invasive cortical neuromodulation for visceral pain. Eur J Pain 15:53–60.

García-Larrea L, Peyron R, Mertens P, Gregoire MC, Lavenne F, Le Bars D, Convers P, Mauguière F, Sindou M, Laurent B (1999) Electrical stimulation of motor cortex for pain control: a combined PET-scan and electrophysiological study. PAIN 83:259–273.

Geisser ME, Glass JM, Rajcevska LD, Clauw DJ, Williams DA, Kileny PR, Gracely RH (2008) A psychophysical study of auditory and pressure sensitivity in patients with fibromyalgia and healthy controls. The Journal of Pain 9:417–422.

Giesecke T, Gracely RH, Grant MAB, Nachemson A, Petzke F, Williams DA, Clauw DJ (2004) Evidence of augmented central pain processing in idiopathic chronic low back pain. Arthritis Rheum 50:613–623.

Giovengo SL, Russell IJ, Larson AA (1999) Increased concentrations of nerve growth factor in cerebrospinal fluid of patients with fibromyalgia. J Rheumatol 26:1564–1569.

Goldenberg DL, Clauw DJ, Palmer RE, Clair AG (2016) Opioid Use in Fibromyalgia: A Cautionary Tale. Mayo Clin Proc 91:640–648.

Gorka Zamora-López CZJK (2010) Cortical Hubs Form a Module for Multisensory Integration on Top of the Hierarchy of Cortical Networks. Frontiers in Neuroinformatics 4.

Goto T, Saitoh Y, Hashimoto N, Hirata M, Kishima H, Oshino S, Tani N, Hosomi K, Kakigi R,

Yoshimine T (2008) Diffusion tensor fiber tracking in patients with central post-stroke pain; correlation with efficacy of repetitive transcranial magnetic stimulation. PAIN 140:509–518.

Gracely RH (2004) Pain catastrophizing and neural responses to pain among persons with fibromyalgia. Brain 127:835–843.

Gracely RH, Petzke F, Wolf JM, Clauw DJ (2002) Functional magnetic resonance imaging evidence of augmented pain processing in fibromyalgia. Arthritis Rheum 46:1333–1343.

Harris RE, Clauw DJ, Scott DJ, McLean SA, Gracely RH, Zubieta J-K (2007) Decreased central mu-opioid receptor availability in fibromyalgia. Journal of Neuroscience 27:10000–10006.

Harris RE, Napadow V, Huggins JP, Pauer L, Kim J, Hampson J, Sundgren PC, Foerster B, Petrou M, Schmidt-Wilcke T, Clauw DJ (2013) Pregabalin rectifies aberrant brain chemistry, connectivity, and functional response in chronic pain patients. Anesthesiology 119:1453–1464.

Harris RE, Sundgren PC, Craig AD, Kirshenbaum E, Sen A, Napadow V, Clauw DJ (2009) Elevated insular glutamate in fibromyalgia is associated with experimental pain. Arthritis Rheum 60:3146–3152.

Harte SE, Ichesco E, Hampson JP, Peltier SJ, Schmidt-Wilcke T, Clauw DJ, Harris RE (2016) Pharmacologic attenuation of cross-modal sensory augmentation within the chronic pain insula. PAIN 157:1933–1945.

Häuser W, Walitt B, Fitzcharles M-A, Sommer C (2014) Review of pharmacological therapies in fibromyalgia syndrome. Arthritis Res Ther 16:201.

Ichesco E, Puiu T, Hampson JP, Kairys AE, Clauw DJ, Harte SE, Peltier SJ, Harris RE, Schmidt-Wilcke T (2016) Altered fMRI resting-state connectivity in individuals with fibromyalgia on acute pain stimulation. European Journal of Pain 20:1079–1089.

Institute of Medicine (US) Committee on Advancing Pain Research, Care, and Education (2011) Relieving Pain in America: A Blueprint for Transforming Prevention, Care, Education, and Research. Washington (DC): National Academies Press (US).

Jensen KB, Kosek E, Petzke F, Carville S, Fransson P, Marcus H, Williams SCR, Choy E, Giesecke T, Mainguy Y, Gracely R, Ingvar M (2009) Evidence of dysfunctional pain inhibition in Fibromyalgia reflected in rACC during provoked pain. PAIN 144:95–100.

Jensen KB, Loitoile R, Kosek E, Petzke F, Carville S, Fransson P, Marcus H, Williams SCR, Choy E, Mainguy Y, Vitton O, Gracely RH, Gollub R, Ingvar M, Kong J (2012) Patients with fibromyalgia display less functional connectivity in the brain's pain inhibitory network. Mol Pain 8:32.

Jensen KB, Petzke F, Carville S, Choy E, Fransson P, Gracely RH, Vitton O, Marcus H, Williams SCR, Ingvar M, Kosek E (2014) Segregating the cerebral mechanisms of antidepressants and placebo in fibromyalgia. J Pain 15:1328–1337.

Jones AK, Qi LY, Fujirawa T, Luthra SK, Ashburner J, Bloomfield P, Cunningham VJ, Itoh M, Fukuda H, Jones T (1991) In vivo distribution of opioid receptors in man in relation to the cortical projections of the medial and lateral pain systems measured with positron emission tomography. Neuroscience Letters 126:25–28.

Khedr EM, Omran EAH, Ismail NM, El-Hammady DH, Goma SH, Kotb H, Galal H, Osman AM, Farghaly HSM, Karim AA, Ahmed GA (2017) Effects of transcranial direct current stimulation on pain, mood and serum endorphin level in the treatment of fibromyalgia: A double blinded, randomized clinical trial. Brain Stimul 10:893–901.

Kutch JJ et al. (2017) Brain signature and functional impact of centralized pain: a multidisciplinary approach to the study of chronic pelvic pain (MAPP) network study. PAIN.

Kwon YH, Ko M-H, Ahn SH, Kim Y-H, Song JC, Lee C-H, Chang MC, Jang SH (2008) Primary motor cortex activation by transcranial direct current stimulation in the human brain. Neuroscience Letters 435:56–59.

Lang N, Siebner HR, Ward NS, Lee L, Nitsche MA, Paulus W, Rothwell JC, Lemon RN, Frackowiak RS (2005) How does transcranial DC stimulation of the primary motor cortex alter regional neuronal activity in the human brain? European Journal of Neuroscience 22:495–504.

Lee MC, Tracey I (2013) Imaging pain: a potent means for investigating pain mechanisms in patients. Br J Anaesth 111:64–72.

Lefaucheur J-P (2016) Cortical neurostimulation for neuropathic pain: state of the art and perspectives. PAIN 157 Suppl 1:S81–S89.

Lefaucheur J-P et al. (2017) Evidence-based guidelines on the therapeutic use of transcranial direct current stimulation (tDCS). Clin Neurophysiol 128:56–92.

Liebetanz D, Nitsche MA, Tergau F, Paulus W (2002) Pharmacological approach to the mechanisms of transcranial DC-stimulation-induced after-effects of human motor cortex excitability. Brain 125:2238–2247.

Liu J, Zhao L, Li G, Xiong S, Nan J, Li J, Yuan K, Deneen von KM, Liang F, Qin W, Tian J (2012) Hierarchical Alteration of Brain Structural and Functional Networks in Female Migraine Sufferers. PLoS ONE 7:e51250.

López-Solà M, Pujol J, Wager TD, Garcia-Fontanals A, Blanco-Hinojo L, Garcia-Blanco S, Poca-Dias V, Harrison BJ, Contreras-Rodríguez O, Monfort J, Garcia-Fructuoso F, Deus J (2014) Altered functional magnetic resonance imaging responses to nonpainful sensory stimulation in fibromyalgia patients. Arthritis Rheumatol 66:3200–3209.

López-Solà M, Woo C-W, Pujol J, Deus J, Harrison BJ, Monfort J, Wager TD (2016) Towards a neurophysiological signature for fibromyalgia. PAIN.

Maarrawi J, Peyron R, Mertens P, Costes N, Magnin M, Sindou M, Laurent B, Garcia-Larrea L

(2013) Brain opioid receptor density predicts motor cortex stimulation efficacy for chronic pain. PAIN 154:2563–2568.

Maarrawi J, Peyron R, Mertens P, Costes N, Magnin M, Sindou M, Laurent B, García-Larrea L (2007) Motor cortex stimulation for pain control induces changes in the endogenous opioid system. Neurology 69:827–834.

Maixner W, Fillingim RB, Williams DA, Smith SB, Slade GD (2016) Overlapping Chronic Pain Conditions: Implications for Diagnosis and Classification. J Pain 17:T93–T107.

Mansour A, Baria AT, Tetreault P, Vachon-Presseau E, Chang P-C, Huang L, Apkarian AV, Baliki MN (2017) Global disruption of degree rank order: Ahallmark of chronic pain. Sci Rep:1–18.

Martenson ME, Halawa OI, Tonsfeldt KJ, Maxwell CA, Hammack N, Mist SD, Pennesi ME, Bennett RM, Mauer KM, Jones KD, Heinricher MM (2016) A possible neural mechanism for photosensitivity in chronic pain. PAIN 157:868–878.

McBeth J, Jones K (2007) Epidemiology of chronic musculoskeletal pain. Best Pract Res Clin Rheumatol.

Meinzer M, Jähnigen S, Copland DA, Darkow R, Grittner U, Avirame K, Rodriguez AD, Lindenberg R, Flöel A (2014) Transcranial direct current stimulation over multiple days improves learning and maintenance of a novel vocabulary. Cortex 50:137–147.

Meissner K, Bingel U, Colloca L, Wager TD, Watson A, Flaten MA (2011) The placebo effect: advances from different methodological approaches. Journal of Neuroscience 31:16117–16124.

Merskey H BN (1994) Classification of Chronic Pain, Second Edition (Revised) Merskey H BN, ed. IASP Press:1–9.

Monte-Silva K, Kuo M-F, Hessenthaler S, Fresnoza S, Liebetanz D, Paulus W, Nitsche MA (2013) Induction of late LTP-like plasticity in the human motor cortex by repeated non-invasive brain stimulation. Brain Stimul 6:424–432.

Moon J-Y, Kim J, Ko T-W, Kim M, Iturria-Medina Y, Choi J-H, Lee J, Mashour GA, Lee U (2017) Structure Shapes Dynamics and Directionality in Diverse Brain Networks: Mathematical Principles and Empirical Confirmation in Three Species. Sci Rep 7:46606.

Moon J-Y, Lee U, Blain-Moraes S, Mashour GA (2015) General relationship of global topology, local dynamics, and directionality in large-scale brain networks. PLoS Comp Biol 11:e1004225.

Napadow V, Kim J, Clauw DJ, Harris RE (2012) Brief Report: Decreased intrinsic brain connectivity is associated with reduced clinical pain in fibromyalgia. Arthritis Rheum 64:2398–2403.

Napadow V, LaCount L, Park K, As-Sanie S, Clauw DJ, Harris RE (2010) Intrinsic brain connectivity in fibromyalgia is associated with chronic pain intensity. Arthritis Rheum 62:2545–2555.

Nguyen J-P, Nizard J, Keravel Y, Lefaucheur J-P (2011) Invasive brain stimulation for the treatment of neuropathic pain. Nat Rev Neurol 7:699–709.

O'Connell NE, Wand BM, Marston L, Spencer S, Desouza LH (2014) Non-invasive brain stimulation techniques for chronic pain. Cochrane Database Syst Rev 4:CD008208.

Ohn SH, Chang WH, Park C-H, Kim ST, Lee JI, Pascual-Leone A, Kim Y-H (2012) Neural correlates of the antinociceptive effects of repetitive transcranial magnetic stimulation on central pain after stroke. Neurorehabil Neural Repair 26:344–352.

Pagano RL, Assis DV, Clara JA, Alves AS, Dale CS, Teixeira MJ, Fonoff ET, Britto LR (2011) Transdural motor cortex stimulation reverses neuropathic pain in rats: a profile of neuronal activation. Eur J Pain 15:268.e1–.e14.

Pagano RL, Fonoff ET, Dale CS, Ballester G, Teixeira MJ, Britto LRG (2012) Motor cortex stimulation inhibits thalamic sensory neurons and enhances activity of PAG neurons: possible pathways for antinociception. PAIN 153:2359–2369.

Petrovic P (2002) Placebo and Opioid Analgesia-- Imaging a Shared Neuronal Network. Science 295:1737–1740.

Petzke F, Clauw DJ, Ambrose K, Khine A, Gracely RH (2003) Increased pain sensitivity in fibromyalgia: effects of stimulus type and mode of presentation. PAIN.

Peyron R, Faillenot I, Mertens P, Laurent B, Garcia-Larrea L (2007) Motor cortex stimulation in neuropathic pain. Correlations between analgesic effect and hemodynamic changes in the brain. A PET study. NeuroImage 34:310–321.

Polanía R, Paulus W, Antal A, Nitsche MA (2011) Introducing graph theory to track for neuroplastic alterations in the resting human brain: A transcranial direct current stimulation study. NeuroImage 54:2287–2296.

Polanía R, Paulus W, Nitsche MA (2012a) Reorganizing the intrinsic functional architecture of the human primary motor cortex during rest with non-invasive cortical stimulation. PLoS ONE 7:e30971.

Polanía R, Paulus W, Nitsche MA (2012b) Modulating cortico-striatal and thalamo-cortical functional connectivity with transcranial direct current stimulation. Hum Brain Mapp 33:2499–2508.

Pujol J, López-Solà M, Ortiz H, Vilanova JC, Ben J Harrison, Yücel M, Soriano-Mas C, Cardoner N, Deus J (2009) Mapping brain response to pain in fibromyalgia patients using temporal analysis of FMRI. PLoS ONE 4:e5224–e5224.

Pujol J, Macià D, Garcia-Fontanals A, Blanco-Hinojo L, López-Solà M, Garcia-Blanco S, Poca-Dias V, Harrison BJ, Contreras-Rodríguez O, Monfort J, Garcia-Fructuoso F, Deus J (2014) The contribution of sensory system functional connectivity reduction to clinical pain in fibromyalgia. PAIN.

Reidler JS, Mendonca ME, Santana MB, Wang X, Lenkinski R, Motta AF, Marchand S, Latif L, Fregni F (2012) Effects of motor cortex modulation and descending inhibitory systems on pain thresholds in healthy subjects. J Pain 13:450–458.

Reis J, Fritsch B (2011) Modulation of motor performance and motor learning by transcranial direct current stimulation. Curr Opin Neurol 24:590–596.

Reis J, Schambra HM, Cohen LG, Buch ER, Fritsch B, Zarahn E, Celnik PA, Krakauer JW (2009) Noninvasive cortical stimulation enhances motor skill acquisition over multiple days through an effect on consolidation. Proc Natl Acad Sci USA 106:1590–1595.

Roizenblatt S, Fregni F, Gimenez R, Wetzel T, Rigonatti SP, Tufik S, Boggio PS, Valle AC (2007) Site-specific Effects of Transcranial Direct Current Stimulation on Sleep and Pain in Fibromyalgia: A Randomized, Sham-controlled Study. Pain Pract 7:297–306.

Rosen AC, Ramkumar M, Nguyen T, Hoeft F (2009) Noninvasive transcranial brain stimulation and pain. Current Science Inc 13:12–17.

Russell IJ, Orr MD, Littman B, Vipraio GA, Alboukrek D, Michalek JE, Lopez Y, Mackillip F (1994) Elevated cerebrospinal fluid levels of substance p in patients with the fibromyalgia syndrome. Arthritis & Rheumatology 37:1593–1601.

Russell IJ, Vaeroy H, Javors M, Nyberg F (1992) Cerebrospinal fluid biogenic amine metabolites in fibromyalgia/fibrositis syndrome and rheumatoid arthritis. Arthritis Rheum 35:550–556.

Sarchielli P, Mancini ML, Floridi A, Coppola F, Rossi C, Nardi K, Acciarresi M, Pini LA, Calabresi P (2007) Increased levels of neurotrophins are not specific for chronic migraine: evidence from primary fibromyalgia syndrome. J Pain 8:737–745.

Schambra HM, Bikson M, Wager TD, DosSantos MF, DaSilva AF (2014) It's All in Your Head: Reinforcing the Placebo Response With tDCS. Brain Stimul 7:623–624.

Schmidt-Wilcke T, Clauw DJ (2010) Pharmacotherapy in fibromyalgia (FM)--implications for the underlying pathophysiology. Pharmacol Ther 127:283–294.

Schmidt-Wilcke T, Ichesco E, Hampson JP, Kairys A, Peltier S, Harte S, Clauw DJ, Harris RE (2014) Resting state connectivity correlates with drug and placebo response in fibromyalgia patients. Neuroimage Clin 6:252–261.

Sehm B, Kipping J, Schafer A, Villringer A, Ragert P (2013) A Comparison between Uni- and Bilateral tDCS Effects on Functional Connectivity of the Human Motor Cortex. Front Hum Neurosci 7:183.

Sehm B, Schafer A, Kipping J, Margulies D, Conde V, Taubert M, Villringer A, Ragert P (2012) Dynamic modulation of intrinsic functional connectivity by transcranial direct current stimulation. Journal of Neurophysiology 108:3253–3263.

Shi H, Yuan C, Dai Z, Ma H, Sheng L (2016) Gray matter abnormalities associated with fibromyalgia: A meta-analysis of voxel-based morphometric studies. Seminars in Arthritis and Rheumatism 46:330–337.

Sluka KA, Clauw DJ (2016) Neurobiology of fibromyalgia and chronic widespread pain. Neuroscience.

Sporns O, Zwi JD (2004) The small world of the cerebral cortex. Neuroinformatics 2:145–162.

Stagg CJ, Best JG, Stephenson MC, O'Shea J, Wylezinska M, Kincses ZT, Morris PG, Matthews PM, Johansen-Berg H (2009) Polarity-sensitive modulation of cortical neurotransmitters by transcranial stimulation. Journal of Neuroscience 29:5202–5206.

Stagg CJ, Nitsche MA (2011) Physiological Basis of Transcranial Direct Current Stimulation. The Neuroscientist.

Stam CJ (2014) Modern network science of neurological disorders. Nat Rev Neurosci 15:683–695.

Tracey I (2005) Nociceptive processing in the human brain. Current Opinion in Neurobiology 15:478–487.

Tracey I (2010) Getting the pain you expect: mechanisms of placebo, nocebo and reappraisal effects in humans. Nat Med 16:1277–1283.

Tsubokawa T, Katayama Y, Yamamoto T, Hirayama T, Koyama S (1991) Treatment of thalamic pain by chronic motor cortex stimulation. Pacing Clin Electrophysiol 14:131–134.

Tsubokawa T, Katayama Y, Yamamoto T, Hirayama T, Koyama S (1993) Chronic motor cortex stimulation in patients with thalamic pain. J Neurosurg 78:393–401.

Valle A, Roizenblatt S, Botte S, Zaghi S, Riberto M, Tufik S, Boggio PS, Fregni F (2009) Efficacy of anodal transcranial direct current stimulation (tDCS) for the treatment of fibromyalgia: results of a randomized, sham-controlled longitudinal clinical trial. J Pain Manag 2:353–361.

van den Heuvel MP, Kahn RS, Goñi J, Sporns O (2012) High-cost, high-capacity backbone for global brain communication. Proc Natl Acad Sci USA 109:11372–11377.

van den Heuvel MP, Pol HEH (2010) Exploring the brain network: A review on resting-state fMRI functional connectivity. European Neuropsychopharmacology 20:519–534.

van den Heuvel MP, Sporns O (2011) Rich-club organization of the human connectome. Journal of Neuroscience 31:15775–15786.

van den Heuvel MP, Sporns O (2013) Network hubs in the human brain. Trends Cogn Sci (Regul Ed) 17:683–696.

Vaseghi B, Zoghi M, Jaberzadeh S (2014) Does anodal transcranial direct current stimulation modulate sensory perception and pain? A meta-analysis study. Clin Neurophysiol.

Vincent A, Lahr BD, Wolfe F, Clauw DJ, Whipple MO, Oh TH, Barton DL, St Sauver J (2013) Prevalence of fibromyalgia: a population-based study in Olmsted County, Minnesota, utilizing the Rochester Epidemiology Project. Arthritis Care Res (Hoboken) 65:786–792.

Wager TD, Fields H (2013) Placebo analgesia. Textbook of Pain.

Wilbarger JL, Cook DB (2011) Multisensory hypersensitivity in women with fibromyalgia: implications for well being and intervention. Arch Phys Med Rehabil 92:653–656.

Wolfe F, Ross K, Anderson J, Russell IJ (1995) The prevalence and characteristics of fibromyalgia in the general population - Wolfe - 2005 - Arthritis & Rheumatism - Wiley Online Library. Arthritis & ….

Younger J, Mackey S (2009) Fibromyalgia symptoms are reduced by low-dose naltrexone: a pilot study. Pain Med 10:663–672.

Younger J, Noor N, McCue R, Mackey S (2013) Low-dose naltrexone for the treatment of fibromyalgia: findings of a small, randomized, double-blind, placebo-controlled, counterbalanced, crossover trial assessing daily pain levels. Arthritis & Rheumatology 65:529–538.

Zaghi S, Acar M, Hultgren B, Boggio PS, Fregni F (2010) Noninvasive brain stimulation with low-intensity electrical currents: putative mechanisms of action for direct and alternating current stimulation. The Neuroscientist 16:285–307.

Zaghi S, Heine N, Fregni F (2009) Brain stimulation for the treatment of pain: A review of costs, clinical effects, and mechanisms of treatment for three different central neuromodulatory approaches. J Pain Manag 2:339–352.

Zhang D, Snyder AZ, Shimony JS, Fox MD, Raichle ME (2010) Noninvasive Functional and Structural Connectivity Mapping of the Human Thalamocortical System. Cerebral Cortex 20:1187–1194.

Zimerman M, Nitsch M, Giraux P, Gerloff C, Cohen LG, Hummel FC (2013) Neuroenhancement of the aging brain: restoring skill acquisition in old subjects. Ann Neurol 73:10–15.

Zubieta J-K, Stohler CS (2009) Neurobiological mechanisms of placebo responses. Ann N Y Acad Sci 1156:198–210.

Chapter 2 : Functional and Neurochemical Disruptions of Brain Hub Topology in Chronic Pain

Introduction

The perception of acute pain is a product of neural activity in a widely distributed brain network, typically following noxious insult. In chronic pain conditions, however, altered processing within this network can create, amplify, or sustain the perception of pain independent of noxious stimulation (Sluka and Clauw, 2016). Therefore, a network approach may offer critical and unique insights into the pathogenesis of chronic pain conditions (Farmer *et al.*, 2012; Kucyi and Davis, 2015).

Brain networks can be modeled using graph theoretical tools as a set of functional interactions made up of nodes (neurons and/or brain regions) and edges (structural or functional connections between nodes). The organization, or topology, of a network is critical to its function because it influences the efficiency and content of information transfer among nodes (Moon *et al.*, 2015; 2017). The human brain network has been described as "small-world," a topology that strikes a balance between segregated processing and rapid information integration (Sporns and Zwi, 2004).

A critical component of small-world architecture is a robust hub structure, wherein hub nodes facilitate efficient information integration across the brain by occupying a highly-connected and functionally-central role in the network (van den Heuvel and Sporns, 2013). Brain networks also have a higher order level of organization called "rich-clubs," in which hubs are more likely to be connected to each other than to nodes with fewer connections (Colizza *et*

al., 2006; Gorka Zamora-López, 2010; van den Heuvel and Sporns, 2011). This rich club forms a densely connected network core wherein hubs are thought to act in concert and link different functional systems in the brain (van den Heuvel and Sporns, 2011; van den Heuvel *et al.*, 2012).

Importantly, while hubs create efficiency, they also create network vulnerability wherein disruption of hub organization can have widespread consequences for information transfer. Work in clinical populations has shown that hubs may be disproportionately affected in neurological disorders (Crossley *et al.*, 2014; Stam, 2014). A recent meta-analysis of 26 diverse brain disorders found that gray matter alterations were more likely to be in hubs and rich club hubs in particular (Crossley *et al.*, 2014). Characterizing hub topology in clinical conditions may therefore provide insight into the pathology of these disorders. Alterations in optimal network structure have been reported in chronic pain disorders (Balenzuela *et al.*, 2010; Liu *et al.*, 2012; Mansour *et al.*, 2017). However, how brain hub topology is altered in chronic pain, and its relationship to underlying neurochemistry and patient self-reported clinical pain is largely unknown. More broadly, it remains unknown how alterations in neurotransmitter levels in a clinical population may relate to changes in hub strength and rich club membership.

Here we used a graph theoretical approach in conjunction with resting state functional MRI (fMRI) and proton magnetic resonance spectroscopy (^{1}H-MRS) to examine hub topology and brain neurochemistry in fibromyalgia (FM), a common chronic pain condition with significant central nervous system contributions (Clauw, 2014). In addition to widespread pain and hyperalgesia without clear evidence of ongoing peripheral inflammation or damage, FM patients display hyper-sensitivity to a variety of non-noxious sensory stimuli (Geisser *et al.*, 2008; Harte *et al.*, 2016; López-Solà *et al.*, 2014; Martenson *et al.*, 2016; Petzke *et al.*, 2003; Wilbarger and Cook, 2011), as well as other brain-related symptoms such as disturbances in

energy, sleep, memory and mood. FM patients consistently display evidence of augmented pain and sensory processing on fMRI (Gracely *et al.*, 2002; López-Solà *et al.*, 2016), and altered functional connectivity in pro- and anti-nociceptive regions (Ichesco *et al.*, 2014; 2016; Jensen *et al.*, 2009; Napadow *et al.*, 2010). Moreover, FM patients have altered levels of excitatory and inhibitory neurotransmitters within the insula and other sensory processing regions (Foerster *et al.*, 2012; Harris *et al.*, 2009). We hypothesized that the FM brain network would have altered hub organization and rich-club membership of pain-associated regions (such as the insula). We further hypothesized that these differences would be related to neurochemistry and clinical pain intensity.

Materials and Methods

Participants. Data from 40 female FM patients and 27 age- and sex-matched HCs were pooled from previous fMRI studies and analyzed retrospectively using a graph-theoretical approach. The data from 31 FM and 27 HCs were previously published in manuscripts focusing on functional connectivity, ^{1}H-MRS, and treatment outcomes (Harris *et al.*, 2009; 2013; Harte *et al.*, 2016; Ichesco *et al.*, 2014; Napadow *et al.*, 2010; 2012; Puiu *et al.*, 2016; Schmidt-Wilcke *et al.*, 2014). Data from the remaining nine FM patients has not been published. The University of Michigan Institutional Review Board approved the studies and written informed consent was obtained from all participants in accordance with the Declaration of Helsinki. The major inclusion criteria for FM patients were: meeting the American College of Rheumatology (ACR) 1990 criteria for FM and at least 6 months of self-reported chronic widespread pain, a score of $\geq$ 40 mm on a 100 mm pain Visual Analog Scale (VAS) at the time of consenting. Both FM and HCs were 18-75 years of age, female, right-handed, and capable of giving written informed consent. Major exclusion criteria for both groups were: pregnant or nursing mothers, contraindications to fMRI, positive

urine drug screen or history of drug or alcohol abuse within the past two years, body mass index greater than 36, severe psychiatric illness, concurrent autoimmune or inflammatory disease that causes pain, or systemic malignancy or infection such as HIV or hepatitis. An additional exclusion criterion for HCs was meeting the ACR 1990 criteria for FM.

Data Acquisition and Preprocessing. Self-reported clinical pain intensity in FM patients was assessed immediately before fMRI using a VAS, with 0 being "no pain" and 10 being the "worst pain imaginable". Depression in FM patients was assessed on the day of the scan; 18 patients received the Hospital Anxiety and Depression scale (HADS) (Zigmond and Snaith, 1983), and 12 patients received the Center for Epidemiological Studies-Depression Scale (CESD-D) (Radloff, 1977). Depression scores were converted to Z-scores in order to combine measures. Each participant completed a resting state fMRI scan and ^{1}H-MRS sequence. Scanning was performed for all subjects on a 3.0 T General Electric (Milwaukee, WI) system with an eight-channel head coil. The MRI scanner at the University of Michigan was upgraded to a new 3.0 T GE system with identical scanning parameters during one of the studies reported on here, so data from 3 FM participants was acquired on the new scanner. Group differences in graph theoretical measures did not change when excluding these participants (data not shown).

Each participant completed a 6-minute resting state fMRI scan as described previously (Harris *et al.*, 2013; Napadow *et al.*, 2010; 2012). Data was collected using a spiral in-out gradient echo T2*-weighted blood oxygenation-level dependent pulse sequence with the following parameters: TR 2000ms/TE 30ms, 180 volumes, 43 AC-PC aligned slices, voxel size 3.13 x 3.13 x 4.0 mm. The first 6 volumes were discarded in order to avoid equilibration effects. A high-resolution structural image was collected for registration purposes (spoiled gradient echo pulse sequence: TR 14/TE 5.5/TI 300ms, 20° flip angle, 124 contiguous axial slices, voxel size 1

x 1 x 1.5mm). Cardiac and respiratory data were collected simultaneously using an infrared pulse oximeter (GE) attached to the right middle finger and a respiration belt placed around the participant's ribcage.

All data were checked for artifacts and motion greater than 2mm or 1° rotation in any direction. No participants were excluded for these reasons. Resting state data were preprocessed using FSL (http://www.fmrib.ox.ac.uk/fsl) and SPM8 (http://www.fil.ion.ucl.ac.uk/spm/software) running on MATLAB R2014a (http://www.mathworks.co.uk/products/matlab/). Physiological correction was done using the RETROICOR (Glover *et al.*, 2000) algorithm in FSL. All other preprocessing steps were done in SPM8 and included slicetiming, motion correction, co-registration of the structural and functional images, normalization to Montreal Neurological Institute (MNI) space and smoothing with an 8mm FWHM Gaussian Kernel. Preprocessed data were entered into the Conn Toolbox (Whitfield-Gabrieli and Nieto-Castanon, 2012), and a nuisance regression using the CompCor method (Behzadi *et al.*, 2007) was performed with six subject-specific realignment parameters, the signal from white matter and CSF, and their first order derivatives included as confounds. Finally, a temporal filter of 0.008 – 0.09 Hz was applied to focus on low-frequency fluctuations (Fox *et al.*, 2005).

During ^{1}H-MRS, the spectroscopic voxel was placed in the right posterior insula as described previously (Figure A.1A; Harris *et al.*, 2008; 2009). Single-voxel point resolved spectroscopy spectra were acquired while participants were at rest with the following parameters: TR 3000ms/TE 30ms, 90-degree flip angle, number of excitations 8, number of averages 128, with a voxel size of 2 x 2 x 3 cm. Shimming was optimized using auto-prescan and the CHEmical Shift Selective (CHESS) water suppression routine was used. Spectra were analyzed

offline with LCModel (Stephan Provencher, Oakville, Ontario, Canada) (Provencher, 1993). Raw spectra were fit with a linear combination of pure metabolite spectra using LCModel (the basis set, which was simulated by Stephan Provencher of LCModel, included the following metabolites: Ala, Asp, Cr, PCr, GABA, Glc, Gln, Glu, GPC, PCh, Ins, Lac, NAA, NAAG, Scyllo, Tau). See Figure A.1B for a representative spectrum. Glutamate + glutamine (Glx) values were calculated as concentrations rescaled using the water peak. Concentrations were corrected for CSF in each participant using Voxel Based Morphometry (VBM) within SPM8 as previously described (Harris *et al.*, 2009). To rule out the possibility of tissue volume biases in the ^{1}H-MRS results, we analyzed the segmented gray/white matter and CSF content of the spectroscopic voxel and found that it was not significantly different between groups (Tables A.1 and A.2). Spectra were excluded if the Cramer-Rao bounds exceeded 20% or if the FWHM was greater than 0.12. One FM participant with poor quality spectra was excluded from analysis.

Graph theoretical analyses. The analysis flow is depicted in Figure 2.1. We defined the brain network using a set of 264 non-overlapping nodes based on resting state and task functional connectivity meta-analyses (Cohen *et al.*, 2008; Jonathan D Power, 2011). This set of nodes has been shown to produce reliable network topologies (Cole *et al.*, 2013; Dosenbach *et al.*, 2007; Jonathan D Power, 2011; Spreng *et al.*, 2013; Vatansever *et al.*, 2015). The 264 nodes were entered into the Conn Toolbox as 10 mm diameter spheres (Jonathan D Power, 2011). We created Fisher z-transformed bivariate correlation (Pearson's r) matrices (264 x 264) for each participant. Matrices were thresholded, over a range of relative thresholds (5 - 40% density, in steps of 5%), to create binary undirected graphs. We calculated the following graph theoretical measures to assess global network properties: global efficiency, Louvain modularity Q score, clustering coefficient, characteristic path length and the rich club coefficient. We also calculated

the nodal measures of degree, betweenness centrality, participation coefficient and eigenvector centrality. See (Rubinov and Sporns, 2010) or (Fornito *et al.*, 2016) for a detailed description and mathematical formulations of these measures. All graph theoretical measures were calculated using the Brain Connectivity Toolbox (Rubinov and Sporns, 2010). To reduce the number of comparisons, for each metric and each node, we averaged across thresholds as previously published (Achard *et al.*, 2012; Lynall *et al.*, 2010).

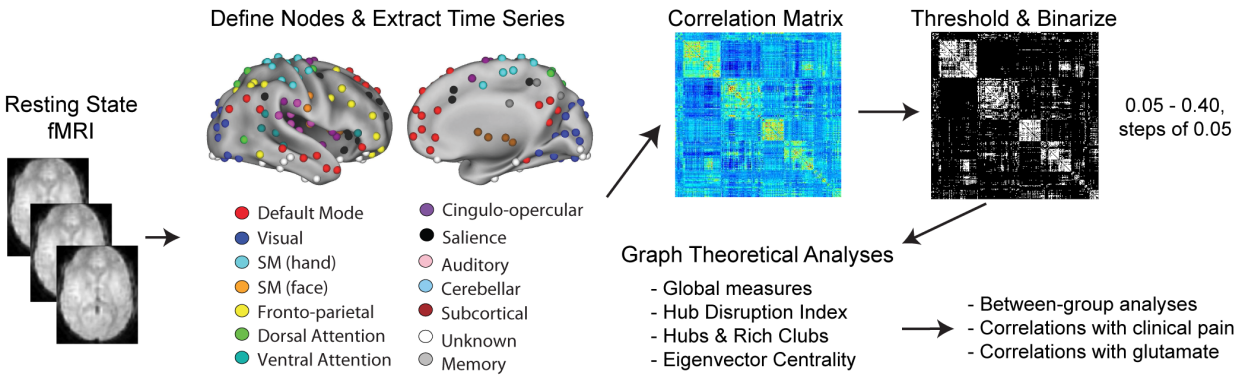

Figure 2.1. Summary of Graph Theoretical Methods. Resting state fMRI data was collected for 40 FM patients and 27 HC. 264 nodes were defined using the Power atlas (Jonathan D Power, 2011) which reliably segregate into large scale resting state networks. Pairwise (Fisher Z-transformed Pearson) correlation matrices were created for each participant, which were thresholded and binarized across a range of network densities. Graph theoretical measures were calculated and between-group differences were assessed using non-parametric permutation testing. Post-hoc correlations between hub measures and clinical pain and glutamate were also performed.

Hub Disruption Index. The hub disruption index (κ) was calculated as previously described (Achard *et al.*, 2012). Briefly, for each graph theory hub measure analyzed here (degree, betweenness, participation coefficient), we plotted the mean value of each node in the HC group versus the difference between an individual participant and the HC group for each corresponding node. The κ is defined as the slope of a line fitted to these data. Between group differences in κ were examined using non-parametric permutation testing (Achard *et al.*, 2012; Fornito *et al.*, 2016; Nichols and Holmes, 2002) under the null hypothesis that FM and HCs do not differ with respect to hub disruption. We randomly reassigned participants to one of two groups and

calculated a two-sample t-statistic. We repeated this procedure 10,000 times to form a randomized null distribution for each metric. We rejected the null hypothesis if the actual t-statistic was greater than or equal to the 95th percentile of the null distribution. Significance was set at $p < 0.05$.

Identification of Hubs. We assigned hub status to a node if the degree or betweenness centrality was greater than one standard deviation above the group mean (Sporns *et al.*, 2007; van den Heuvel and Sporns, 2011). We further distinguished between provincial hubs (hubs that have connections mainly within one module) and connector hubs (hubs that have connections between many modules). Hubs with a participation coefficient less than 0.5 were classified as provincial hubs, and hubs with a participation coefficient greater than 0.5 were defined as connector hubs (van den Heuvel and Sporns, 2011). Analyses of between group differences on nodal measures were restricted to hub regions. As outlined above, we performed non-parametric permutation testing on hub degree, betweenness centrality and participation coefficient to identify the specific hub differences between FM and HCs. Significance was set at $p < 0.05$.

Rich Club Organization. We assessed rich-club organization in the average FM and HC brain networks by computing the rich-club coefficients ϕ (k) over a range of degree (k), as previously described (van den Heuvel and Sporns, 2011). Briefly, the degree of each node was calculated for the FM and HC networks and all nodes that had a degree $\leq$ k were ignored. For the remaining nodes in the network, we calculated the rich-club coefficient ϕ (k) as the number of connections between the remaining nodes divided by the total number of possible connections. Random networks can also have an increasing function of ϕ (k) by chance alone; hence the ϕ (k) is typically normalized by a set of random networks. We created 1000 random networks with similar degree distribution and density, and for each level of k, calculated the average rich-club

coefficient ϕ_{random}. We determined statistical significance of ϕ (k) at each level of k with permutation testing (Fornito *et al.*, 2016; van den Heuvel and Sporns, 2011). Using the random networks created above, we obtained a null distribution of ϕ_{random} (k) values. P-values were estimated as the proportion of ϕ_{random} (k) that exceeded the observed ϕ (k) for FM and HC separately. This was repeated over all levels of k and a Bonferroni correction (0.05/28) was applied so that $p < 0.001$ was deemed significant at 5% density. The range of k in which ϕ (k) is significantly different from ϕ_{random} (k), and where the ϕ_{norm} (k) is greater than one, is the rich-club regime. Differences between FM and HC in ϕ (k) at each level of k were tested in SPSS 24 (Armonk, New York) using independent samples t-tests. To assess how rich club membership varied with clinical pain, we separated the FM group into age-matched tertiles (high n=12, medium n=16, low n=12) based on the VAS clinical pain rating. Differences in ϕ (k) between the tertiles were examined using a 1-way analysis of variance (ANOVA). A Bonferroni correction was applied (0.05/28) and significance set at $p < 0.001$. For visualization purposes, rich club nodes were displayed at k = 22, the highest level of k that was significantly different from random networks for the FM and HC groups, and also corresponded to nodes with a degree greater than one standard deviation above the group mean.

Examining the relationship between hub status, clinical pain and Glx. For correlations between hub measures and clinical pain and Glx, we performed Pearson correlations in SPSS. To test for differences in clinical variables and Glx between the FM tertiles, we performed 1-way ANOVAs in SPSS. All analyses controlled for age and significance was set at $p < 0.05$. To test the hypothesis that higher levels of posterior insular Glx influence clinical pain indirectly through greater eigenvector centrality in the insula, we conducted mediation analyses using MPLUS v. 8. Posterior insula Glx was used as the independent variable, and clinical pain on the

VAS was used as the dependent variable. Eigenvector centrality values from two nodes overlapping the ^{1}H-MRS voxel for the posterior insula (nodes 43 and 67) were standardized and averaged, and this value was used as the mediating variable. Indirect effects were evaluated by constructing 95% bias-corrected bootstrapped confidence intervals using 20,000 resamples. All models controlled for participant age.

Visualization. The visualization of 264 nodes on a brain surface was created in Caret (Dickson *et al.*, 2001; Van Essen *et al.*, 2005). All other brain surfaces were created using BrainNet viewer (Xia *et al.*, 2013).

Results

Clinical Characteristics

There was no significant difference in age between FM and HC participants (mean ± SD HC: 36.2 ± 12.4, FM: 39.0 ± 11.0, $t = 0.97$, $p = 0.34$). Other patient characteristics and a list of current medications in the FM patients are listed in Tables A.3 and A.4, respectively.

Fibromyalgia and Control Participants had Similar Global Network Properties

Our initial aim was to characterize the global brain network properties of FM patients and controls. At every density of functional connections tested (5 - 40%), FM and HC networks had small-world organization, defined as high clustering (local connectivity) and a low average path length between nodes. As these measures did not differ significantly between groups, we averaged all graph theory metrics across densities to reduce the number of comparisons when performing permutation testing to assess group differences (Achard *et al.*, 2012; Lynall *et al.*, 2010). There were no significant differences between groups in the clustering coefficient, average path length, modularity or global efficiency of the reconstructed brain network (all $p > 0.4$, Table A.5).

Differences in Hub Status Between Fibromyalgia Patients and Controls

The hub status of a node can be assessed by measuring the number of connections a node has (degree), the number of shortest paths in a network that pass through the given node (betweenness centrality), or the amount of connectivity to diverse functional systems (participation coefficient) (Sporns *et al.*, 2007). For degree, betweenness centrality, and participation coefficient, we calculated the hub disruption index (κ) (Achard *et al.*, 2012) to investigate brain regions with increased or decreased hub status in FM. A negative κ value indicates that hub nodes in HC are reduced in FM, and non-hubs in HC are classified as hubs in FM. The κ was significantly more negative in the FM group for degree (κ_D mean ± SD, HC: 0.00 ± 0.24, FM: -0.16 ± 0.28, t = 2.50, p = 0.015, Figure 2.2A), betweenness centrality (κ_{BC} mean ± SD, HC: 0.00 ± 0.27, FM: -0.16 ± 0.21, t = 2.58, p = 0.012, Figure 2.2B) and participation coefficient (κ_{PC} mean ± SD, HC: 0.00 ± 0.38, FM: -0.36 ± 0.47, t = 3.48, p = 0.00008, Figure 2.2C).

To determine exactly which hubs were altered, we assigned hub status to nodes whose degree or betweenness centrality was greater than one standard deviation above the mean, for each group separately (Figure 2.3A). See Tables A.6 and A.7 for a list of hub brain regions. FM patients had higher degree in the right mid insula, bilateral anterior insula, bilateral superior temporal gyrus (STG), left precuneus, right inferior temporal gyrus, and the right inferior parietal lobule. HCs had higher degree in left primary somatosensory cortex (S1), left middle temporal gyrus and five nodes in the visual cortex (Figure 2.3B). Results for betweenness centrality were similar (Figure 2.3C) and all differences are listed in Table 2.1.

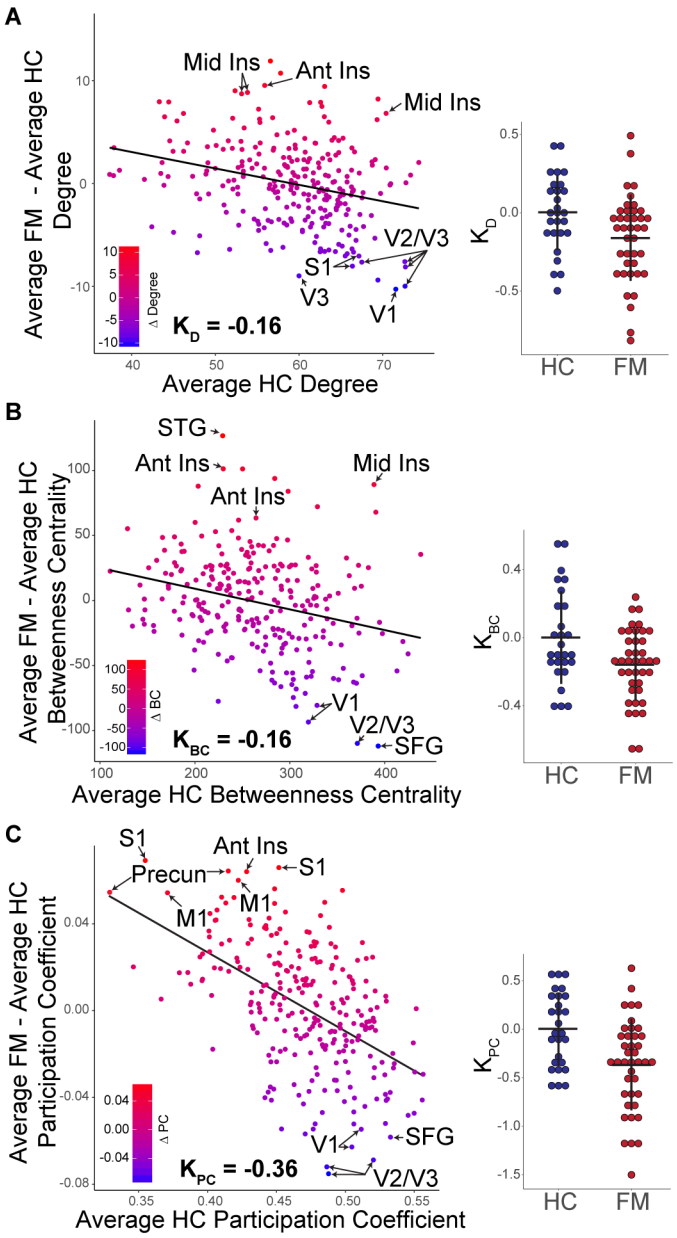

Figure 2.2. Large scale hub reorganization in FM. The hub disruption index (κ) measured by (A) degree (κ_D), (B) betweenness centrality (κ_{BC}) and (C) participation coefficient (κ_{PC}) is plotted as the mean value of each node in HC (x axis) versus the difference between FM and HC for each corresponding node (y axis). A negative slope (κ) indicates that hubs in HC are decreased in FM and non-hubs in HC have increased hubness in FM. Boxplots showing each participants κ value are plotted for each measure. Across all measures, the anterior insula has shown an increase in hub strength in FM patients, while the visual cortex hub strength has decreased. FM, fibromyalgia; HC, healthy control; M1, primary motor cortex; S1, primary somatosensory cortex; STG, superior temporal gyrus, Ant Ins, anterior insula; Mid Ins, mid insula; Precun, precuneus; V1, primary visual cortex; V2, secondary visual cortex; V3, visual association cortex; SFG, superior frontal gyrus

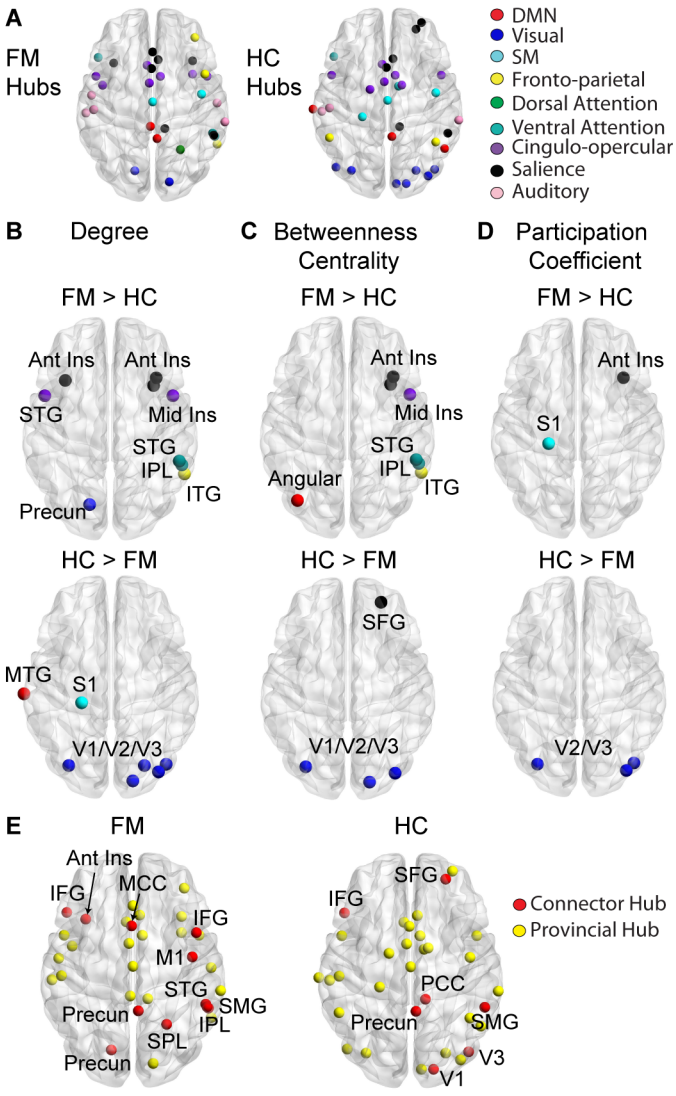

Figure 2.3. Altered hub topology in FM. Hubs were defined for each group separately as greater than one standard deviation above the mean group degree or betweenness centrality. All FM and HC hubs, as defined by degree, are depicted in (A). Between group differences in hub regions were assessed using non-parametric permutation testing for (B) degree, (C) betweenness centrality, and (D) participation coefficient. The anterior insula consistently had significantly stronger hub status in FM patients across all measures. Hubs can be further classified based on the level of inter- versus intra-modular connectivity. Connector hubs have connections to many different functional systems, while provincial hubs have connections mainly within the same system. Connector and provincial hubs and are depicted for FM and HC in (E). The anterior insula is also a connector hub in FM. FM, fibromyalgia; HC, healthy control; S1, primary somatosensory cortex; SMA, supplementary motor area; SMG, supramarginal gyrus; V1, primary visual cortex; V2, secondary visual cortex; V3, visual association cortex; PCC, posterior cingulate; Precun, precuneus; SPL, superior parietal lobule; IPL, inferior parietal lobule; STG, superior temporal gyrus; IFG, inferior frontal gyrus; MCC, mid cingulate cortex; SFG, superior frontal gyrus; ITG, inferior temporal gyrus; Ant Ins, anterior insula; Mid Ins, mid insula

Table 2.1: Differences in hub strength between FM patients and HCs

	Brain Region (Node #)	HC (mean ± SD)	FM (mean ± SD)	t	p-value
Degree					
FM > HC	R mid insula (56)	70.40 ± 14.02	77.22 ± 13.83	-1.96	0.05
	L STG (58)	69.44 ± 12.81	77.64 ± 14.69	-2.42	0.02
	L precuneus (166)	61.27 ± 16.74	69.13 ± 14.89	-1.96	0.05
	R ITG (179)	56.58 ± 10.10	68.48 ± 14.64	-3.94	0.001
	L anterior insula (208)	62.58 ± 15.21	70.46 ± 15.52	-2.06	0.04
	R anterior insula (209)	62.73 ± 14.87	70.22 ± 12.30	-2.16	0.03
	R anterior insula (211)	55.90 ± 17.62	65.43 ± 14.80	-2.31	0.02
	R IPL (235)	63.06 ± 13.59	72.48 ± 13.06	-2.83	0.006
	R STG (240)	57.80 ± 14.08	68.51 ± 14.50	-3.02	0.004
HC > FM	L S1 (23)	67.16 ± 13.54	60.11 ± 14.53	2.03	0.04
	L MTG (83)	69.42 ± 14.79	60.04 ± 12.99	2.67	0.009
	R V1 (141)	71.56 ± 16.58	61.30 ± 13.52	2.67	0.009
	R V3 (153)	72.71 ± 13.05	64.61 ± 12.85	2.51	0.01
	R V2 (165)	72.64 ± 10.79	65.05 ± 11.82	2.72	0.008
	R V3 (169)	67.50 ± 11.42	59.86 ± 15.82	2.29	0.02
	L V2/V3 (172)	72.67 ± 15.71	62.69 ± 15.67	2.55	0.01
Betweenness Centrality					
FM > HC	R mid insula (56)	388.72 ± 161.53	477.85 ± 151.78	-2.27	0.03
	L angular (87)	250.20 ± 85.32	351.37 ± 141.23	-3.65	0.001
	R ITG (179)	284.10 ± 136.62	377.93 ± 182.49	-2.40	0.02
	R anterior insula (209)	264.38 ± 106.18	327.81 ± 139.77	-2.11	0.04
	R anterior insula (211)	229.85 ± 113.63	331.08 ± 161.44	-3.01	0.003
	R IPL (235)	298.21 ± 140.01	382.18 ± 163.62	-2.25	0.03
	R STG (240)	229.25 ± 97.51	356.00 ± 158.52	-4.05	0.001
HC > FM	R V1 (141)	328.67 ± 177.66	248.07 ± 127.56	2.03	0.04
	R V3 (169)	316.24 ± 116.45	244.84 ± 98.52	2.62	0.01
	L V2/V3 (172)	371.17 ± 177.75	261.35 ± 153.61	2.62	0.01
	R SFG (219)	393.14 ± 171.72	281.26 ± 129.02	2.88	0.005

Table 2.1. Differences in hub strength between FM patients and HCs. FM, fibromyalgia; HC, healthy control; SD, standard deviation; R, right; L, left; STG, superior temporal gyrus; ITG, inferior temporal gyrus; IPL, inferior parietal lobule; S1, primary somatosensory cortex; MTG, mid temporal gyrus; V1, primary visual cortex; V2, secondary visual cortex; V3, visual association cortex; SFG, superior frontal gyrus

Fibromyalgia Participants Exhibit Altered Connector and Provincial Hubs

Hubs can be further delineated into provincial or connector hubs based on whether the connections are mainly to nodes within the same system, or module, or between nodes in different modules (Sporns *et al.*, 2007). In FM patients, the right anterior insula had a significantly higher participation coefficient relative to HC ($t = -2.14$, $p = 0.035$) and met criteria for a connector hub (Figure 2.3D-E). The mid cingulate and primary motor cortex (M1) were

also connector hubs in FM, while these regions were provincial hubs in HC. In HC, nodes in V1, V3 and the SFG were classified as connector hubs. HCs had significantly higher participation coefficients in bilateral V2/V3 (right $t = 2.83$, $p = 0.006$, $t = 2.766$, $p = 0.007$, left $t = 2.57$, $p = 0.013$). In both groups, the precuneus, inferior frontal gyrus and supramarginal gyrus were classified as connector hubs and the mid insula, supplementary motor area (SMA) and S1 were provincial hubs, although FM patients had significantly higher participation coefficients in left S1 ($t = -2.20$, $p = 0.031$).

Altered Rich Club Membership in Fibromyalgia

Next, we examined higher order rich club classification in patients and controls. The rich club curves for the group averaged networks at 5% density are displayed in Figure 2.4A. Both FM and HC brain networks had a rich club organization, which differed from random networks, but the rich club coefficients were not significantly different between groups. In FM, the rich-club regime (defined as $\phi(k)$ significantly different from $\phi_{random}(k)$, and $\phi_{norm}(k) > 1$) was between $k = 4$ to $k = 6$ and $k = 8$ to $k = 22$. In HC, the rich-club regime was over a range of $k = 2$ to $k = 22$. The illustrated rich club regions for FM and HC ($k = 22$; the highest level of k that was significantly different from random networks for both groups, which also corresponds to nodes with a degree greater than one standard deviation above the group mean) are depicted in Figure 2.4B & C. While there was no significant difference in the level of rich club organization between FM and HCs, the hubs that constituted the rich club were different between groups. Most importantly, the bilateral anterior insulae were members of the rich club in FM patients but not controls. Results were similar for most other network densities tested, and are illustrated in Figure A.2.

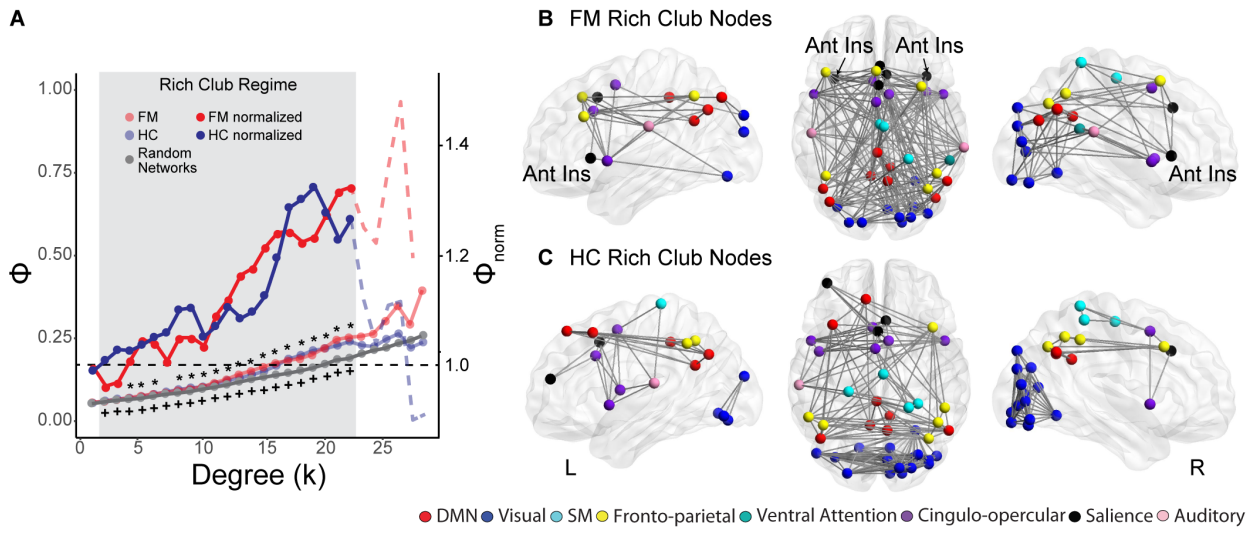

Figure 2.4. Rich Club Membership is altered in FM. (A) Both FM and HC have significant rich club organization compared to random networks. The rich club regime (compared to random networks) for FM was between k = 4 and k = 6 and k = 8 and k = 22, and for HC was between k = 2 and k = 22. There was no significant difference in the rich club coefficient (ϕ) between FM and HC at any k level. Normalized rich club curves are also depicted which show an increasing ϕ_{norm} over a range of k for both groups. However, rich club membership was different between groups. FM and HC rich club nodes are depicted in (B) and (C), respectively, for k = 22, the highest significant k level. The FM rich club includes the bilateral anterior insula, whereas the HC rich club contains more nodes in the visual cortex. The data depicted are from 5% network density; results are similar for other thresholds (See Supplementary Fig. 1). FM, fibromyalgia; HC, healthy control; Ant Ins, anterior insula

Rich Club Membership is Associated with Clinical Pain

To determine if rich club membership was related to clinical pain, we divided the FM group into age-matched tertiles based on the level of clinical pain on the day of the scan (Figure 2.5). As expected, the tertiles had significantly different pain ratings (VAS mean ± SD, high: 7.0 ± 1.2, medium: 5.1 ± 1.5, low: 2.5 ± 1.6, $F_{(2,37)} = 29.02$, $p < 10^{-8}$). There were no significant differences between the tertiles in age ($F_{(2,37)} = 0.55$, $p = 0.58$) or depression ($F_{(2,37)} = 1.07$, $p = 0.35$). The rich club coefficient, ϕ (k), was not significantly different between the tertiles for any level of k; however, the hubs comprising the rich club in each tertile were markedly different. The rich club nodes in the high pain group were predominantly in S1/M1, STG, and the anterior and posterior insula. The medium pain group rich club included fewer S1/M1 regions and the anterior insula, with a general shift towards more posterior and default mode network (DMN) regions. Finally, the rich club in the low pain group appeared more similar to HC and primarily

contained nodes in the frontoparietal, DMN and visual networks. Results were similar across all other thresholds tested and are illustrated in Figure A.3.

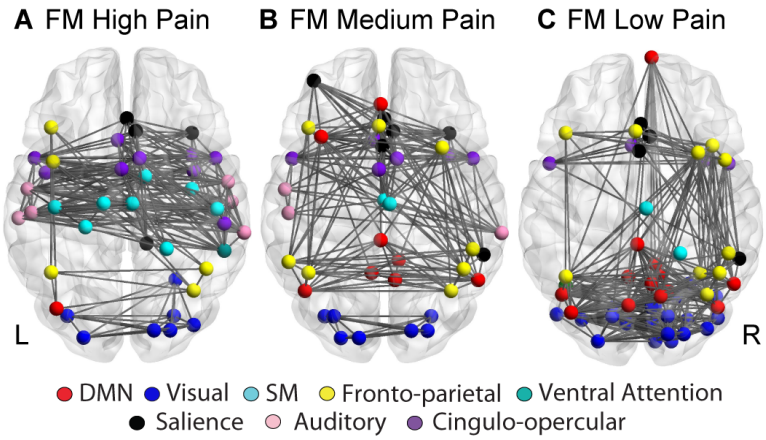

Figure 2.5. Rich club membership varies with clinical pain. The high pain FM group (A) had rich club nodes primarily in bilateral S1, M1, SMA and the right posterior insula. The rich club in the medium pain FM group (B) contained fewer S1/M1 nodes and more nodes in the default mode network. In the low pain group (C), there was a shift in rich club membership to posterior default mode and visual regions. The data depicted are from 5% network density; results are consistent across thresholds (See Supplementary Fig. 2). FM, fibromyalgia; M1, primary motor cortex; S1, primary somatosensory cortex; SMA, supplementary motor area

Differences in eigenvector centrality between FM and HC, and the relationship to clinical pain and rich club membership

To investigate the nature or quality of edges made in the reconstructed brain network, we calculated the eigenvector centrality of each node. The eigenvector centrality accounts for the quantity and quality of connections by taking into account the degree of a node and the degree of that node's neighbors. FM patients, compared to HC, had higher eigenvector centrality in the left anterior insula ($t = -2.38$, $p = 0.02$), bilateral STG (right $t = -1.99$, $p = 0.049$, left $t = -2.34$, $p = 0.022$), right inferior parietal lobule ($t = -2.22$, $p = 0.03$), left precuneus ($t = -2.29$, $p = 0.025$), and right inferior temporal gyrus ($t = -3.01$, $p = 0.003$). HCs had higher eigenvector centrality in the left middle temporal gyrus ($t = 2.39$, $p = 0.019$), right V1 ($t = 1.99$, $p = 0.049$), and right V3

(t = 2.15, p = 0.035). The left anterior insula and STG were members of the rich club in FM, while the right V1 and V3 belonged to the rich club in HC.

We then correlated the eigenvector centrality with the level of clinical pain in FM patients. The eigenvector centrality of 14 nodes in bilateral S1/M1, three nodes in the bilateral STG, two nodes in the right posterior insula, and one node each in the right SMA and right supramarginal gyrus positively correlated with clinical pain (all $r > 0.3$, $p < 0.05$, Figure 2.6 and Table A.8). Five of these nodes (three in bilateral M1, one in the supramarginal gyrus, and one in the right posterior insula) belonged to the rich club only in the high pain FM tertile.

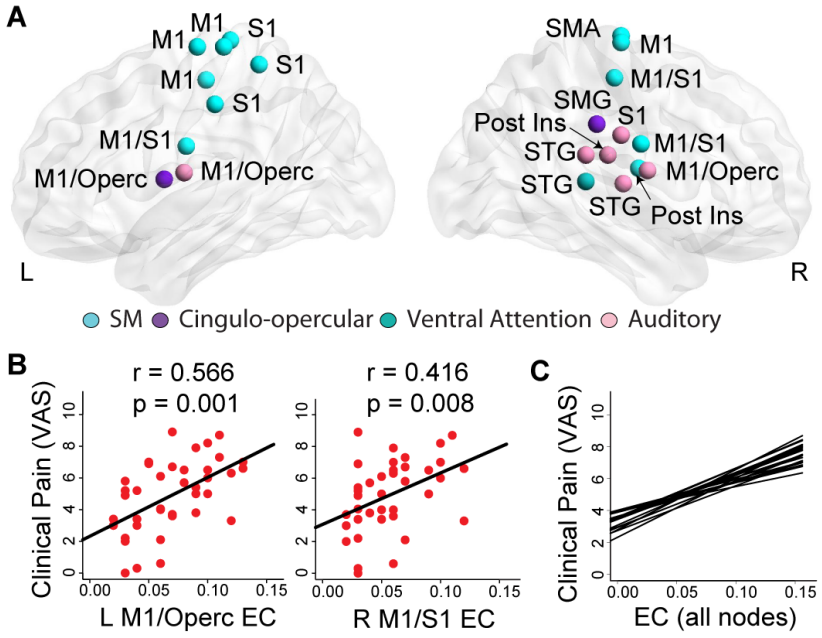

Figure 2.6. Correlations with clinical pain in FM. (A) Within FM patients, there were positive correlations between clinical pain and eigenvector centrality (a measure of how connected a brain region is to other highly connected regions) in 14 bilateral S1/M1 nodes, three nodes in right STG, two nodes in the right posterior insula, and one node each in the right SMA, and right SMG. Representative correlations are shown in (B) for left M1/operculum and right M1/S1 and regression lines for all 21 correlations are depicted in (C). FM, fibromyalgia; M1, primary motor cortex; S1, primary somatosensory cortex; STG, superior temporal gyrus; SMA, supplementary motor area; SMG, supramarginal gyrus; VAS, visual analog scale.

Graph Theory Metrics Mediate the Relationship between Glutamate within the Posterior Insula and Clinical Pain Intensity.

As the right posterior insula was a member of the rich club in FM patients with the highest levels of clinical pain, we sought to examine the relationship between hub strength, clinical pain and Glx. Right posterior insula Glx (CSF corrected values) was significantly different between the FM pain tertiles and HC ($F_{(3,62)}$ = 4.37, p = 0.007). Specifically, the high pain group had significantly higher Glx in the right posterior insula compared to the low pain group (mean ± SD high: 12.76 ± 1.13, low: 11.20 ± 1.42, p = 0.013) and compared to HC (mean ± SD HC: 10.97, p = 0.001).

Two nodes overlapped with the ^{1}H-MRS voxel in the right posterior insula (Figure 2.7A). The standardized and averaged eigenvector centrality of these two posterior insula nodes positively correlated with clinical pain (r = 0.419, p = 0.008, Figure 2.7B) and Glx (r = 0.320, p = 0.05; Figure 2.7B). In mediation analyses, higher posterior insula Glx was associated with greater clinical pain indirectly through increased averaged posterior insula eigenvector centrality (B = .132; 95% CI= .016, .399). The direct effect of insula Glx on clinical pain was also significant (B= .387, p = .026). The R^2 value for clinical pain in this model was .422. See Figure 2.7C for standardized estimates and confidence intervals of each path in the model.

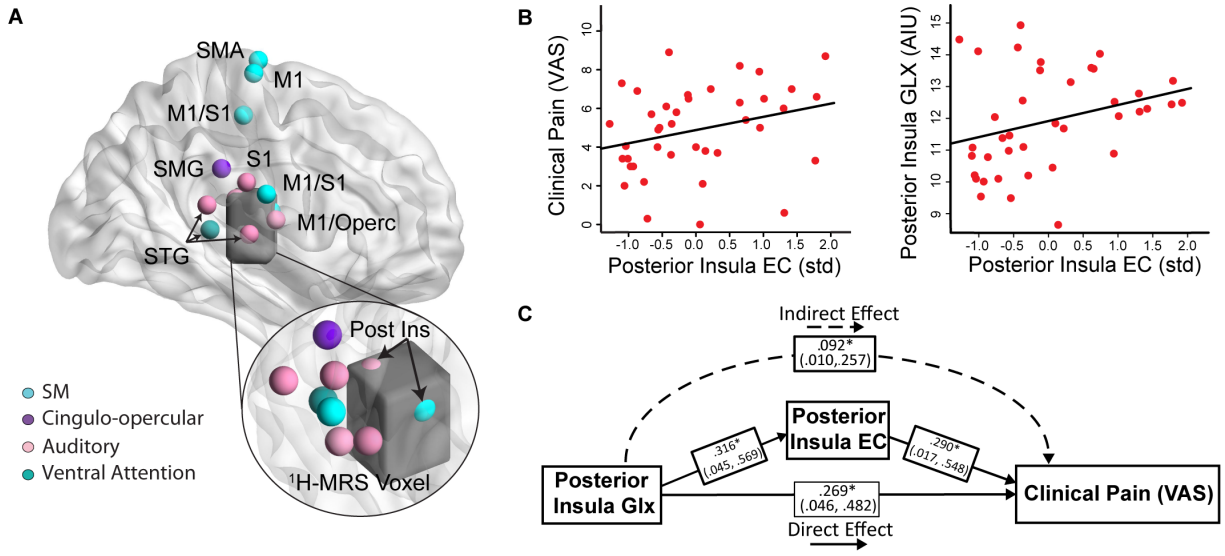

Figure 2.7. The relationship between clinical pain, eigenvector centrality and posterior insula Glx. (A) Glutamate + glutamine (Glx) was measured in the right posterior insula using ^{1}H-MRS (voxel shown in dark gray). The overlap between the ^{1}H-MRS voxel and 2 nodes from the Power's atlas is shown in the inset. (B) In FM, clinical pain and posterior insula Glx positively correlated with the averaged, standardized eigenvector centrality in these 2 posterior insula nodes. (C) In a mediation analysis, posterior insula eigenvector centrality significantly mediated the relationship between Glx in the posterior insula and clinical pain. Standardized values are shown for ease of interpretation. FM, fibromyalgia; Glx, glutamate + glutamine; SM, sensorimotor network; EC, eigenvector centrality; H-MRS, proton magnetic resonance spectroscopy; AIU, arbitrary institutional units

Discussion

In this study we have shown that hubs, the brain regions that create efficiency and route information across networks, are altered in FM patients. Brain regions that were hubs in FM, such as the anterior insula and STG, were non-hubs with low degree or centrality in HCs. Conversely, hubs in HCs, such as the visual cortex and SFG, were non-hubs in FM patients. We also found a reorganization of nodes with high between-network connectivity. In FM, nodes in the anterior insula, S1 and M1 had the greatest increase in participation coefficient relative to the HC group. In HCs, the nodes with the highest participation coefficient were again in the visual cortex and cuneus. The anterior insulae were consistently ranked as hubs in the FM group and were significantly different from HCs on multiple measures, indicating that the anterior insulae had more connections, were more central to information flow, and were more connected to other

nodes with high degree and nodes outside its own module. We also examined a higher-order hub structure (the rich club) and found that rich club membership was altered in FM and varied with the level of clinical pain. Finally, this study demonstrates, for the first time to our knowledge, a neurochemical correlate of altered hub topology and its relationship to the perception of pain. Taken together, these data suggest that, within the chronic pain network, the brain regions most crucial for information processing and integration are located in regions such as the insulae that are known to be pro-nociceptive.

Physical and biological systems share an optimal pattern of network organization that is characterized by high clustering, short average path length, hierarchical modularity, scale-free degree distribution and highly interconnected hub nodes, which together form a rich club. In the case of the brain, this optimal topology is consistently disrupted in disease states. However, there is little consensus within each disorder as to the specific nature of this network disruption (Stam, 2014). From all the organizational principles listed above, one consistent finding has been abnormalities in hub topology, which have been reported for a range of neurological disorders, including schizophrenia (Crossley *et al.*, 2016; Lynall *et al.*, 2010; Rubinov and Bullmore, 2013; van den Heuvel *et al.*, 2013), Huntington's disease (Harrington *et al.*, 2015), Alzheimer's disease (Buckner *et al.*, 2009; Dai *et al.*, 2015) and depression (Wu *et al.*, 2016) (see (Crossley *et al.*, 2014) for recent meta-analysis).

Previous studies have examined network connectivity and topology in other chronic pain conditions. A study of chronic back pain patients found increased functional connectivity between hubs in the DMN and the insula relative to HCs (Tagliazucchi *et al.*, 2010). Similarly, increased cross-network communication between the DMN and the salience network was found in patients with chronic pain due to ankylosing spondylitis, which also correlated with the level

of clinical pain (Hemington *et al.*, 2015). The most comprehensive analysis to date found altered whole-brain degree rank order in three different chronic pain populations relative to HCs (Mansour *et al.*, 2017). Additionally, the level of disruption correlated with the level of clinical pain. However, this study did not examine hubs specifically. Instead, it assessed the modular structure of the network and the variability in community membership. The insula was a member of the sensorimotor network in the majority of HCs; however, allegiance in chronic pain conditions was split between the sensorimotor, default mode and subcortical networks. Our finding of increased hub strength and inter-network communication in the anterior insula in FM relative to HCs is consistent with these studies.

A key attribute of brain networks is the existence of a rich club organization, in which high degree hubs form a densely interconnected core. The rich club may also serve to integrate information from different modules in the brain since rich club hubs are often distributed across the brain and include many different resting state networks (van den Heuvel and Sporns, 2011). In the current study, we found both FM and HC networks possessed, by global assessment, a similar level of rich club organization. However, the specific membership of the rich club varied between groups - the visual network was dominant in HCs, while a more distributed organization was present in FM that included the bilateral anterior insulae. The rich club visual nodes in HCs formed a stand-alone network, which is consistent with previous studies showing a low level of integration in the functional rich club of healthy adults (Grayson *et al.*, 2014). It is interesting to note that in FM, the visual nodes were integrated into the rest of the rich club. Balenzuela and colleagues reported a disruption in the community membership in chronic back pain patients such that the insula was abnormally integrated into the auditory system and dorsal visual stream (Balenzuela *et al.*, 2010). Given our previous findings of visual hypersensitivity and increased

insular activation during an unpleasant visual stimulus in FM (Harte *et al.*, 2016), it is possible that altered rich club membership and integration contributes to the phenomenon of multi-modal sensory sensitivity observed in many chronic pain patients.

In an analysis of functional hubs in migraine, the insula, S1, M1 and the orbitofrontal cortex were the most strongly interconnected regions and members of the rich club in patients with the longest disease duration compared to HCs (Liu *et al.*, 2015). This is consistent with our findings but this previous study did not examine the relationship of rich club membership and clinical pain. Within our FM patients, rich club membership varied as a function of clinical pain. In general, the distribution of rich club nodes shifted from the default mode, frontoparietal and visual networks in the low pain FM group, to the sensorimotor, cingulo-opercular and salience networks in the high pain FM group. Patients with the highest levels of clinical pain had rich club nodes mainly in S1, M1, SMA, STG, operculum, anterior and posterior insula. The high pain rich club had just one DMN node and seven nodes in the visual network, while the low pain group had 13 DMN and 20 visual network regions. Overall, the low pain rich club resembled HCs more closely than the high pain rich club. This suggests that the intensity of chronic pain is related to, and perhaps determined by, rich club membership.

Although the posterior insula did not meet hub criteria in the FM group, the connectivity of this structure with other highly connected nodes (as measured with eigenvector centrality) was positively correlated with the level of ongoing clinical pain. The right posterior insula was a member of the rich club only in the high pain FM tertile. We previously showed that posterior insula Glx is elevated in FM patients relative to HCs (Harris *et al.*, 2009). Here we found that posterior insula Glx was significantly higher in the high pain tertile compared to the low pain FM group. Importantly, we demonstrated that eigenvector centrality of nodes, within the posterior

insula region showing elevated Glx, mediates the relationship between this neurotransmitter and clinical pain. Thus, altered neurochemistry in an individual hub could alter functional network properties that result in the experience of pain. This is consistent with recent preclinical studies in rodents demonstrating a causal influence of excitatory-inhibitory balance in the insula on pain (Harte *et al.*, 2017; Watson, 2016).

Why might hubs be preferentially affected in chronic pain? Stam hypothesized that since hubs are damaged or reorganized in many different neurological disorders, there must be a general mechanism that makes hub brain regions more vulnerable (Stam, 2014). Briefly, he suggests that, in the acute phase, traffic to a failing node is rerouted to existing hub regions, which become overloaded. This would be observed as an increase in the degree or centrality of hubs relative to healthy networks. In the chronic phase, new hubs appear to avoid or compensate for hub overload. This would be reflected as a decrease in the degree or centrality of "healthy" hubs and the appearance of new hubs.

In the chronic pain patients studied here, we demonstrated an appearance of new hubs (anterior insula, STG) and a disappearance of "healthy" hubs (visual cortex, SFG). This may be due to a barrage of nociceptive input, although this is unlikely given the lack of convincing evidence of peripheral pathology in FM (Clauw, 2014). It is more likely that the reorganization of hubs stems from an underlying alteration in excitatory neurotransmission in pro-nociceptive brain regions (Watson, 2016). The mediation analyses described here were consistent with a model in which higher levels of Glx in the posterior insula increase the eigenvector centrality of posterior insular nodes and, consequently, clinical pain. Longitudinal analyses will be required to determine if these effects are in fact causal in chronic pain patients.

Our study has limitations. First, a general methodological limitation of graph theoretical analyses is the arbitrary thresholding and binarization process, which leads to the loss of information, specifically, anticorrelations. However, binary networks, such as those used here, retain the most significant correlations and may be less sensitive to noise and therefore easier to interpret (Rubinov and Sporns, 2010). We examined a relatively small number of female participants with FM, so it remains unknown if our findings are generalizable to males or other chronic pain conditions. Additionally, many of the FM patients studied here were taking medications to manage their symptoms and it is unclear how these treatments may be impacting our results. Future studies are necessary to replicate our findings in larger sample sizes using fully weighted networks.

In conclusion, we demonstrated altered hub topology in FM patients, and showed that disruptions in the excitatory tone within the insula altered the strength of this region as a hub and was associated with the intensity of clinical pain. Although cross-sectional in nature, these data suggest the possibility that disruption and reallocation of rich club hub membership plays a causal role in the symptomatology of a common chronic pain condition.

Acknowledgements

We thank Drs. UnCheol Lee and Hyoungkyu Kim for insightful discussions. This work was supported in part by NIH grant R01 AT007550 to RE Harris; a grant from Cerephex Corporation (Los Altos, California) to DJ Clauw, GM Mashour and RE Harris; a grant from Pfizer Inc (Groton, Connecticut) to RE Harris; a pilot grant from the Functional MRI Laboratory of the University of Michigan (PF U034199); and a grant from Forest Laboratories (MD-SAV-09) to DJ Clauw.

References

Achard S, Delon-Martin C, Vértes PE, Renard F, Schenck M, Schneider F, et al. Hubs of brain functional networks are radically reorganized in comatose patients. Proc. Natl. Acad. Sci. U.S.A. 2012; 109: 20608–20613.

Balenzuela P, Chernomoretz A, Fraiman D, Cifre I, Sitges C, Montoya P, et al. Modular Organization of Brain Resting State Networks in Chronic Back Pain Patients. Frontiers in Neuroinformatics 2010; 4

Behzadi Y, Restom K, Liau J, Liu TT. A component based noise correction method (CompCor) for BOLD and perfusion based fMRI. NeuroImage 2007; 37: 90–101.

Buckner RL, Sepulcre J, Talukdar T. Cortical hubs revealed by intrinsic functional connectivity: mapping, assessment of stability, and relation to Alzheimer's disease. Journal of … 2009

Clauw DJ. Fibromyalgia: a clinical review. 2014. p. 1547–1555.

Cohen AL, Fair DA, Dosenbach NUF, Miezin FM, Dierker D, Van Essen DC, et al. Defining functional areas in individual human brains using resting functional connectivity MRI. NeuroImage 2008; 41: 45–57.

Cole MW, Reynolds JR, Power JD, Repovs G, Anticevic A, Braver TS. Multi-task connectivity reveals flexible hubs for adaptive task control. Nature Neuroscience 2013

Colizza V, Flammini A, Serrano MA, Vespignani A. Detecting rich-club ordering in complex networks. Nat Phys 2006; 2: 110–115.

Crossley NA, Mechelli A, Ginestet C, Rubinov M, Bullmore ET, McGuire P. Altered Hub Functioning and Compensatory Activations in the Connectome: A Meta-Analysis of Functional Neuroimaging Studies in Schizophrenia. Schizophr Bull 2016; 42: 434–442.

Crossley NA, Mechelli A, Scott J, Carletti F, Fox PT, McGuire P, et al. The hubs of the human connectome are generally implicated in the anatomy of brain disorders. Brain 2014; 137: 2382–2395.

Dai Z, Yan C, Li K, Wang Z, Wang J, Cao M, et al. Identifying and Mapping Connectivity Patterns of Brain Network Hubs in Alzheimer's Disease. Cerebral Cortex 2015; 25: 3723–3742.

Dickson J, Drury H, Van Essen DC. 'The surface management system' (SuMS) database: a surface-based database to aid cortical surface reconstruction, visualization and analysis. Philos. Trans. R. Soc. Lond., B, Biol. Sci. 2001; 356: 1277–1292.

Dosenbach NUF, Fair DA, Miezin FM, Cohen AL, Wenger KK, Dosenbach RAT, et al. Distinct brain networks for adaptive and stable task control in humans. Proc. Natl. Acad. Sci. U.S.A. 2007; 104: 11073–11078.

Farmer MA, Baliki MN, Apkarian AV. A dynamic network perspective of chronic pain.

Neuroscience Letters 2012; 520: 197–203.

Foerster BR, Petrou M, Edden RAE, Sundgren PC, Schmidt-Wilcke T, Lowe SE, et al. Reduced insular γ-aminobutyric acid in fibromyalgia. Arthritis Rheum 2012; 64: 579–583.

Fornito A, Zalesky A, Bullmore E. Fundamentals of Brain Network Analysis - Alex Fornito, Andrew Zalesky, Edward Bullmore - Google Books. 2016.

Fox MD, Snyder AZ, Vincent JL, Corbetta M, Van Essen DC, Raichle ME. The human brain is intrinsically organized into dynamic, anticorrelated functional networks. Proc. Natl. Acad. Sci. U.S.A. 2005; 102: 9673–9678.

Geisser ME, Glass JM, Rajcevska LD, Clauw DJ, Williams DA, Kileny PR, et al. A psychophysical study of auditory and pressure sensitivity in patients with fibromyalgia and healthy controls. The Journal of Pain 2008; 9: 417–422.

Glover GH, Li TQ, Ress D. Image-based method for retrospective correction of physiological motion effects in fMRI: RETROICOR. Magn. Reson. Med. 2000; 44: 162–167.

Gorka Zamora-López CZJK. Cortical Hubs Form a Module for Multisensory Integration on Top of the Hierarchy of Cortical Networks. Frontiers in Neuroinformatics 2010; 4

Gracely RH, Petzke F, Wolf JM, Clauw DJ. Functional magnetic resonance imaging evidence of augmented pain processing in fibromyalgia. Arthritis Rheum 2002; 46: 1333–1343.

Grayson DS, Ray S, Carpenter S, Iyer S, Dias T. Structural and functional rich club organization of the brain in children and adults. PLoS ONE 2014

Harrington DL, Rubinov M, Durgerian S, Mourany L, Reece C, Koenig K, et al. Network topology and functional connectivity disturbances precede the onset of Huntington's disease. Brain 2015; 138: 2332–2346.

Harris RE, Napadow V, Huggins JP, Pauer L, Kim J, Hampson J, et al. Pregabalin rectifies aberrant brain chemistry, connectivity, and functional response in chronic pain patients. Anesthesiology 2013; 119: 1453–1464.

Harris RE, Sundgren PC, Craig AD, Kirshenbaum E, Sen A, Napadow V, et al. Elevated insular glutamate in fibromyalgia is associated with experimental pain. Arthritis Rheum 2009; 60: 3146–3152.

Harris RE, Sundgren PC, Pang Y, Hsu M, Petrou M, Kim S-H, et al. Dynamic levels of glutamate within the insula are associated with improvements in multiple pain domains in fibromyalgia. Arthritis Rheum 2008; 58: 903–907.

Harte SE, Clauw DJ, Hayes JM, Feldman EL. Reduced intraepidermal nerve fiber density after a sustained increase in insular glutamate: a proof-of-concept study examining the pathogenesis of small fiber …. PAIN 2017

Harte SE, Ichesco E, Hampson JP, Peltier SJ, Schmidt-Wilcke T, Clauw DJ, et al. Pharmacologic attenuation of cross-modal sensory augmentation within the chronic pain insula. PAIN 2016; 157: 1933–1945.

Hemington KS, Wu Q, Kucyi A, Inman RD, Davis KD. Abnormal cross-network functional connectivity in chronic pain and its association with clinical symptoms. Brain Struct Funct 2015

Ichesco E, Puiu T, Hampson JP, Kairys AE, Clauw DJ, Harte SE, et al. Altered fMRI resting-state connectivity in individuals with fibromyalgia on acute pain stimulation. European Journal of Pain 2016; 20: 1079–1089.

Ichesco E, Schmidt-Wilcke T, Bhavsar R, Clauw DJ, Peltier SJ, Kim J, et al. Altered resting state connectivity of the insular cortex in individuals with fibromyalgia. J Pain 2014; 15: 815–826.e1.

Jensen KB, Kosek E, Petzke F, Carville S, Fransson P, Marcus H, et al. Evidence of dysfunctional pain inhibition in Fibromyalgia reflected in rACC during provoked pain. PAIN 2009; 144: 95–100.

Kucyi A, Davis KD. The dynamic pain connectome. Trends Neurosci. 2015; 38: 86–95.

Liu J, Zhao L, Lei F, Zhang Y, Yuan K, Gong Q, et al. Disrupted resting-state functional connectivity and its changing trend in migraine suffers. Hum Brain Mapp 2015; 36: 1892–1907.

Liu J, Zhao L, Li G, Xiong S, Nan J, Li J, et al. Hierarchical Alteration of Brain Structural and Functional Networks in Female Migraine Sufferers. PLoS ONE 2012; 7: e51250.

López-Solà M, Pujol J, Wager TD, Garcia-Fontanals A, Blanco-Hinojo L, Garcia-Blanco S, et al. Altered functional magnetic resonance imaging responses to nonpainful sensory stimulation in fibromyalgia patients. Arthritis Rheumatol 2014; 66: 3200–3209.

López-Solà M, Woo C-W, Pujol J, Deus J, Harrison BJ, Monfort J, et al. Towards a neurophysiological signature for fibromyalgia. PAIN 2016

Lynall M-E, Bassett DS, Kerwin R, McKenna PJ, Kitzbichler M, Muller U, et al. Functional connectivity and brain networks in schizophrenia. Journal of Neuroscience 2010; 30: 9477–9487.

Mansour A, Baria AT, Tetreault P, Vachon-Presseau E, Chang P-C, Huang L, et al. Global disruption of degree rank order: Ahallmark of chronic pain. Sci Rep 2017: 1–18.

Martenson ME, Halawa OI, Tonsfeldt KJ, Maxwell CA, Hammack N, Mist SD, et al. A possible neural mechanism for photosensitivity in chronic pain. PAIN 2016; 157: 868–878.

Moon J-Y, Kim J, Ko T-W, Kim M, Iturria-Medina Y, Choi J-H, et al. Structure Shapes Dynamics and Directionality in Diverse Brain Networks: Mathematical Principles and Empirical Confirmation in Three Species. Sci Rep 2017; 7: 46606.

Moon J-Y, Lee U, Blain-Moraes S, Mashour GA. General relationship of global topology, local dynamics, and directionality in large-scale brain networks. PLoS Comp Biol 2015; 11:

e1004225.

Napadow V, Kim J, Clauw DJ, Harris RE. Brief Report: Decreased intrinsic brain connectivity is associated with reduced clinical pain in fibromyalgia. Arthritis Rheum 2012; 64: 2398–2403.

Napadow V, LaCount L, Park K, As-Sanie S, Clauw DJ, Harris RE. Intrinsic brain connectivity in fibromyalgia is associated with chronic pain intensity. Arthritis Rheum 2010; 62: 2545–2555.

Nichols TE, Holmes AP. Nonparametric permutation tests for functional neuroimaging: a primer with examples. Hum Brain Mapp 2002; 15: 1–25.

Petzke F, Clauw DJ, Ambrose K, Khine A, Gracely RH. Increased pain sensitivity in fibromyalgia: effects of stimulus type and mode of presentation. PAIN 2003

Power JD, Cohen AL, Nelson SM, et al. Functional network organization of the human brain. Neuron 2011; 72(4):665-678.

Provencher SW. Estimation of metabolite concentrations from localized in vivo proton NMR spectra. Magn. Reson. Med. 1993; 30: 672–679.

Puiu T, Kairys AE, Pauer L, Schmidt-Wilcke T, Ichesco E, Hampson JP, et al. Association of Alterations in Gray Matter Volume With Reduced Evoked-Pain Connectivity Following Short-Term Administration of Pregabalin in Patients With Fibromyalgia. Arthritis Rheumatol 2016; 68: 1511–1521.

Radloff LS. The CES-D scale: A self-report depression scale for research in the general population. Applied psychological measurement 1977

Rubinov M, Bullmore E. Schizophrenia and abnormal brain network hubs. Dialogues Clin Neurosci 2013; 15: 339–349.

Rubinov M, Sporns O. Complex network measures of brain connectivity: Uses and interpretations. NeuroImage 2010

Schmidt-Wilcke T, Ichesco E, Hampson JP, Kairys A, Peltier S, Harte S, et al. Resting state connectivity correlates with drug and placebo response in fibromyalgia patients. Neuroimage Clin 2014; 6: 252–261.

Sluka KA, Clauw DJ. Neurobiology of fibromyalgia and chronic widespread pain. Neuroscience 2016

Sporns O, Honey CJ, Kötter R. PLOS ONE: Identification and Classification of Hubs in Brain Networks. PLoS ONE 2007

Sporns O, Zwi JD. The small world of the cerebral cortex. Neuroinformatics 2004; 2: 145–162.

Spreng RN, Sepulcre J, Turner GR, Stevens WD, Schacter DL. Intrinsic architecture underlying the relations among the default, dorsal attention, and frontoparietal control networks of the

human brain. J Cogn Neurosci 2013; 25: 74–86.

Stam CJ. Modern network science of neurological disorders. Nat Rev Neurosci 2014; 15: 683–695.

Tagliazucchi E, Balenzuela P, Fraiman D, Chialvo DR. Brain resting state is disrupted in chronic back pain patients. Neuroscience Letters 2010; 485: 26–31.

van den Heuvel MP, Kahn RS, Goñi J, Sporns O. High-cost, high-capacity backbone for global brain communication. Proc. Natl. Acad. Sci. U.S.A. 2012; 109: 11372–11377.

van den Heuvel MP, Sporns O, Collin G, Scheewe T, Mandl RCW, Cahn W, et al. Abnormal rich club organization and functional brain dynamics in schizophrenia. JAMA Psychiatry 2013; 70: 783–792.

van den Heuvel MP, Sporns O. Rich-club organization of the human connectome. Journal of Neuroscience 2011; 31: 15775–15786.

van den Heuvel MP, Sporns O. Network hubs in the human brain. Trends Cogn. Sci. (Regul. Ed.) 2013; 17: 683–696.

Van Essen DC, Harwell J, Hanlon D, Dickson J. Surface-based atlases and a database of cortical structure and function. …) Databasing the Brain: From Data to …; 2005.

Vatansever D, Menon DK, Manktelow AE, Sahakian BJ, Stamatakis EA. Default Mode Dynamics for Global Functional Integration. Journal of Neuroscience 2015; 35: 15254–15262.

Watson CJ. Insular balance of glutamatergic and GABAergic signaling modulates pain processing. PAIN 2016; 157: 2194–2207.

Whitfield-Gabrieli S, Nieto-Castanon A. Conn: A Functional Connectivity Toolbox for Correlated and Anticorrelated Brain Networks. Brain Connectivity 2012; 2: 125–141.

Wilbarger JL, Cook DB. Multisensory hypersensitivity in women with fibromyalgia: implications for well being and intervention. Arch Phys Med Rehabil 2011; 92: 653–656.

Wu H, Sun H, Xu J, Wu Y, Wang C, Xiao J, et al. Changed Hub and Corresponding Functional Connectivity of Subgenual Anterior Cingulate Cortex in Major Depressive Disorder. Front Neuroanat 2016; 10: 120.

Xia M, Wang J, He Y. BrainNet Viewer: a network visualization tool for human brain connectomics. PLoS ONE 2013

Zigmond AS, Snaith RP. The hospital anxiety and depression scale. Acta psychiatrica scandinavica 1983

Chapter 3 : Changes in Resting State Functional Connectivity after Repetitive Transcranial Direct Current Stimulation Applied to Motor Cortex in Fibromyalgia Patients[1]

Introduction

Fibromyalgia (FM) is a chronic centralized pain condition characterized by widespread pain, fatigue, sleep problems, cognitive dysfunction, and mood disturbances (Wolfe et al., 1990). While the exact pathophysiology of FM remains unknown, a prevailing hypothesis states that a sensory processing dysfunction within the central nervous system creates, amplifies, or sustains the perception of chronic pain (Schmidt-Wilcke and Clauw, 2011). In support of this hypothesis, brain network alterations seen in these patients fall into two broad categories: decreased descending anti-nociceptive transmission, and/or enhanced pro-nociceptive processing (Jensen et al., 2009; Napadow et al., 2010; Jensen et al., 2012; Napadow et al., 2012).

Motor cortical dysfunction has been suggested in a number of chronic pain conditions, including FM. In general, the primary motor cortex (M1) shows increased cortical excitability at baseline and heightened responses to sensory stimuli, which may be suggestive of a reduction in inhibitory activity (Saavedra et al., 2014). Noninvasive brain stimulation has emerged as an attractive therapeutic option for chronic pain conditions given its ability to target specific cortical regions. Some studies report that transcranial direct current stimulation (tDCS) over M1 relieves

[1] This chapter was previously published in the journal *Arthritis Research & Therapy:* Cummiford, C. M., Nascimento, T. D., Foerster, B. R., Clauw, D. J., Zubieta, J. K., Harris, R. E., & DaSilva, A. F. (2016). Changes in resting state functional connectivity after repetitive transcranial direct current stimulation applied to motor cortex in fibromyalgia patients. *Arthritis Res Ther*, 1–12. http://doi.org/10.1186/s13075-016-0934-0

pain in FM (Fregni et al., 2006; Valle et al., 2009; Fagerlund et al., 2015). However, a recent review did not find a significant difference between sham and real M1 tDCS on short-term pain relief (O'Connell et al., 2014). The lack of effect may be due to significant heterogeneity between the studies (i.e., stimulation parameters, number of treatment sessions, type of chronic pain) included in the review. It is also possible that sham tDCS produces a significant placebo response. Consistent with previous work implicating the endogenous opioid system in placebo analgesia (Petrovic, 2002; Wager et al., 2007), we recently showed that sham tDCS caused the release of endogenous opioids in the PAG, precuneus and thalamus (DosSantos et al., 2014).

While placebo responses are clearly present in tDCS, the specific neurobiology underlying the analgesic effects of real tDCS are less clear. During and immediately after stimulation, tDCS may alter excitability by modulating resting membrane potential. Longer lasting effects may be due to changes in synaptic plasticity via mechanisms similar to long-term potentiation or depression (Dayan et al., 2013). M1 tDCS can alter the functional connectivity (FC) of regions under the stimulating electrode (Polanía et al., 2012a), as well as spatially distant but structurally connected regions, such as the thalamus (Polanía et al., 2012b) and DLPFC (Sehm et al., 2012; Lindenberg et al., 2013). Real tDCS also acts on the endogenous opioid system (DosSantos et al., 2014), similar to invasive motor cortex stimulation (Maarrawi et al., 2007; 2013). However, these studies were conducted in healthy participants and examined FC during or shortly after M1 tDCS. There have been no investigations of how M1 tDCS alters resting state FC in chronic pain patients treated repeatedly, as they might be in clinical practice.

We measured clinical pain and resting state FC in twelve FM patients at baseline, after five days of sham and after five days of real tDCS. We were interested in three questions: Does baseline connectivity predict clinical treatment response? Are there differences in FC after sham

and real tDCS? And do changes in FC relate to analgesia? We hypothesized that strong M1 – thalamus connectivity at baseline would predict a better clinical response, as shown in previous M1 stimulation studies (Goto et al., 2008; Ohn et al., 2012). In addition, since we found a trend towards decreased glutamate + glutamine (Glx) in the thalamus after real tDCS in these same patients (Foerster et al., 2014), and given the strong structural connectivity between M1 and the thalamus (Zhang et al., 2010), we hypothesized that real tDCS would decrease FC between the thalamus and brain regions involved in pain perception.

Patients and Methods

Patients. We recruited thirteen female patients with FM (age 27-64, mean ± SD: 47.6 ± 10.6 years) for this study. One patient dropped out after the baseline visit, the remaining twelve patients completed the entire protocol. All patients met the 1990 criteria of the American College of Rheumatology for FM (Wolfe et al., 1990), had symptoms for at least one year and reported pain on more than 50% of days. Inclusion criteria were: right-handed, a BMI of 36 or less and agreement to delay taking new medications or treatments for FM during the study. Exclusion criteria were: pregnant or breastfeeding, participation in other clinical trials, currently taking opiates, history of autoimmune or chronic inflammatory disease that causes pain, substance abuse or severe psychiatric illness, and contraindications with magnetic resonance imaging procedures. The University of Michigan Institutional Review Board approved this study and all subjects gave written informed consent. The effect of tDCS on brain metabolites in these same subjects is described in a previous report (Foerster et al., 2014).

Study Design. Our within-subjects crossover design had three phases: a baseline pain assessment and functional magnetic resonance imaging (fMRI) session #1, sham tDCS for five consecutive days followed by pain assessment and fMRI #2, and real tDCS for five consecutive

days followed by pain assessment and fMRI #3 (Figure B.1). Sham and real tDCS phases were separated by a 7-11 day washout period (mean = 9.9 days). We chose to perform real tDCS for five consecutive days because previous studies in FM patients have shown a meaningful reduction in clinical pain using this protocol (Fregni et al., 2006; Fagerlund et al., 2015). We did not use a randomized design in order to limit carry over from real to sham tDCS (Brunoni and Fregni, 2011). All participants were debriefed during a final follow-up visit. Patients were also offered a clinical referral for an outpatient clinic at our institution for continuation of care with regular therapy for their symptoms.

Clinical Pain Outcomes. Clinical pain intensity was assessed as an "average" experience for the week before each assessment using a visual analog scale (VAS), with 0 being "no pain" and 10 being the "worst possible pain". Clinical pain was also assessed using the short-form McGill Pain Questionnaire (Melzack, 1987) and affective state was measured using the Positive and Negative Affect Schedule (PANAS) (Watson et al., 1988). We are missing McGill baseline pain data for one patient, PANAS scores across all conditions for one patient and PANAS baseline only scores for two patients. Clinical results have been published previously (Foerster et al., 2014) and are reproduced in Table B.1. Differences in clinical variables across conditions were assessed with repeated measures ANOVA in SPSS v22. Significance was set at an alpha level of $p < 0.05$. The changes in clinical pain scores used in neuroimaging analyses were calculated by subtracting sham – baseline VAS and real – sham VAS.

tDCS Protocol. The tDCS protocol was performed as described previously (DaSilva et al., 2011). Briefly, for both sham and real tDCS sessions, the anode electrode was placed on the scalp over the left motor cortex and the cathode over the right supraorbital cortex. Positions were determined individually using the EEG 10/20 system, respectively C3 and FP2. Electrodes were

placed by the same operators (AFD and TDN) for all patients. Active stimulation consisted of 2 mA of current applied continuously for 20 minutes. During sham tDCS, the current was applied for 30 seconds at the beginning and end of the session. Patients were blinded to type (i.e. real vs. sham) of treatment they were receiving. This protocol is identical to that used in previous studies of M1 tDCS in FM patients (Fregni et al., 2006; Fagerlund et al., 2015).

Neuroimaging Methods. Resting state fMRI sessions were performed on a Philips Ingenia 3T system (Best, Netherlands) with a 15 channel receive head coil. Each scan lasted 10 minutes and parameters include: a T2*-weighted BOLD echo-planar imaging (EPI) sequence (TR=2000ms, TE=30ms, flip angle 77 degrees, 30 slices, voxel size = 3.44 x 3.33 x 4.00mm). Physiological data (cardiac and respiratory volume) were collected simultaneously. A high-resolution structural image was acquired for normalization purposes (TR/TE = 9.8/4.6 ms, flip angle 8 degrees, 151 slices, voxel size = 1 x 1 x 1 mm). fMRI data were checked for quality and head motion greater than 3 mm; no data were excluded. Resting state fMRI data was preprocessed using SPM8 (http://www.fil.ion.ucl.ac.uk/spm/software/spm8/) running on Matlab R2010a (Mathworks, Sherborn, MA, USA) and included physiological artifact correction, slice timing correction, realignment, coregistration, normalization to MNI space and smoothing (FWHM=8mm).

Seed-to-whole brain FC analyses were performed using the Conn Toolbox (Whitfield-Gabrieli and Nieto-Castanon, 2012). Seeds were chosen based on the following criteria: 1) location under stimulating anode (left precentral gyrus and left postcentral gyrus (M1/S1), WFU PickAtlas, http://www.nitrc.org/projects/wfu_pickatlas), 2) structural connectivity to left M1 and S1 (right pre and postcentral gyri, bilateral ventral lateral (VL) and ventral posterior lateral (VPL) thalamus, WFU PickAtlas), and 3) our previous tDCS studies (PAG (DosSantos et al., 2014)). The time-series for each seed region was extracted and white matter, cerebrospinal fluid

signal and realignment parameters were entered into the analysis as regressors of no interest. A band-pass filter (.008-.09 Hz) was applied to remove linear drift artifacts and high-frequency noise. First level analyses were performed by correlating the time series from each seed region with the rest of the voxels in the brain, creating seed-to-whole-brain Fisher-transformed correlation maps. These maps were imported into SPM8 for group level analyses.

For prediction analyses, we performed seed-to-whole brain regression analyses with baseline FC maps and change in clinical pain (real – baseline) as a regressor of interest. Main effects were calculated using repeated measures ANOVA design with baseline, sham and real tDCS FC maps. The contrasts of interest were baseline versus sham, and sham versus real tDCS. We also examined the change in FC across the entire study using the contrast baseline versus real tDCS. To examine correlations between changes in connectivity and changes in clinical pain, we first created difference images by subtracting first level connectivity maps for each subject (sham – baseline, real – sham, real – baseline). We then preformed a regression analysis with VAS change scores as a regressor of interest. All analyses controlled for differences in age. Results were thresholded at uncorrected $p<0.001$ on the voxel level and $p<0.05$ FWE correction for multiple comparisons at the cluster level with a cluster size of > 5 voxels. For a-priori regions that did not meet this stringent threshold, we performed small volume corrections (SVC) using the anatomically (WFU PickAtlas) defined ROIs used as seed regions or functionally defined ROIs from our previous findings in FM (Napadow et al., 2010). Significance for SVC was set at $p<0.05$ FWE at the cluster level with a cluster size of > 5 voxels. The Fisher-transformed correlation values were extracted using MarsBaR software (http://marsbar.sourceforge.net) and post-hoc analyses performed in SPSS v22.

Results

Clinical Pain Reduction with Sham and Real tDCS

As reported previously (Foerster et al., 2014), there was a trend towards improvement in VAS clinical pain during the sham period (mean difference ± SE, sham minus baseline: -1.042 ± 0.572; 95% CI: -0.218 to 2.301; p = 0.096), and there was no significant difference in pain relief between sham and real tDCS (mean difference ± SE, real minus sham: -0.750 ± 0.494; 95% CI: -1.838 to 0.338; p = 0.157). However, clinical pain significantly decreased across the entire study from baseline to after real tDCS (mean difference ± SE real minus baseline: -1.792 ± 0.762; 95% CI: -3.470 to -0.114; p = 0.038). There were no significant differences in clinical pain as measured by the McGill Pain questionnaire or PANAS positive affect. There was a significant difference between baseline and real tDCS in PANAS negative affect (mean difference ± SE real minus baseline: -3.0 ± 1.067; 95% CI: -5.461 to -0.539; p = 0.023). Clinical results for each patient individually across the study are presented in Table B.2.

Stronger Baseline FC is Associated with Subsequent Analgesia

To examine common predictive ability of baseline FC for reductions in pain across sham and real tDCS (as this was where the significant clinical effect on pain was found), we used pre-defined ROIs and correlated baseline FC with improvements in clinical pain across the entire study period (real – baseline). Patients who had stronger connectivity at baseline between the left M1 seed and left VL thalamus (p = 0.011 FWE, SVC), between the left S1 seed and left anterior insula (p = 0.001 FWE), and between the left VL thalamus seed and PAG (p = 0.007 FWE, SVC) had greater improvement in clinical pain scores across sham and real tDCS periods (Figure 3.1 and Table 3.1). Importantly, these correlations were also significant when looking at change in clinical pain from baseline to sham or from sham to real tDCS alone (with one

exception: left VL – PAG baseline FC and real – sham clinical pain, p = 0.057; Table B.3). There were no regions that showed significant correlations between less connectivity at baseline and better treatment response (Figure B.2). In post-hoc analyses, there were no significant correlations between baseline connectivity of these regions and the change McGill clinical pain or the change in positive and negative affect.

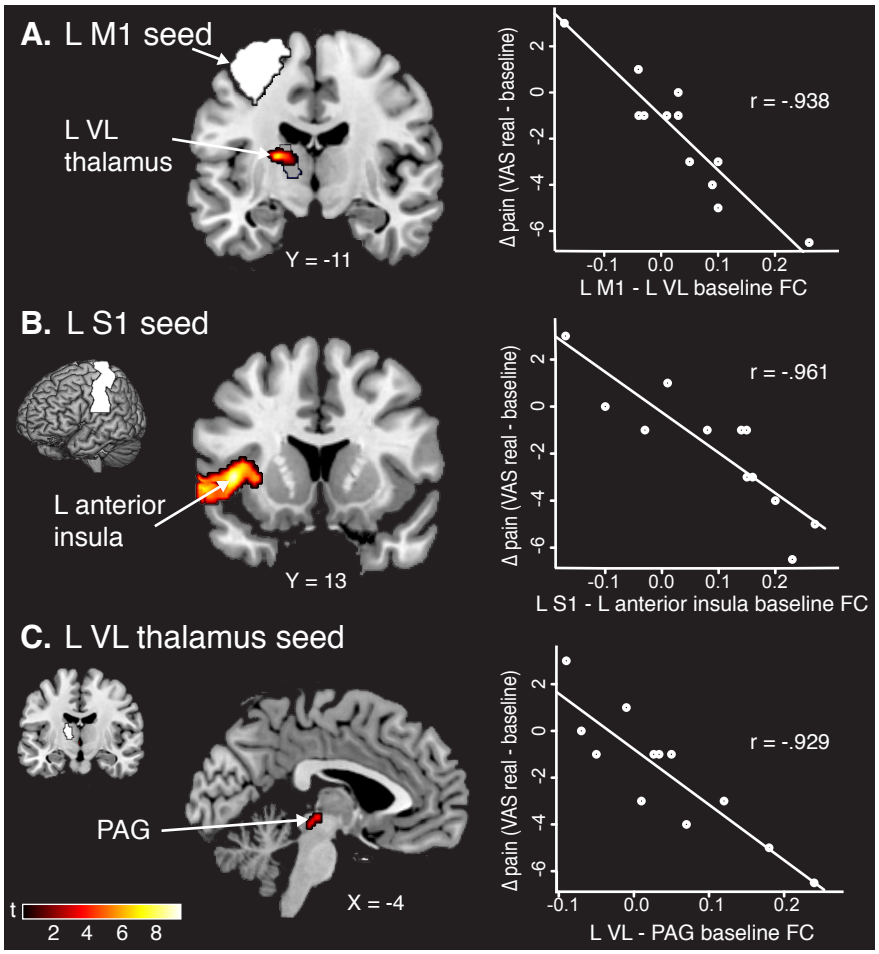

Figure 3.1. Stronger FC at baseline predicts analgesia. ***A,*** *Patients with higher L M1 (seed in white) – L VL (anatomical region outlined in black) connectivity at baseline had a greater reduction in clinical pain across sham and real tDCS periods (displayed at p = 0.005).* ***B,*** *Stronger L S1 (seed in white) – L anterior insula FC at baseline predicted a better clinical response.* ***C,*** *Connectivity between the L VL thalamus (seed in white) and the PAG at baseline also predicted patients that would respond to sham and real tDCS treatment. M1, primary motor cortex; VL, ventral lateral; S1, primary somatosensory cortex; PAG, periaqueductal gray; VAS, visual analog scale; L, left; R, right; FC, functional connectivity (fisher-transformed r-values).*

Table 3.1. Predicting changes in clinical pain from baseline FC

Seed FC Region	MNI coordinates (x y z)			r value	T	Cluster size	Cluster p-value
L M1							
L VL thalamus	-18	-14	12	-0.938	5.41	7	0.011 FWE*
L S1							
L anterior insula	-42	14	2	-0.961	9.38	396	0.001 FWE
L VL thalamus							
PAG	-6	-26	-8	-0.929	5.25	8	0.007 FWE*

Table 3.1. Predicting changes in clinical pain from baseline FC. FC, functional connectivity; L, left; M1, primary motor cortex; VL, ventral lateral; S1, primary somatosensory cortex; PAG, periaqueductal gray; MNI, Montreal Neurological Institute
** = Significant at $p < 0.05$ with small volume correction*

Sham tDCS is Associated with Decreases in FC

Since previous studies have shown a placebo analgesic response on experimental and clinical pain during sham tDCS (Vaseghi et al., 2014), we examined whether sham tDCS changed resting state FC (sham – baseline, Table 3.2). After five sessions of sham tDCS, FM patients had reduced FC between the left VPL thalamus seed and left S1 ($p = 0.016$ FWE), left amygdala/parahippocampal gyrus ($p = 0.004$ FWE) and right inferior parietal lobule (IPL, $p = 0.013$ FWE; Figure 3.2A). FC also decreased between the right VPL thalamus seed and left IPL ($p = 0.049$ FWE; Figure 3.2B), between the PAG seed and precuneus ($p = 0.001$ FWE; Figure 3.2C), and between the right M1 seed and right cerebellum ($p = 0.002$ FWE). There were no significant increases in FC after sham compared to baseline (Figure B.3).

Table 3.2. Main effect of sham tDCS on FC

Seed FC Region	MNI coordinates (x y z)			T	Cluster size	Cluster p-value
Baseline > Sham						
L VPL						
L S1	-62	-16	42	6.80	304	0.016 FWE
L parahipp/amyg	-32	-14	-26	6.70	408	0.004 FWE
R IPL	44	-36	32	5.69	320	0.013 FWE
R VPL						
L IPL	-34	-36	34	5.28	230	0.049 FWE
R M1 (precentral gyrus)						
R cerebellum	16	-74	-36	5.91	485	0.002 FWE
PAG						
precuneus	-20	-84	24	4.88	618	0.000 FWE
Baseline < Sham						
N.S.						

Table 3.2. Main effect of sham tDCS on FC. tDCS, transcranial direct current stimulation; FC, functional connectivity; L, left; R, right; VPL, ventral posterior lateral; S1, primary somatosensory cortex; parahipp/amyg, parrahippocampal gyrus & amygdala; IPL, inferior parietal lobule; M1, primary motor cortex; PAG, periaqueductal gray; N.S., not significant; MNI, Montreal Neurological Institute

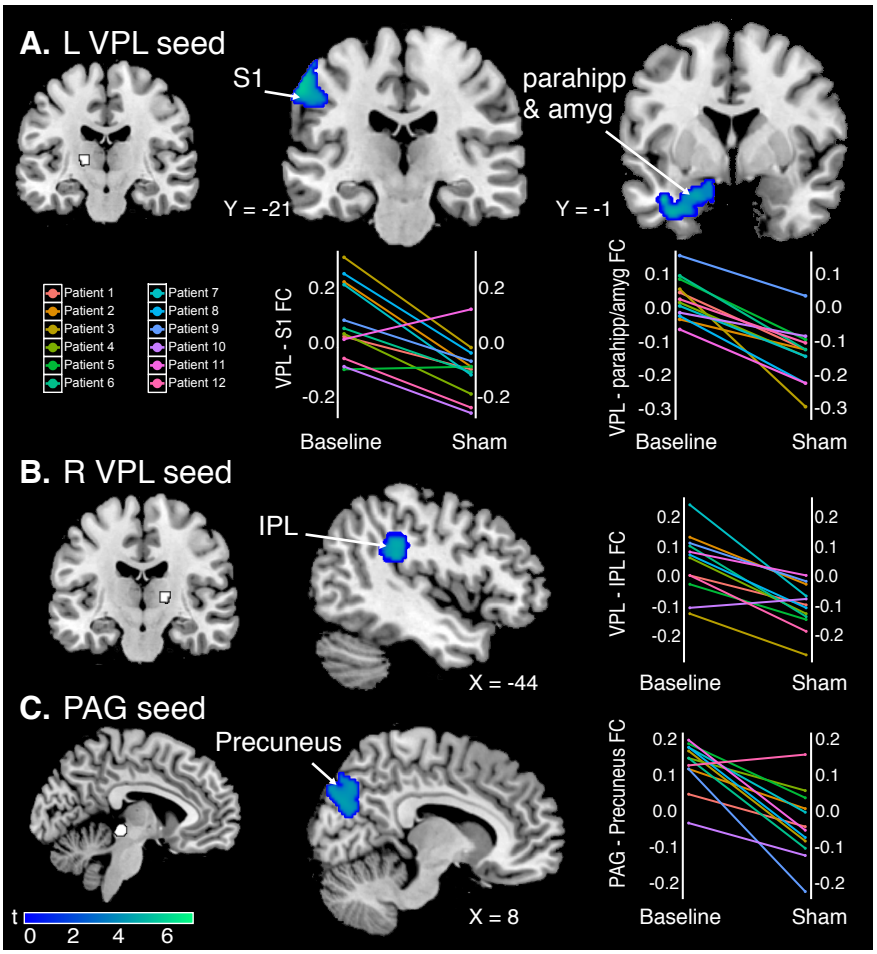

Figure 3.2. Sham tDCS decreases FC compared to baseline. ***A,*** *Decreased connectivity between the left VPL (seed in white) and left S1, left parahippocampal gryus and amygdala after sham tDCS compared to baseline. Plots show changes in FC from baseline to after the sham treatment period for each FM patient.* ***B,*** *Decreased connectivity between the right VPL (seed in white) and left IPL.* ***C,*** *Decreased connectivity between the PAG (seed in white) and precuneus. VPL, ventral posterior lateral; S1, primary somatosensory cortex; parahipp, parahippocampal gyrus; amyg, amygdala; IPL, inferior parietal lobule; PAG, periaqueductal gray; L, left; R, right; FC, functional connectivity (fisher transformed r-values).*

To determine if changes in FC related to changes in clinical pain during the sham period, we ran a regression analysis with each participants connectivity difference map (sham – baseline) with change in VAS (sham – baseline) as a regressor of interest (Table 3.3). The change in connectivity between the left VL thalamus seed and the left posterior insula was positively correlated with change in clinical pain (p = 0.001 FWE); patients with reduced connectivity between the left VL thalamus and posterior insula had a greater reduction in pain intensity after sham tDCS (Figure 3.3A). Reduced connectivity between the right VPL thalamus

seed and right M1 (p = 0.001 FWE), right S1 (p = 0.008 FWE) and left M1 (p = 0.046 FWE) also correlated with reduced pain after sham tDCS (Figure 3.3B). Decreased FC between the right S1 seed and the cerebellum (p = 0.001 FWE) was also positively correlated with change in pain. These changes in connectivity were not significantly correlated with changes in positive and negative affect or McGill clinical pain. There were no significant relationships between increases in connectivity and decreases in clinical pain (Figure B.4).

Table 3.3. Correlations between change in FC and change in clinical pain (VAS) for sham vs baseline

Seed FC Region	MNI coordinates (x y z)			r value	T	Cluster size	Cluster p-value
L VL thalamus							
L posterior insula	-48	-12	0	0.979	12.33	313	0.001 FWE
R VPL thalamus							
R M1	56	-12	42	0.969	9.85	603	0.000 FWE
R S1	44	-34	54	0.917	7.46	235	0.008 FWE
L M1	-46	-6	26	0.936	9.41	158	0.046 FWE
R S1 (postcentral gyrus)							
cerebellum	36	-52	-20	0.937	7.63	355	0.001 FWE

Table 3.3. Correlations between change in FC and change in clinical pain (VAS) for sham vs baseline. FC, functional connectivity; VAS, visual analog scale; L, left; R, right; VL, ventral lateral; VPL, ventral posterior lateral; M1, primary motor cortex; S1, primary somatosensory cortex; MNI, Montreal Neurological Institute

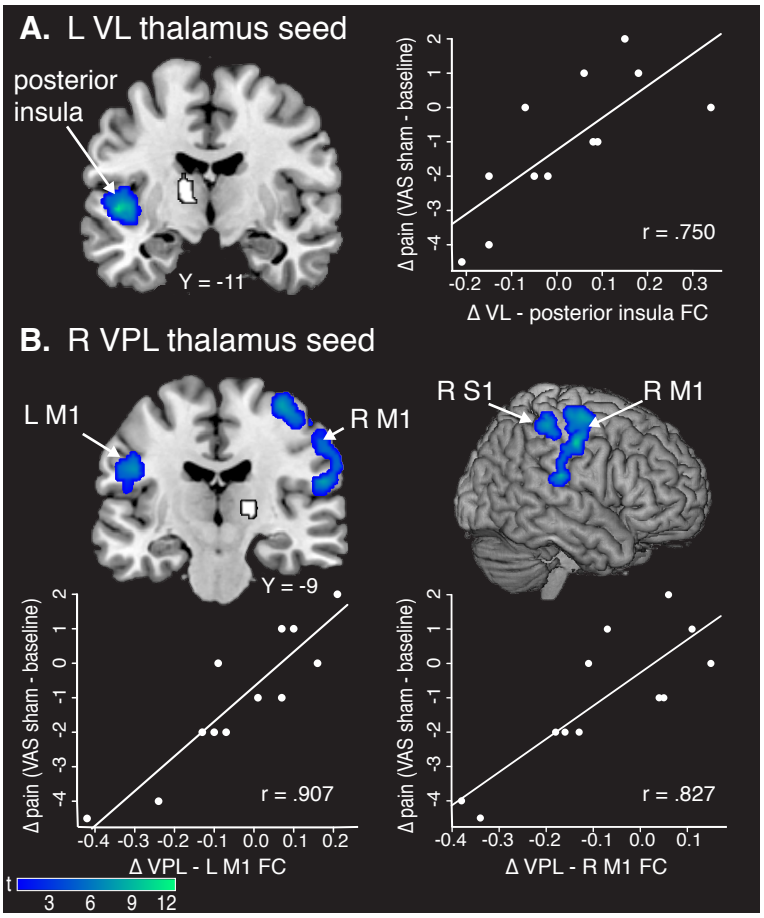

Figure 3.3. Correlations between changes in FC and changes in clinical pain after sham tDCS. ***A,*** *Decreased FC between the left VL thalamus (seed in white) and left posterior insula was correlated with a reduction in clinical pain after sham tDCS.* ***B,*** *Decreased FC between the right VPL thalamus (seed in white) and left M1, right M1, and right S1 correlated with reduced clinical pain after sham tDCS. VL, ventral lateral; VPL, ventral posterior lateral; M1, primary motor cortex; S1, primary somatosensory cortex; VAS, visual analog scale; L, left; R, right; FC, functional connectivity (fisher transformed r-values).*

Real tDCS is Also Associated with Decreases in FC

Next, we measured changes in FC between sham and real tDCS (Table 3.4). After real tDCS, FC decreased between the left VL thalamus seed and the medial prefrontal cortex (mPFC, p = 0.006 FWE) and left supplementary motor area (SMA, p = 0.043 FWE; Figure 3.4A). FC also decreased between the right VL thalamus seed and the cerebellum (p = 0.001 FWE) and left SMA (p = 0.016 FWE; Figure 3.4B). There were no significant increases in FC (Figure B.3).

Table 3.4. Main effect of real tDCS on FC

Seed FC Region	MNI coordinates (x y z)			T	Cluster size	Cluster p-value
Sham > Real						
L VL thalamus						
mPFC	4	56	8	5.66	362	0.006 FWE
L SMA	-2	24	56	5.49	228	0.043 FWE
L OFG	-10	40	-22	5.91	185	0.08 FWE**
R VL thalamus						
cerebellum	16	-46	-22	6.88	1122	0.000 FWE
L SMA	-6	22	58	6.16	313	0.016 FWE
Sham < Real						
N.S.						

*Table 3.4. Main effect of real tDCS on FC. tDCS, transcranial direct current stimulation; FC, functional connectivity; L, left; R, right; VL, ventral lateral; mPFC, medial prefrontal cortex; SMA, supplementary motor area; OFG, orbitofrontal gyrus; N.S., not significant; MNI, Montreal Neurological Institute; ** = Trend at p < 0.05 FWE correction for multiple comparisons*

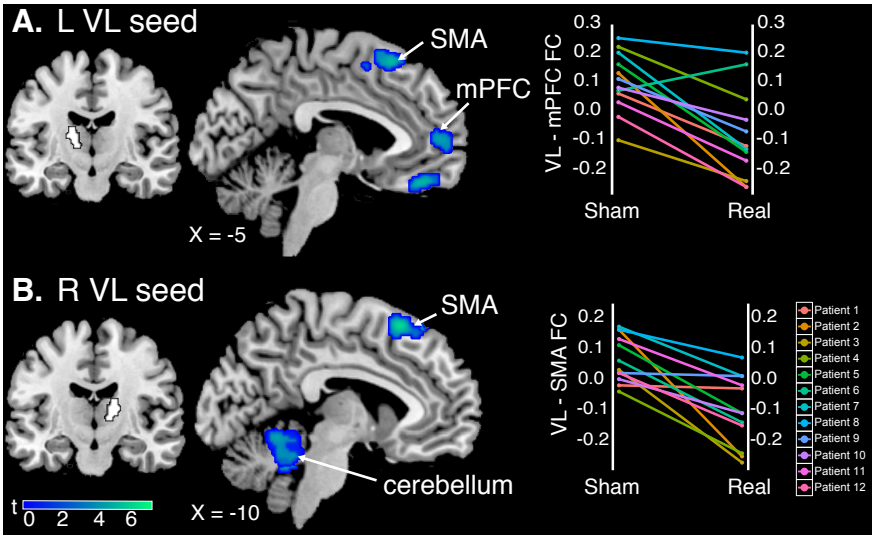

*Figure 3.4. Real tDCS decreases FC compared to sham. **A,** Decreased connectivity between the left VL (seed in white) and SMA and mPFC after real tDCS. Plots show changes in FC between sham and real tDCS for each FM patient. **B,** Decreased connectivity between the right VL (seed in white) and SMA and cerebellum after real tDCS. VL, ventral lateral; SMA, supplementary motor area; mPFC, medial prefrontal cortex; L, left; R, right; FC, functional connectivity (fisher transformed r-values).*

When comparing baseline to real tDCS, we found significant decreases in connectivity between the left VPL thalamus seed and the left IPL (p = 0.041 FWE) and between the PAG seed and the posterior cingulate (p = 0.007 FWE; Figure B.4 and Table B.4). There were no significant increases in FC.

We did not find any regions that met whole brain correction in a regression analysis measuring changes in connectivity in relation to changes in pain after real tDCS compared to sham, however there were regions that met significance using SVC with *a-priori* ROIs (Table 3.5). The change in connectivity between the left VPL thalamus and left M1/S1 ($p = 0.007$ FWE, SVC) and right posterior insula ($p = 0.007$ FWE, SVC) was positively correlated with the change in clinical pain (Figure 3.5). The change in left VL thalamus to right posterior insula connectivity was also positively correlated with change in pain ($p = 0.022$ FWE, SVC). Patients with reduced connectivity between the VL/VPL thalamus and M1/S1 and posterior insula had a greater reduction in pain intensity after real tDCS. In post-hoc analyses, these changes in connectivity were also correlated with the change in McGill clinical pain (Table B.6). However, there were no significant relationships between FC and changes in positive or negative affect. In an analysis examining changes in connectivity and changes in clinical pain from baseline to real tDCS, we found that patients with reduced connectivity between left S1 and left SMA had a greater reduction in clinical pain ($p = 0.013$ FWE, Figure B.5 and Table B.5). Again, there were no significant relationships between increases in connectivity and decreases in clinical pain either between sham and real tDCS or between baseline and real tDCS (Figure B.6).

Table 3.5. Correlations between change in FC and change in clinical pain (VAS) for real vs sham

Seed FC Region	MNI coordinates (x y z)			r value	T	Cluster size	Cluster p-value
L VL thalamus							
R posterior insula	42	-24	20	0.887	5.08	5	0.022 FWE*
L VPL thalamus							
L M1/S1	-48	-18	50	0.923	6.45	89	0.007 FWE*
R posterior insula	46	-30	24	0.927	7.64	23	0.007 FWE*

*Table 3.5. Correlations between change in FC and change in clinical pain (VAS) for real vs sham. FC, functional connectivity; VAS, visual analog scale; L, left; R, right; VL, ventral lateral; VPL, ventral posterior lateral; M1, primary motor cortex; S1, primary somatosensory cortex; MNI, Montreal Neurological Institute; * = Significant at $p < 0.05$ with small volume correction*

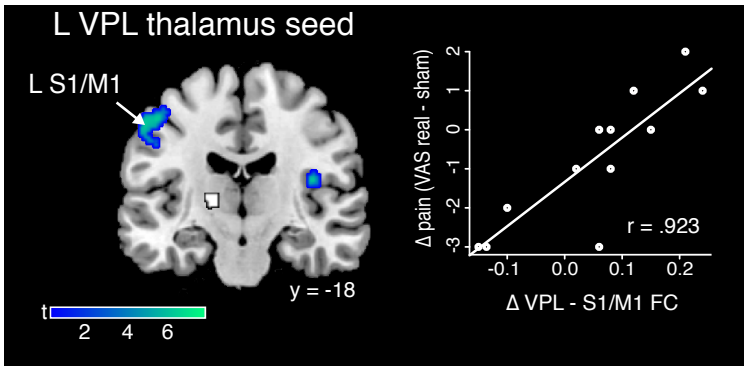

Figure 3.5. Correlation between change in FC and change in clinical pain after real tDCS. Patients with reduced FC between the L VPL thalamus (seed in white) and left S1/M1 and right posterior insula had greater reductions in clinical pain after real tDCS compared to sham (displayed at p = 0.005). VPL, ventral posterior lateral; S1, primary somatosensory cortex; M1, primary motor cortex; VAS, visual analog scale; L, left; R, right; FC, functional connectivity (fisher transformed r-values).

Discussion

This study shows for the first time that a clinically relevant schedule of repetitive M1 tDCS sessions alters FC in FM patients. Real tDCS (versus sham) reduced FC between the VL thalamus and SMA, mPFC, and the cerebellum. These changes in FC were distinct from those observed after sham tDCS. Sham tDCS (compared to baseline) decreased connectivity between the VPL thalamus and S1, IPL, and the parahippocampal gyrus/amygdala and between the PAG and precuneus. However, after both sham and active tDCS, we found a relationship between decreases in FC among pro-nociceptive brain regions and reductions in clinical pain. Patients with decreased connectivity between the VL thalamus and posterior insula and between the VPL thalamus and M1/S1 had greater reductions in clinical pain after sham and real tDCS. In addition, our data indicate that FM patients with stronger baseline connectivity between left M1 and left VL thalamus, between left S1 and left anterior insula, and between left VL thalamus and the PAG have a better analgesic response across the entire study. Although we see distinct main effects for sham and active tDCS, the overlapping results that relate to clinical changes in pain

may point to a shared placebo response in both sham and active conditions. A summary of the results is depicted in Figure 3.6.

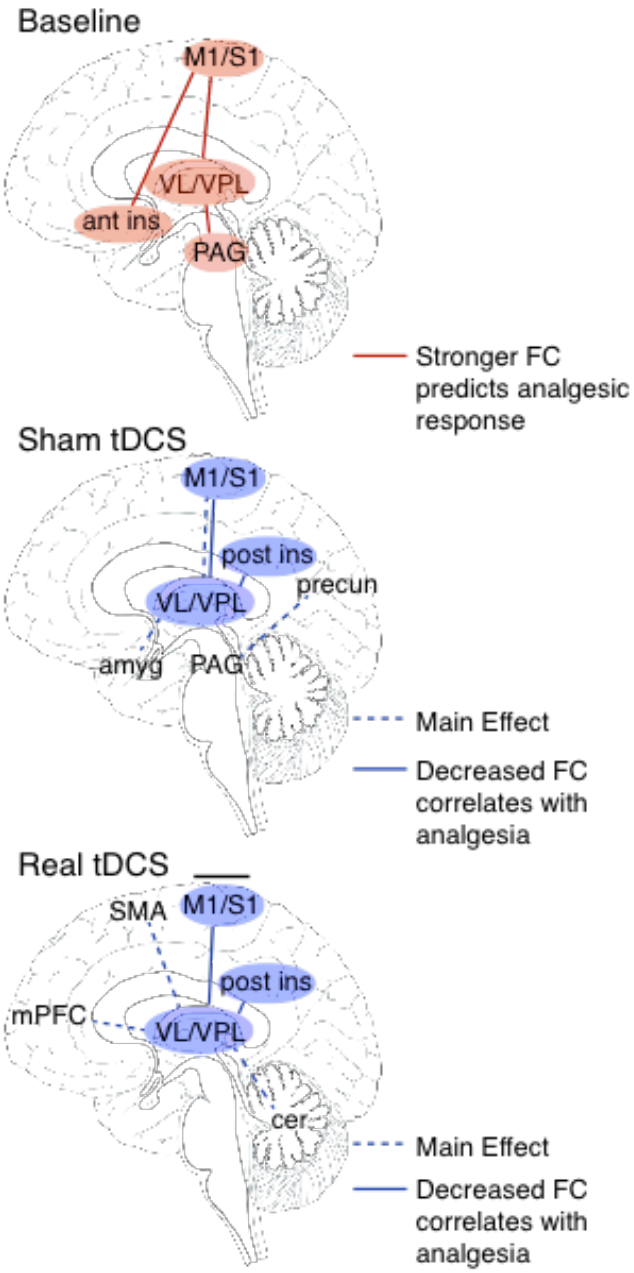

Figure 3.6. Summary of results. Stronger corticothalamic FC and FC between regions with high densities of opioid receptors at baseline predicted a better clinical response across the entire study. Changes in FC were observed after sham tDCS, which could be attributed to placebo analgesia or regression to the mean. Real tDCS caused some distinct long-lasting changes in FC (compared to sham) and may relieve pain via the inhibition of thalamic activity and subsequent decreases in FC, both of which could be caused by the release of endogenous opioids. M1, primary motor cortex; S1, primary somatosensory cortex; VL, ventral lateral; VPL, ventral posterior lateral; Ant Ins, anterior insula; PAG, periaqueductal gray; Post Ins, posterior insula; Amyg, amygdala; Precun, precuneus; SMA, supplemental motor area; mPFC, medial prefrontal cortex; Cer, cerebellum; FC, functional connectivity.

Our findings are somewhat at odds with the existing literature. For example, some studies have reported increases in thalamic blood flow (García-Larrea et al., 1999) or increased M1 – thalamus connectivity after M1 stimulation (Polanía et al., 2012b; Sours et al., 2014). We suggest that these conflicting results can be explained by the timing of stimulation and measurement. In the other studies, neural activity was measured during or immediately after M1 stimulation, which likely has a different neural signature than after one week of repetitive stimulation. In support of this notion, Garcia-Larrea and colleagues noted that 30 minutes after M1 stimulation stopped, thalamic blood flow reverted to baseline levels (García-Larrea et al., 1999). Therefore, the initial or acute changes in thalamic activity may cause a cascade of other events that are important for analgesia (Garcia-Larrea and Peyron, 2007), leading to the distinct long-term changes that we observe.

How might M1 stimulation promote analgesia in chronic pain patients? One hypothesis states that M1 stimulation suppresses pain perception directly by inhibiting activity in the lateral thalamus (Plow et al., 2012; Kuo et al., 2014). Compared to healthy controls, FM patients have increased activity in pain processing structures during experimental pain and increased connectivity in ascending pro-nociceptive pathways at rest (see Cagnie et al., 2014 for a recent review on neuroimaging findings in FM), although the specific role of the thalamus in FM remains unclear. Both increases and decreases in thalamic activity or connectivity during experimental pain or at rest have been reported (Burgmer et al., 2009; Jensen et al., 2009; Cifre et al., 2012; Jensen et al., 2012). In the current study, we found that strong M1 – VL thalamus connectivity at baseline predicted a greater reduction in pain across sham and real tDCS periods. This is consistent with work in central post-stroke pain where analgesic response to repetitive transcranial magnetic stimulation over M1 was found to be best in patients with intact

thalamocortical tracts (as measured by diffusion tensor imaging) (Goto et al., 2008; Ohn et al., 2012). Invasive motor cortex stimulation (MCS) decreases thalamic hyperactivity (Tsubokawa et al., 1993), likely by activating GABAergic divisions of the thalamus and increasing inhibition (Lucas et al., 2011). In healthy rodents and in a rodent model of neuropathic pain, MCS decreases the firing rate of VPL thalamic neurons specifically (Pagano et al., 2011; 2012). In a previous study using the same patients reported here, we found a trend towards decreased glutamate + glutamine (Glx) in the bilateral thalamus after real tDCS compared to sham (Foerster et al., 2014). The decreases in FC between the thalamus and SMA, mPFC and cerebellum after real tDCS in this study lends support to the hypothesis that M1 stimulation disrupts thalamic activity.

Another hypothesis is that M1 stimulation causes analgesia indirectly via the facilitation of descending anti-nociceptive pathways and release of endogenous opioids (Garcia-Larrea and Peyron, 2007). Maarrawi and colleagues hypothesized that neuropathic pain patients with higher levels of endogenous opioids at baseline would be least likely to benefit from any additional opioid release caused by MCS, and indeed, patients with lower baseline binding potential for an opioid agonist (reflecting either fewer opioid receptors or higher levels of endogenous opioids) in the thalamus, insula and PAG were the least likely to benefit from MCS (Maarrawi et al., 2013). The relationship between opioids and BOLD fMRI signal deserves further study, but in healthy controls morphine administration decreases activity in S1, thalamus and PAG (Becerra et al., 2006) while naloxone (an opioid antagonist) increases activity in S1, thalamus, insula and PAG (Borras, 2004). In our study, stronger M1- thalamus, S1 – insula, and thalamus – PAG connectivity at baseline predicted a better treatment response. Since both sham and real tDCS also cause endogenous opioid release (DosSantos et al., 2014), this finding may suggest that

patients with connectivity between regions under the stimulating anode (M1/S1) and regions with a high density of opioid receptors are the most likely to benefit from tDCS. We also found decreases in FC in many of these regions after sham and real tDCS, which could also reflect opioid release.

Placebo analgesia is a well-documented psychobiological event, and imaging studies have found overlap between brain networks involved in pain processing and those implicated in the placebo response (Tracey, 2010; Meissner et al., 2011). The decreases in FC found after sham (compared to baseline) are consistent with previous studies of placebo analgesia showing decreased activity in the thalamus, S1, amygdala and insula (Wager, 2004; Price et al., 2007; Wager et al., 2011). Importantly, the similarity of FC results related to changes in clinical pain between baseline and sham and between sham and real sessions may suggest a shared placebo component across conditions. However, the changes in FC after the sham period in this study cannot be interpreted solely as a placebo effect since we lacked a control group that received no treatment for comparison. Therefore, any changes from baseline to sham could also reflect regression to the mean or the natural course of the disease (Wager and Fields, 2013). Regression to the mean also may account for a portion of the change in clinical pain after both the sham and real tDCS periods.

Our study was limited by the small sample size, which may have contributed to the lack of a significant clinical effect between sham and active conditions and reduced statistical power. This pilot study did not aim to validate the efficacy of M1 tDCS as a treatment for FM; rather our goal was to determine if a clinically relevant schedule of tDCS sessions altered resting state FC in FM patients. However, as with most pain treatments wherein only a portion have a clinically meaningful response, half of the patients in this study did report a drop in pain on the

VAS (active – sham), and this change was correlated with reductions in thalamo-cortical connectivity. This study is significantly limited by the lack of counterbalancing between sham and active conditions. Therefore, we cannot rule out carry-over effects from the sham period. However, sham and active phases were separated by a wash out period of at least one week, so we find this unlikely. Another limitation is that the stimulation sessions were single blinded. Finally, research has shown that stimulating for 30 seconds at the beginning and end of the sham condition can mimic the sensation during active treatment and that patients can not differentiate between sham and real at 1 mA (Gandiga et al., 2006). However, the credibility of sham tDCS and the effectiveness of patient blinding at 2 mA has recently been questioned (O'Connell et al., 2014). Given our repeated measures design, it is likely that the patients became aware of the condition differences. Our results should be interpreted with caution and additional studies will be needed to replicate our findings.

Conclusion

Our results support the hypothesis that repetitive M1 tDCS causes lasting changes in FC and may relieve pain by altering thalamic activity. Analgesia may result from the inhibition of thalamic activity and subsequent decreases in FC, both of which could be caused by the release of endogenous opioids. Future studies that combine fMRI and PET within the same patients after repetitive M1 tDCS are needed to test this hypothesis. It is possible that there is a significant placebo component common to both sham and real tDCS. Future studies should include a no-treatment control group to test this hypothesis. It remains to be seen if similar changes in FC are observed for tDCS in other chronic pain conditions.

Acknowledgments

This study was funded by a MICHR Clinical Trial Planning Program and CTSA high-tech funding grant, University of Michigan (Principal Investigators: A.F.D. and R.E.H.). C.C. was supported by T32 NS076401. R.E.H was funded by NIH/NCCAM: R01 AT007550. A.F.D. was supported by NIH/NIDCR R56 DE022637-01. The authors would like to thank Suzan Lowe, B.A., R.T., for expert technical assistance with fMRI data collection.

References

Becerra L, Harter K, Gonzalez RG, Borsook D (2006) Functional Magnetic Resonance Imaging Measures of the Effects of Morphine on Central Nervous System Circuitry in Opioid-Naive Healthy Volunteers. Anesth Analg 103:208–216.

Borras MC (2004) FMRI Measurement of CNS Responses to Naloxone Infusion and Subsequent Mild Noxious Thermal Stimuli in Healthy Volunteers. Journal of Neurophysiology 91:2723–2733.

Brunoni AR, Fregni F (2011) Clinical trial design in non-invasive brain stimulation psychiatric research. Int J Methods Psychiatr Res 20:e19–e30.

Burgmer M, POGATZKIZAHN E, Gaubitz M, WESSOLECK E, Heuft G, Pfleiderer B (2009) Altered brain activity during pain processing in fibromyalgia. NeuroImage 44:502–508.

Cagnie B, Coppieters I, Denecker S, Six J, Danneels L, Meeus M (2014) Central sensitization in fibromyalgia? A systematic review on structural and functional brain MRI. Seminars in Arthritis and Rheumatism.

Cifre I, Sitges C, Fraiman D, Muñoz MÁ, Balenzuela P, González-Roldán A, Martínez-Jauand M, Birbaumer N, Chialvo DR, Montoya P (2012) Disrupted functional connectivity of the pain network in fibromyalgia. Psychosom Med 74:55–62.

DaSilva AF, Volz MS, Bikson M, Fregni F (2011) Electrode positioning and montage in transcranial direct current stimulation. J Vis Exp.

Dayan E, Censor N, Buch ER, Sandrini M, Cohen LG (2013) Noninvasive brain stimulation: from physiology to network dynamics and back. Nature Neuroscience 16:838–844.

DosSantos MF, Martikainen IK, Nascimento TD, Love TM, DeBoer MD, Schambra HM, Bikson M, Zubieta J-K, DaSilva AF (2014) Building up analgesia in humans via the endogenous μ-opioid system by combining placebo and active tDCS: a preliminary report. PLoS ONE 9:e102350.

Fagerlund AJ, Hansen OA, Aslaksen PM (2015) Transcranial direct current stimulation as a

treatment for patients with fibromyalgia. PAIN 156:62–71.

Foerster BR, Nascimento TD, DeBoer M, Bender MA, Rice IC, Truong DQ, Bikson M, Clauw DJ, Zubieta J-K, Harris RE, DaSilva AF (2014) Excitatory and Inhibitory Brain Metabolites as Targets and Predictors of Effective Motor Cortex tDCS Therapy in Fibromyalgia. Arthritis Rheumatol.

Fregni F, Gimenes R, Valle AC, Ferreira MJL, Rocha RR, Natalle L, Bravo R, Rigonatti SP, Freedman SD, Nitsche MA, Pascual-Leone A, Boggio PS (2006) A randomized, sham-controlled, proof of principle study of transcranial direct current stimulation for the treatment of pain in fibromyalgia. Arthritis Rheum 54:3988–3998.

Gandiga PC, Hummel FC, Cohen LG (2006) Transcranial DC stimulation (tDCS): a tool for double-blind sham-controlled clinical studies in brain stimulation. Clinical Neurophysiology 117:845–850 Available at: http://eutils.ncbi.nlm.nih.gov/entrez/eutils/elink.fcgi?dbfrom=pubmed&id=16427357&retmode=ref&cmd=prlinks.

Garcia-Larrea L, Peyron R (2007) Motor cortex stimulation for neuropathic pain: From phenomenology to mechanisms. NeuroImage 37 Suppl 1:S71–S79.

García-Larrea L, Peyron R, Mertens P, Gregoire MC, Lavenne F, Le Bars D, Convers P, Mauguière F, Sindou M, Laurent B (1999) Electrical stimulation of motor cortex for pain control: a combined PET-scan and electrophysiological study. PAIN 83:259–273.

Goto T, Saitoh Y, Hashimoto N, Hirata M, Kishima H, Oshino S, Tani N, Hosomi K, Kakigi R, Yoshimine T (2008) Diffusion tensor fiber tracking in patients with central post-stroke pain; correlation with efficacy of repetitive transcranial magnetic stimulation. PAIN 140:509–518.

Jensen KB, Kosek E, Petzke F, Carville S, Fransson P, Marcus H, Williams SCR, Choy E, Giesecke T, Mainguy Y, Gracely R, Ingvar M (2009) Evidence of dysfunctional pain inhibition in Fibromyalgia reflected in rACC during provoked pain. PAIN 144:95–100.

Jensen KB, Loitoile R, Kosek E, Petzke F, Carville S, Fransson P, Marcus H, Williams SCR, Choy E, Mainguy Y, Vitton O, Gracely RH, Gollub R, Ingvar M, Kong J (2012) Patients with fibromyalgia display less functional connectivity in the brain's pain inhibitory network. Mol Pain 8:32.

Kuo M-F, Paulus W, Nitsche MA (2014) Therapeutic effects of non-invasive brain stimulation with direct currents (tDCS) in neuropsychiatric diseases. NeuroImage 85 Pt 3:948–960.

Lindenberg R, Nachtigall L, Meinzer M, Sieg MM, Flöel A (2013) Differential effects of dual and unihemispheric motor cortex stimulation in older adults. Journal of Neuroscience 33:9176–9183.

Lucas JM, Ji Y, Masri R (2011) Motor cortex stimulation reduces hyperalgesia in an animal model of central pain. PAIN 152:1398–1407.

Maarrawi J, Peyron R, Mertens P, Costes N, Magnin M, Sindou M, Laurent B, Garcia-Larrea L (2013) Brain opioid receptor density predicts motor cortex stimulation efficacy for chronic pain. PAIN 154:2563–2568.

Maarrawi J, Peyron R, Mertens P, Costes N, Magnin M, Sindou M, Laurent B, García-Larrea L (2007) Motor cortex stimulation for pain control induces changes in the endogenous opioid system. Neurology 69:827–834.

Meissner K, Bingel U, Colloca L, Wager TD, Watson A, Flaten MA (2011) The placebo effect: advances from different methodological approaches. Journal of Neuroscience 31:16117–16124.

Melzack R (1987) The short-form McGill pain questionnaire. PAIN.

Napadow V, Kim J, Clauw DJ, Harris RE (2012) Brief Report: Decreased intrinsic brain connectivity is associated with reduced clinical pain in fibromyalgia. Arthritis Rheum 64:2398–2403.

Napadow V, LaCount L, Park K, As-Sanie S, Clauw DJ, Harris RE (2010) Intrinsic brain connectivity in fibromyalgia is associated with chronic pain intensity. Arthritis Rheum 62:2545–2555.

O'Connell NE, Wand BM, Marston L, Spencer S, Desouza LH (2014) Non-invasive brain stimulation techniques for chronic pain. Cochrane Database Syst Rev 4:CD008208.

Ohn SH, Chang WH, Park C-H, Kim ST, Lee JI, Pascual-Leone A, Kim Y-H (2012) Neural correlates of the antinociceptive effects of repetitive transcranial magnetic stimulation on central pain after stroke. Neurorehabil Neural Repair 26:344–352.

Pagano RL, Assis DV, Clara JA, Alves AS, Dale CS, Teixeira MJ, Fonoff ET, Britto LR (2011) Transdural motor cortex stimulation reverses neuropathic pain in rats: a profile of neuronal activation. Eur J Pain 15:268.e1–.e14.

Pagano RL, Fonoff ET, Dale CS, Ballester G, Teixeira MJ, Britto LRG (2012) Motor cortex stimulation inhibits thalamic sensory neurons and enhances activity of PAG neurons: possible pathways for antinociception. PAIN 153:2359–2369.

Petrovic P (2002) Placebo and Opioid Analgesia-- Imaging a Shared Neuronal Network. Science 295:1737–1740.

Plow EB, Pascual-Leone A, Machado A (2012) Brain stimulation in the treatment of chronic neuropathic and non-cancerous pain. J Pain 13:411–424.

Polanía R, Paulus W, Nitsche MA (2012a) Reorganizing the intrinsic functional architecture of the human primary motor cortex during rest with non-invasive cortical stimulation. PLoS ONE 7:e30971.

Polanía R, Paulus W, Nitsche MA (2012b) Modulating cortico-striatal and thalamo-cortical

functional connectivity with transcranial direct current stimulation. Hum Brain Mapp 33:2499–2508.

Price DD, Craggs J, Nicholas Verne G, Perlstein WM, Robinson ME (2007) Placebo analgesia is accompanied by large reductions in pain-related brain activity in irritable bowel syndrome patients. PAIN 127:63–72.

Saavedra LC, Mendonca M, Fregni F (2014) Medical Hypotheses. Medical Hypotheses 83:332–336.

Schmidt-Wilcke T, Clauw DJ (2011) Fibromyalgia: from pathophysiology to therapy. Nat Rev Rheumatol 7:518–527.

Sehm B, Schafer A, Kipping J, Margulies D, Conde V, Taubert M, Villringer A, Ragert P (2012) Dynamic modulation of intrinsic functional connectivity by transcranial direct current stimulation. Journal of Neurophysiology 108:3253–3263.

Sours C, Alon G, Roys S, Gullapalli RP (2014) Modulation of resting state functional connectivity of the motor network by transcranial pulsed current stimulation. Brain Connectivity 4:157–165.

Tracey I (2010) Getting the pain you expect: mechanisms of placebo, nocebo and reappraisal effects in humans. Nat Med 16:1277–1283.

Tsubokawa T, Katayama Y, Yamamoto T, Hirayama T, Koyama S (1993) Chronic motor cortex stimulation in patients with thalamic pain. J Neurosurg 78:393–401.

Valle A, Roizenblatt S, Botte S, Zaghi S, Riberto M, Tufik S, Boggio PS, Fregni F (2009) Efficacy of anodal transcranial direct current stimulation (tDCS) for the treatment of fibromyalgia: results of a randomized, sham-controlled longitudinal clinical trial. J Pain Manag 2:353–361.

Vaseghi B, Zoghi M, Jaberzadeh S (2014) Does anodal transcranial direct current stimulation modulate sensory perception and pain? A meta-analysis study. Clin Neurophysiol.

Wager TD (2004) Placebo-Induced Changes in fMRI in the Anticipation and Experience of Pain. Science 303:1162–1167.

Wager TD, Atlas LY, Leotti LA, Rilling JK (2011) Predicting individual differences in placebo analgesia: contributions of brain activity during anticipation and pain experience. Journal of Neuroscience 31:439–452.

Wager TD, Fields H (2013) Placebo analgesia. Textbook of Pain.

Wager TD, Scott DJ, Zubieta J-K (2007) Placebo effects on human mu-opioid activity during pain. Proc Natl Acad Sci USA 104:11056–11061.

Watson D, Clark LA, Tellegen A (1988) Development and validation of brief measures of

positive and negative affect: the PANAS scales. J Pers Soc Psychol 54:1063–1070.

Whitfield-Gabrieli S, Nieto-Castanon A (2012) Conn: A Functional Connectivity Toolbox for Correlated and Anticorrelated Brain Networks. Brain Connectivity 2:125–141.

Wolfe F et al. (1990) The american college of rheumatology 1990 criteria for the classification of fibromyalgia. Arthritis Rheum 33:160–172.

Zhang D, Snyder AZ, Shimony JS, Fox MD, Raichle ME (2010) Noninvasive Functional and Structural Connectivity Mapping of the Human Thalamocortical System. Cerebral Cortex 20:1187–1194.

Chapter 4 : Conclusions and Future Directions

This dissertation investigated alterations in functional brain network hubs in FM and how non-invasive brain stimulation can alter brain network connectivity to produce analgesia in these patients. The main contributions of this research are a better understanding of how functional hubs, the regions most fundamental to efficiency and information transfer in the brain, are reorganized in FM and how increases in an excitatory neurotransmitter may influence hub status and lead to increases in clinical pain. Further, this dissertation adds to the knowledge of how a clinically relevant schedule of M1 tDCS treatment alters brain connectivity to cause analgesia. By identifying brain network alterations present in an individual patient, combined with the analgesic mechanism of action of noninvasive brain stimulation at a particular site, treatment may be personalized to the type of central alteration present in each patient.

Summary of Findings

In Chapter 2, we applied a brain network based approach to examine hub topology in FM. Resting state functional MRI data from 40 FM patients and 27 healthy volunteers were analyzed using graph theoretical techniques. We also measured the concentration of Glx in the right posterior insula using ^{1}H-MRS in each participant. We identified significant disruptions in hub rank order in FM patients as compared to healthy volunteers. In general, brain regions that were hubs in FM patients, such as the superior temporal gyrus, mid and anterior insula, were non-hubs with low degree or centrality in healthy controls. Conversely, hubs in healthy controls, such as primary and secondary visual cortices and superior frontal gyrus, were non-hubs in FM. In FM, but not controls, the anterior insula was a connector hub with significantly higher inter-

modular connectivity. Both FM and healthy control networks had a rich club organization, however the membership of hubs within the rich club was different between groups. In FM, the bilateral anterior insulae was a member of the rich club and the visual network was integrated with the rest of the rich club. In healthy volunteers, the visual network was segregated into its own module distinct from other rich club nodes.

Among FM patients, rich club membership varied with the intensity of clinical pain: the posterior insula as well as M1 and S1 belonged to the rich club only in FM patients with the highest pain levels. The rich club in the low pain FM group more closely resembled that of healthy controls. Further, we found that the eigenvector centrality (a measure of how connected a brain region is to other highly connected regions) of two nodes in the posterior insula and 14 bilateral M1 and S1 nodes positively correlated with clinical pain. The two posterior insula nodes overlapped with the spectroscopic voxel where we measured each participant's level of Glx. We demonstrated that eigenvector centrality in the posterior insula mediated the relationship between levels of Glx within this structure and the patient's clinical pain report. These data are consistent with preclinical findings in rodents wherein increasing endogenous levels of glutamate in the insula led to increases in hyperalgesia and allodynia (Watson, 2016).

Taken together, these findings demonstrate an altered hub topology in the chronic pain state of FM and suggest that, within the chronic pain network, pro-nociceptive regions (such as the insulae) appear to have acquired hub status that would redefine information processing and integration for the network. Moreover, the intensity of chronic pain may be related to the composition of hubs in the rich club. Finally, these data are the first to suggest that disruptions in the excitatory tone within the insula could alter the strength of the insula as a hub and subsequently lead to increased clinical pain.

In Chapter 3, we had three goals: first, determine if functional connectivity at baseline can predict treatment response to M1 tDCS in FM patients. Second, examine if and how functional connectivity changes after the treatment, and third, assess if these changes relate to analgesia. Twelve FM patients underwent a resting state functional connectivity fMRI scan at baseline, after five days of sham tDCS and after 5 days of real M1 tDCS. Clinical pain intensity was measured at all three time points. Stronger baseline functional connectivity between M1 (under the stimulating anode) and the ventral lateral thalamus, S1 to the anterior insula, and ventral lateral thalamus to the PAG predicted greater analgesia after sham and real tDCS. These findings are consistent with data from invasive motor cortex stimulation wherein patients with intact thalamocortical tracts have the best analgesic response (Goto et al., 2008; Ohn et al., 2012). Additionally, since M1 tDCS may act via the endogenous opioid system (DosSantos et al., 2012), our findings also suggest that patients who have strong connectivity between regions under the stimulating anode and regions with a high density of opioid receptors may be most likely to benefit from this treatment.

Both sham and real tDCS caused reductions in functional connectivity. Sham tDCS (compared to baseline) reduced functional connectivity between the ventral posterior lateral thalamus, S1 and the amygdala, findings which are consistent with neural responses during placebo analgesia (Wager, 2004; Price et al., 2007; Wager et al., 2011). Real tDCS (compared to sham) reduced functional connectivity between the ventral lateral thalamus, medial prefrontal and supplementary motor cortices. Interestingly, decreased functional connectivity between the ventral lateral/ventral posterior lateral thalamus and posterior insula, M1 and S1 correlated with reductions in clinical pain after *both* sham and active treatment. In total, these results suggest that while there may be a placebo response common to both sham and real tDCS, repetitive M1 tDCS

causes distinct changes in functional connectivity that last beyond the stimulation period. The majority of the findings we report in Chapter 3 center on reductions in connectivity between the thalamus and other cortical regions. This lends support to the hypothesis that the analgesic actions M1 tDCS may stem from reductions in pro-nociceptive thalamic hyperactivity (Kuo et al., 2014).

Implications and Conclusions

The Motor Cortex Plays a Role in Pain Perception

The primary motor cortex (M1) is not classically defined as a member of the 'pain matrix', although its role in chronic pain is beginning to be examined. M1 shares many connections with the sensory nuclei of the thalamus and other pain processing regions and may therefore be an important modulator of pain perception by virtue of its connectivity patterns (Saavedra et al., 2014). M1 stimulation with tDCS increases pain and sensory thresholds in healthy volunteers (Reidler et al., 2012; Vaseghi et al., 2014) and causes lasting clinical pain reduction in FM (Fregni et al., 2006; Valle et al., 2009; Fagerlund et al., 2015).

However, in FM patients, motor cortex excitability at baseline and in response to sensory stimuli is abnormally increased (Mhalla:2010iy; Cook et al., 2004). We found that the bilateral M1 were hubs and members of the rich club in the FM patients with the highest intensity of clinical pain. Additionally, as measured with eigenvector centrality, the more connected M1 was to other high degree nodes, then the greater the clinical pain rating. If we conclude from these data that M1 is a hyperactive hub in FM, then why would anodal stimulation of M1, presumably an excitatory intervention, lead to reductions in functional connectivity and analgesia?

The most common way to measure the effect of M1 tDCS on cortical excitability is to measure motor evoked potentials. Anodal stimulation increases the amplitude of motor evoked

potentials, while cathodal stimulation decreases it (Nitsche and Paulus, 2000). These results have led to the convenient interpretation that anodal tDCS is excitatory and cathodal tDCS is inhibitory, although this may not be true in all circumstances. Antal and colleagues found that when healthy subjects are simultaneously given anodal M1 tDCS and performing a motor task that presumably activates M1, the motor evoked potential amplitude is lower compared to anodal M1 stimulation given while participants were at rest (Antal et al., 2007). These results suggest that tDCS-induced plasticity may be dependent on the baseline state of the targeted brain region. According to the Bienenstock-Cooper-Munro (BCM) model of plasticity, synaptic potentiation is more likely to occur if postsynaptic activity is low. Synaptic depression, on the other hand, is more likely to occur if postsynaptic activity is high (Bienenstock et al., 1982) (see (Lefaucheur et al., 2017) for a discussion of this model in the context of noninvasive brain stimulation). This model may explain why changes in cortical excitability after tDCS depend on whether the participant is at rest or performing a task that engages the area being targeted. In the case of our findings, if M1 is active at rest (as one might conclude from our results that show M1 has many more connections at rest in a patient with high pain compared to low pain), then anodal M1 tDCS might act in an inhibitory manner. Therefore, M1 tDCS might be causing analgesia in some patients by decreasing the hub status of M1 regions – a hypothesis that is supported by our findings in Chapter 3 where anodal M1 tDCS caused reductions in functional connectivity between M1, S1 and other cortical regions.

The Insular Cortex may be a "Pain Hub" and a Target of M1 tDCS

The insula is highly connected to the rest of the brain, which may explain why it is implicated is so many functions, including somatosensory, autonomic, interoception, salience detection and cognitive processes (Borsook et al., 2016). One general hypothesis is that the

insula performs a role in converting salient physiological inputs into higher level cognitive states or emotions (Borsook et al., 2016). There is evidence that the anterior insula acts as in a causal manner to coordinate and change brain dynamics in many large scale networks (Uddin, 2015). The insula's role as a sensory integration region that is critical for pain perception is supported by studies in which direct electrical stimulation of the posterior insula elicited painful sensations (Ostrowsky et al., 2002; Mazzola et al., 2009) and insular lesions alter pain perception (Garcia-Larrea and Peyron, 2013). Activity in the posterior insula also tracked over time with experimental heat pain intensity ratings (Segerdahl et al., 2015).

In the first study of this dissertation, we found that the anterior insula was a hub, and had many connections to brain regions outside its own functional system in FM patients but not healthy controls. This region was also a member of the rich club – the functional backbone of connectivity that influences information integration across the whole brain network. In FM patients with the highest pain, this was also true for the posterior insula. In the second study of this dissertation, we showed that FM patients who experienced the greatest analgesic effect after M1 tDCS also had reductions in functional connectivity between the ventral lateral/ventral posterior lateral thalamus and the posterior insula. This finding met our criteria for statistical significance, however, we did observe other reductions in functional connectivity after M1 tDCS between the anterior and posterior insula and other cortical regions, some of which also correlated with analgesia. These observations were not reported in Chapter 3 because they were not significant after correcting for multiple comparisons. It is possible that the sample size (n=12) was too small to detect significant decreases in connectivity in the insula. Another possibility is that the graph theoretical measures used in Chapter 2 would have detected a change

in insular hub status after tDCS. This should be investigated in future studies with a larger number of patients.

Glutamate and GABA Influence Pain Perception and are Altered by M1 tDCS

Patients with FM have elevated levels of Glx in the posterior insula compared to healthy volunteers (Harris et al., 2009). Moreover, higher Glx is associated with lower experimental pain thresholds in these patients. After a non-pharmacological treatment, the FM patients with reductions in Glx within the posterior insula also experience decreases in clinical pain and sensitivity to experimental pain stimuli (Harris et al., 2008). Similarly, an effective pharmacological analgesic treatment reduced insular Glx in FM (Harris et al., 2013). FM patients also have lower GABA concentrations in the anterior insula relative to healthy controls, and patients with lower GABA levels in the posterior insula were more sensitive to experimental pressure pain (Foerster et al., 2012). Alterations in the excitatory-inhibitory balance in the insula have also been found in other chronic pain conditions (Petrou et al., 2012; As-Sanie et al., 2016).

In Chapter 2 we found that the high pain FM group had significantly higher concentrations of Glx in the posterior insula compared to the low pain FM group. There were two nodes in the posterior insula that overlapped with the spectroscopic voxel; hence, we sought to examine the relationship between graph theoretical measures, Glx and clinical pain in FM patients. We demonstrated that the eigenvector centrality of posterior insula nodes mediated the relationship between Glx and clinical pain. These data are consistent with a recent preclinical study wherein either increasing glutamate or decreasing GABA led to increased hyperalgesia and allodynia in naïve rats (Watson, 2016). Further, rats with a chronic constriction injury to the sciatic nerve, a rodent model for chronic neuropathic pain, had higher glutamate levels in the insula compared to controls. Following a microinjection of a glutamate receptor antagonist or

GABA into the insular region, the nociceptive behaviors in the injured rats decreased. Together, these data indicate that the excitatory-inhibitory balance in the insula exerts a causal influence on pain perception.

In addition to the functional connectivity changes after M1 tDCS that we report in Chapter 3, our laboratory previously examined changes in excitatory and inhibitory neurotransmitters after treatment in the same FM patients studied here (Foerster et al., 2014). We found that five days of M1 tDCS treatment significantly decreased Glx in the ACC compared to sham. There was a trend towards decreased Glx in the bilateral thalami after M1 tDCS compared to sham, although this did not meet statistical significance. Finally, M1 tDCS increased GABA in the anterior insula relative to the baseline scan (Foerster et al., 2014). The authors did not find any significant changes in anterior insula Glx, or posterior insula Glx or GABA. It is possible that the study was underpowered (n=12) to detect changes in posterior insula neurochemistry.

Taken together, it is clear that glutamate and GABA in the insula impact pain perception and are altered in chronic pain. Therefore, treatments that decrease glutamate and/or increase GABA in the insula may be effective analgesics in some patients. Our conclusion from these data is that molecular alterations of the excitatory tone of the insula can impact the functionally derived hub status of this region and lead to subsequent changes in the clinical pain percept. Future tDCS studies with a larger number of participants should confirm the impact of M1 stimulation on insular Glx and GABA. If the null results are confirmed, other tDCS targets that may change the excitatory-inhibitory tone in the insula should be explored.

Future Directions

Biomarkers for Chronic Pain

A biomarker is broadly defined as a biochemical, physiological or anatomical trait that reliably predicts a biological state (Fidalgo et al., 2014). Ideally, biomarkers should identify or predict individuals with a disease and they should change with successful treatment. In chronic pain, biomarkers would be helpful to patients who desire validation of an oftentimes invisible condition, and useful for researchers and clinicians to obtain additional information about the status or trajectory of a disease beyond the patient self-report (Davis et al., 2017). Neuroimaging has the potential to generate biomarkers based on brain activity related to pain perception, although this goal should be pursued with care (see Davis et al., 2017 for an extensive discussion of the ethics and challenges of developing biomarkers for chronic pain). Multivariate pattern analysis and machine learning have been used to identify patterns in neuroimaging data that are predictive of pain or disease status (Wager et al., 2013; Ung et al., 2014; López-Solà et al., 2016). Network topology and functional connectivity (as examined in this dissertation) also have the potential to serve as biomarkers for chronic pain. Future studies should replicate our findings in Chapter 2 and determine if the hub status of insular, M1 and S1 regions track with changes in clinical pain over time or decrease with successful treatment. It also remains unclear if our findings translate into other chronic centralized pain conditions. Larger studies with diverse individuals (age, sex, race, ethnicity) and different chronic pain conditions are warranted.

Personalized Treatment

Given the many legal and ethical challenges of chronic pain biomarkers (Davis et al., 2017), it is our conclusion that the best use of a brain biomarker would be to optimize treatment by tailoring interventions based on an individual patient's neurobiology. Despite its clinical

promise, tDCS still faces many engineering and research challenges, such as the fine-tuning of stimulation parameters (intensity, duration of stimulation, number of treatments required, etc.) and the delineation of which brain regions should be targeted to produce the maximum treatment benefit. Biomarkers may serve as a guidepost for new targets in noninvasive brain stimulation research and clinical trials (Fidalgo et al., 2014).

There are many ways in which tDCS could be personalized to an individual patient. The histology of brain regions varies between individuals and, therefore, applying stimulation based on group-average coordinates is not the best approach. Structural MRI data can be used to determine the shape and position of the stimulating electrode with more precision than a group average placement. Computational modeling has shown that this approach can lead to stronger current in the targeted brain regions (Cancelli et al., 2015b). M1 cortical excitability (measured using hand motor evoked potentials) was higher using a personalized electrode compared to non-personalized fit based on the standard electroencephalography 10-20 International system as typically done (Cancelli et al., 2015a). This approach was recently used clinically to reduce fatigue in multiple sclerosis (Cancelli et al., 2017).

Structural and functional connectivity could also be used to determine the best stimulation target. For example, participants with stronger dorsolateral prefrontal cortex (DLPFC) – thalamus structural connectivity experienced more pain relief during anodal DLPFC stimulation (presumably via a top-down activation of descending analgesic pathways from the DLPFC to the PAG that pass through the thalamus) (Lin et al., 2017). The structural connectivity also related to the functional connectivity between these two regions. The functional connectivity profile of the DLPFC is more similar within an individual subject on different days than to an average population map (Fox et al., 2013). Fox et al. identified regions

of the DLPFC that produced a more effective antidepressant response when stimulated compared to other DLPFC sites and that this difference related to functional connectivity (Fox et al., 2012). Effective sites had strong anti-correlated connectivity between that region and the subgenual ACC. The specific region of the DLPFC with the strongest anti-correlation to the ACC varied between patients. In another example, corticostriatal connectivity predicted treatment response to dorsomedial prefrontal cortex transcranial magnetic stimulation (Dunlop et al., 2016). In this case, the non-responders (50%) had less corticostriatal connectivity at baseline compared to responders. Treatment responses may depend on structural and functional brain circuitry and may help explain the wide variances of clinical outcomes after tDCS treatment. By using connectivity at baseline to guide treatment, some of this variance may be reduced.

The findings of this dissertation suggest that anodal M1 tDCS may be most effective in alleviating pain in those FM patients where the insula, M1 and S1 are acting as highly connected hub regions in the brain network. More specifically, patients with high M1-thalamus-PAG connectivity at baseline might respond best to M1 tDCS. For patients with a different hub topology or connectivity pattern, an alternative stimulation site may produce better results. We would predict that patients with stronger DLPFC – thalamus – PAG connectivity would be better candidates for tDCS targeted to the DLPFC. These possibilities should be examined in future studies.

Developing New Targets for tDCS Treatment of Chronic Pain

As we have outlined above, M1 stimulation may not be the best treatment approach in all chronic pain patients. New targets for brain stimulation should be explored and the research presented in this dissertation suggests that targeting hub brain regions for a tDCS "attack" (i.e. decreasing or reorganizing the hub structure in chronic pain patients) could be a successful

treatment approach. Graph theoretical analyses applied to computer simulations of human brain networks have the potential to model the consequences of targeting a novel region without the expense or risk of human trials (Medaglia, 2017).

A recent study used network control theory to predict the effects of stimulating different brain regions using a computational model of a structural brain network (Muldoon et al., 2016). In this context, 'control' refers to the ability to manipulate local activity in order to drive the global network towards a desired state. Regions with high degree (strongly connected hubs) had the highest average controllability, while brain regions with few connections had low controllability. Stimulating brain regions with high controllability resulted in the large changes to the functional state of the brain network (measured as the change in functional connectivity in the computational model after stimulation), and the amount of this global activation was unconstrained by the underlying structural connectivity. On the other hand, stimulating regions with low controllability led to focal activation only, and this activation was constrained and predicted by structural connectivity. In general, based on a model using structural brain data from healthy volunteers, regions of the medial DMN had high controllability and produced large functional effects on the rest of the brain network when stimulated. The postcentral gyrus (S1) had medium controllability and stimulating this region led to moderate changes in functional connectivity across the whole brain network. The results of this study suggest two classes of therapeutic interventions: a 'broad reset' where stimulating a highly connected hub leads to widespread activation and alteration of global brain dynamics, and 'focal' targeting wherein stimulating sparsely connected regions alters the functional dynamics of relatively few areas. The controllability measure could be used to predict network-wide effects of stimulation on a specific brain region. Applying these principles to our data, we would predict that hubs in FM

(anterior insula in all patients; S1, M1 and posterior insula in high pain patients) would have high controllability and stimulation would lead to large effects on global network dynamics. Conversely, stimulating non-hubs (visual cortex) would produce focal changes in connectivity. As we discuss in Chapter 1, the CNS alterations observed in FM are not limited to any one brain region or pathway. Therefore, future tDCS studies should examine the analgesic effects of targeting hub brain regions.

Concluding Remarks

Chronic pain is an enormous personal, societal and economic burden. Individuals who suffer from a chronic widespread pain have a reduced quality of life and excess mortality rates (Clauw, 2014; Macfarlane et al., 2017). Chronic pain is a leading cause of disability and costs for medical treatment and lost productivity exceed $550 billion annually in the United States (Institute of Medicine (US) Committee on Advancing Pain Research, Care, and Education, 2011).

Simultaneously, the United States is in the midst of an opioid epidemic. In 2015, there were 33,091 deaths due to an opioid overdose (Rudd et al., 2016), and most of these individuals first encountered an opioid for the management of acute or chronic pain (Schneiderhan et al., 2017). Paradoxically, there is no evidence that opioids effectively treat chronic pain and may instead lead to poorer long-term outcomes (Brummett et al., 2015; Goldenberg et al., 2016). In the United States, there are three drugs currently approved by the US Food and Drug Administration (FDA) for the treatment of FM. However, only 30-40% of patients experience a meaningful reduction in pain while taking these drugs and there are substantial side effects (see (Häuser et al., 2014)for a review on the efficacy of pharmacological therapies). Noninvasive

brain stimulation has emerged as a potential treatment for chronic centralized pain conditions, although the outcomes of clinical trials have been mixed (O'Connell et al., 2014).

This research offers new insight into the neurobiology of chronic centralized pain conditions, identifies a candidate diagnostic marker of chronic pain, and may contribute to the understanding of how non-invasive brain stimulation treatments cause analgesia. This knowledge could lead to more informed stimulation sites and personalized treatment based on brain network organization and connectivity in an individual patient. Longitudinal studies are needed to determine causality and to measure if network organization changes with successful treatment. Future studies should also examine the effect on brain network connectivity at other stimulation sites.

References

Antal A, Terney D, Poreisz C, Paulus W (2007) Towards unravelling task-related modulations of neuroplastic changes induced in the human motor cortex. Eur J Neurosci 26:2687–2691.

Arnold LM, Choy E, Clauw DJ, Goldenberg DL, Harris RE, Helfenstein M, Jensen TS, Noguchi K, Silverman SL, Ushida T, Wang G (2016) Fibromyalgia and Chronic Pain Syndromes: A White Paper Detailing Current Challenges in the Field. Clin J Pain 32:737–746.

As-Sanie S, Kim J, Schmidt-Wilcke T, Sundgren PC, Clauw DJ, Napadow V, Harris RE (2016) Functional Connectivity is Associated With Altered Brain Chemistry in Women With Endometriosis-Associated Chronic Pelvic Pain. J Pain 17:1–13.

Bienenstock EL, Cooper LN, Munro PW (1982) Theory for the development of neuron selectivity: orientation specificity and binocular interaction in visual cortex. J Neurosci 2:32–48.

Borsook D, Veggeberg R, Erpelding N, Borra R, Linnman C, Burstein R, Becerra L (2016) The Insula: A “Hub of Activity” in Migraine. The Neuroscientist 22:632–652.

Brummett CM, Urquhart AG, Hassett AL, Tsodikov A, Hallstrom BR, Wood NI, Williams DA, Clauw DJ (2015) Characteristics of fibromyalgia independently predict poorer long-term analgesic outcomes following total knee and hip arthroplasty. Arthritis Rheumatol 67:1386–1394.

Cancelli A, Cottone C, Di Giorgio M, Carducci F, Tecchio F (2015a) Personalizing the Electrode to Neuromodulate an Extended Cortical Region. Brain Stimul 8:555–560.

Cancelli A, Cottone C, Giordani A, Migliore S, Lupoi D, Porcaro C, Mirabella M, Rossini PM, Filippi MM, Tecchio F (2017) Personalized, bilateral whole-body somatosensory cortex stimulation to relieve fatigue in multiple sclerosis. Mult Scler:1352458517720528.

Cancelli A, Cottone C, Parazzini M, Fiocchi S, Truong D, Bikson M, Tecchio F, Parazzini M (2015b) Transcranial Direct Current Stimulation: Personalizing the neuromodulation. Conf Proc IEEE Eng Med Biol Soc 2015:234–237.

Clauw DJ (2014) Fibromyalgia: a clinical review. In, pp 1547–1555.

Cook DB, Lange G, Ciccone DS, Liu W-C, Steffener J, Natelson BH (2004) Functional imaging of pain in patients with primary fibromyalgia. J Rheumatol 31:364–378.

Davis KD, Flor H, Greely HT, Iannetti GD, Mackey S, Ploner M, Pustilnik A, Tracey I, Treede R-D, Wager TD (2017) Brain imaging tests for chronic pain: medical, legal and ethical issues and recommendations. Nat Rev Neurol.

DosSantos MF, Love TM, Martikainen IK, Nascimento TD, Fregni F, Cummiford C, Deboer MD, Zubieta J-K, Dasilva AFM (2012) Immediate effects of tDCS on the μ-opioid system of a chronic pain patient. Front Psychiatry 3:93.

Dunlop K, Woodside B, Olmsted M, Colton P, Giacobbe P, Downar J (2016) Reductions in Cortico-Striatal Hyperconnectivity Accompany Successful Treatment of Obsessive-Compulsive Disorder with Dorsomedial Prefrontal rTMS. Neuropsychopharmacology 41:1395–1403.

Fagerlund AJ, Hansen OA, Aslaksen PM (2015) Transcranial direct current stimulation as a treatment for patients with fibromyalgia. PAIN 156:62–71.

Fidalgo TM, Morales-Quezada JL, Muzy GSC, Chiavetta NM, Mendonca ME, Santana MVB, Goncalves OF, Brunoni AR, Fregni F (2014) Biological markers in noninvasive brain stimulation trials in major depressive disorder: a systematic review. J ECT 30:47–61.

Foerster BR, Nascimento TD, DeBoer M, Bender MA, Rice IC, Truong DQ, Bikson M, Clauw DJ, Zubieta J-K, Harris RE, DaSilva AF (2014) Excitatory and Inhibitory Brain Metabolites as Targets and Predictors of Effective Motor Cortex tDCS Therapy in Fibromyalgia. Arthritis Rheumatol.

Foerster BR, Petrou M, Edden RAE, Sundgren PC, Schmidt-Wilcke T, Lowe SE, Harte SE, Clauw DJ, Harris RE (2012) Reduced insular γ-aminobutyric acid in fibromyalgia. Arthritis Rheum 64:579–583.

Fox MD, Buckner RL, White MP, Greicius MD, Pascual-Leone A (2012) Efficacy of transcranial magnetic stimulation targets for depression is related to intrinsic functional connectivity with the subgenual cingulate. Biol Psychiatry 72:595–603.

Fox MD, Liu H, Pascual-Leone A (2013) Identification of reproducible individualized targets for treatment of depression with TMS based on intrinsic connectivity. NeuroImage 66:151–160.

Fregni F, Gimenes R, Valle AC, Ferreira MJL, Rocha RR, Natalle L, Bravo R, Rigonatti SP, Freedman SD, Nitsche MA, Pascual-Leone A, Boggio PS (2006) A randomized, sham-controlled, proof of principle study of transcranial direct current stimulation for the treatment of pain in fibromyalgia. Arthritis Rheum 54:3988–3998.

Garcia-Larrea L, Peyron R (2013) Pain matrices and neuropathic pain matrices: a review. PAIN 154 Suppl 1:S29–S43.

Goldenberg DL, Clauw DJ, Palmer RE, Clair AG (2016) Opioid Use in Fibromyalgia: A Cautionary Tale. Mayo Clin Proc 91:640–648.

Goto T, Saitoh Y, Hashimoto N, Hirata M, Kishima H, Oshino S, Tani N, Hosomi K, Kakigi R, Yoshimine T (2008) Diffusion tensor fiber tracking in patients with central post-stroke pain; correlation with efficacy of repetitive transcranial magnetic stimulation. PAIN 140:509–518.

Harris RE, Napadow V, Huggins JP, Pauer L, Kim J, Hampson J, Sundgren PC, Foerster B, Petrou M, Schmidt-Wilcke T, Clauw DJ (2013) Pregabalin rectifies aberrant brain chemistry, connectivity, and functional response in chronic pain patients. Anesthesiology 119:1453–1464.

Harris RE, Sundgren PC, Craig AD, Kirshenbaum E, Sen A, Napadow V, Clauw DJ (2009) Elevated insular glutamate in fibromyalgia is associated with experimental pain. Arthritis Rheum 60:3146–3152.

Harris RE, Sundgren PC, Pang Y, Hsu M, Petrou M, Kim S-H, McLean SA, Gracely RH, Clauw DJ (2008) Dynamic levels of glutamate within the insula are associated with improvements in multiple pain domains in fibromyalgia. Arthritis Rheum 58:903–907.

Häuser W, Walitt B, Fitzcharles M-A, Sommer C (2014) Review of pharmacological therapies in fibromyalgia syndrome. Arthritis Res Ther 16:201.

Institute of Medicine (US) Committee on Advancing Pain Research, Care, and Education (2011) Relieving Pain in America: A Blueprint for Transforming Prevention, Care, Education, and Research. Washington (DC): National Academies Press (US).

Kuo M-F, Paulus W, Nitsche MA (2014) Therapeutic effects of non-invasive brain stimulation with direct currents (tDCS) in neuropsychiatric diseases. NeuroImage 85 Pt 3:948–960.

Lefaucheur J-P et al. (2017) Evidence-based guidelines on the therapeutic use of transcranial direct current stimulation (tDCS). Clin Neurophysiol 128:56–92.

Lin RL, Douaud G, Filippini N, Okell TW, Stagg CJ, Tracey I (2017) Structural Connectivity Variances Underlie Functional and Behavioral Changes During Pain Relief Induced by Neuromodulation. Sci Rep 7:41603.

López-Solà M, Woo C-W, Pujol J, Deus J, Harrison BJ, Monfort J, Wager TD (2016) Towards a neurophysiological signature for fibromyalgia. PAIN.

Macfarlane GJ, Barnish MS, Jones GT (2017) Persons with chronic widespread pain experience excess mortality: longitudinal results from UK Biobank and meta-analysis. Annals of the Rheumatic Diseases 76:1815–1822.

Mazzola L, Isnard J, Peyron R, Guénot M, Mauguière F (2009) Somatotopic organization of pain responses to direct electrical stimulation of the human insular cortex. PAIN 146:99–104.

Medaglia JD (2017) Graph Theoretic Analysis of Resting State Functional MR Imaging. Neuroimaging Clin N Am 27:593–607.

Muldoon SF, Pasqualetti F, Gu S, Cieslak M, Grafton ST, Vettel JM, Bassett DS (2016) Stimulation-Based Control of Dynamic Brain Networks. PLoS Comp Biol 12:e1005076.

Nitsche MA, Paulus W (2000) Excitability changes induced in the human motor cortex by weak transcranial direct current stimulation. The Journal of Physiology 527 Pt 3:633–639.

O'Connell NE, Wand BM, Marston L, Spencer S, Desouza LH (2014) Non-invasive brain stimulation techniques for chronic pain. Cochrane Database Syst Rev 4:CD008208.

Ohn SH, Chang WH, Park C-H, Kim ST, Lee JI, Pascual-Leone A, Kim Y-H (2012) Neural correlates of the antinociceptive effects of repetitive transcranial magnetic stimulation on central pain after stroke. Neurorehabil Neural Repair 26:344–352.

Ostrowsky K, Magnin M, Ryvlin P, Isnard J, Guénot M, Mauguière F (2002) Representation of pain and somatic sensation in the human insula: a study of responses to direct electrical cortical stimulation. Cereb Cortex 12:376–385.

Petrou M, Pop-Busui R, Foerster BR, Edden RA, Callaghan BC, Harte SE, Harris RE, Clauw DJ, Feldman EL (2012) Altered Excitation-inhibition Balance in the Brain of Patients with Diabetic Neuropathy. Academic Radiology 19:607–612.

Price DD, Craggs J, Nicholas Verne G, Perlstein WM, Robinson ME (2007) Placebo analgesia is accompanied by large reductions in pain-related brain activity in irritable bowel syndrome patients. PAIN 127:63–72.

Reidler JS, Mendonca ME, Santana MB, Wang X, Lenkinski R, Motta AF, Marchand S, Latif L, Fregni F (2012) Effects of motor cortex modulation and descending inhibitory systems on pain thresholds in healthy subjects. J Pain 13:450–458.

Rudd RA, Seth P, David F, Scholl L (2016) Increases in Drug and Opioid-Involved Overdose Deaths - United States, 2010-2015. MMWR Morb Mortal Wkly Rep 65:1445–1452.

Saavedra LC, Mendonca M, Fregni F (2014) Medical Hypotheses. Medical Hypotheses 83:332–336.

Schneiderhan J, Clauw D, Schwenk TL (2017) Primary Care of Patients With Chronic Pain. JAMA 317:2367–2368.

Segerdahl AR, Mezue M, Okell TW, Farrar JT, Tracey I (2015) The dorsal posterior insula subserves a fundamental role in human pain. Nature Neuroscience 18:499–500.

Uddin LQ (2015) Salience processing and insular cortical function and dysfunction. Nat Rev Neurosci 16:55–61.

Ung H, Brown JE, Johnson KA, Younger J, Hush J, Mackey S (2014) Multivariate classification of structural MRI data detects chronic low back pain. Cerebral Cortex 24:1037–1044.

Valle A, Roizenblatt S, Botte S, Zaghi S, Riberto M, Tufik S, Boggio PS, Fregni F (2009) Efficacy of anodal transcranial direct current stimulation (tDCS) for the treatment of fibromyalgia: results of a randomized, sham-controlled longitudinal clinical trial. J Pain Manag 2:353–361.

Vaseghi B, Zoghi M, Jaberzadeh S (2014) Does anodal transcranial direct current stimulation modulate sensory perception and pain? A meta-analysis study. Clin Neurophysiol.

Wager TD (2004) Placebo-Induced Changes in fMRI in the Anticipation and Experience of Pain. Science 303:1162–1167.

Wager TD, Atlas LY, Leotti LA, Rilling JK (2011) Predicting individual differences in placebo analgesia: contributions of brain activity during anticipation and pain experience. Journal of Neuroscience 31:439–452.

Wager TD, Atlas LY, Lindquist MA, Roy M, Woo C-W, Kross E (2013) An fMRI-Based Neurologic Signature of Physical Pain. N Engl J Med 368:1388–1397 Available at: http://www.nejm.org/doi/full/10.1056/NEJMoa1204471.

Watson CJ (2016) Insular balance of glutamatergic and GABAergic signaling modulates pain processing. PAIN 157:2194–2207.

Appendix A : Supplementary Figures and Tables

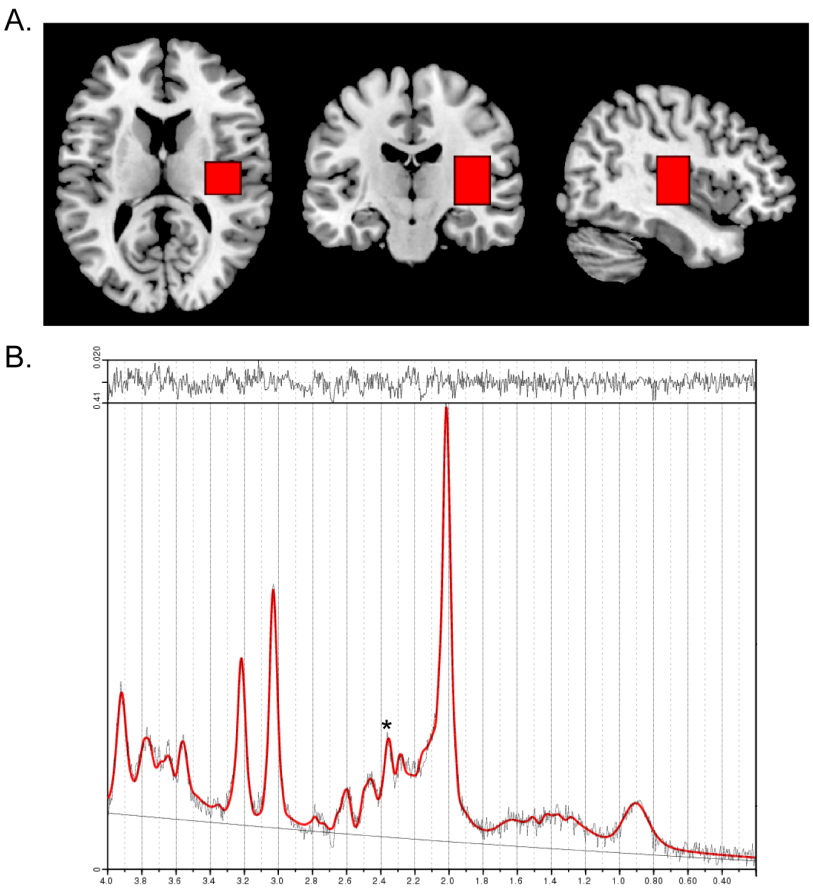

*Figure A.1. Right Posterior Insula ^{1}H-MRS Voxel Placement and Resulting Spectrum. The placement of the spectroscopic voxel in the right posterior insula is shown in (A) in axial, coronal and sagittal images. A representative spectrum fit with LCModel (red trace) is depicted in panel (B). The peak resonance for glutamate + glutamine (Glx) is marked with * at 2.35 parts per million. Glx concentrations were rescaled using the water peak and corrected for CSF.*

Table A.1: No Significant Differences in Grey/White Matter or CSF Volume in the ^{1}H-MRS Voxel between FM and HC

Right Posterior Insula ^{1}H-MRS Voxel	FM(mean ± SD)	HC (mean ± SD)	Statistics
Grey Matter	0.3390 ± 0.08	0.3259 ± 0.08	t=-0.641, p=0.524
White Matter	0.6196 ± 0.09	0.6334 ± 0.08	t=0.591, p=0.557
CSF	0.0394 ± 0.02	0.0391 ± 0.01	t=-0.065,p=0.948

Table A.1. No Significant Differences in Grey/White Matter or CSF Volume in the ^{1}H-MRS Voxel between FM and HC. FM, fibromyalgia; HC, healthy control; SD, standard deviation; ^{1}H-MRS, proton magnetic resonance spectroscopy

Table A.2: No Significant Differences in Grey/White Matter or CSF Volume of the ^{1}H-MRS Voxel between FM Pain Tertiles

Right Posterior Insula ^{1}H-MRS Voxel	High Pain FM (mean ± SD)	Medium Pain FM (mean ± SD)	Low Pain FM (mean ± SD)	Statistics
Grey Matter	0.3259 ± 0.08	0.3605 ± 0.09	0.3441 ± 0.08	F=1.208, p=0.314
White Matter	0.6333 ± 0.10	0.5968 ± 0.10	0.6112 ± 0.08	F=1.188, p=0.321
CSF	0.0391 ± 0.02	0.0401 ± 0.02	0.0429 ± 0.01	F=0.454,p=0.715

Table A.2. No Significant Differences in Grey/White Matter or CSF Volume of the ^{1}H-MRS Voxel between FM Pain Tertiles. FM, fibromyalgia; SD, standard deviation; ^{1}H-MRS, proton magnetic resonance spectroscopy

Table A.3: Participant Demographics

	FM (n=40, unless otherwise noted)	HC (n=27, unless otherwise noted)	Statistics
Age (mean ± SD)	39.03 ± 11.04	36.22 ± 12.43	t = 0.969, p = 0.336
Race	92.5% Caucasian, 5% African American, 2.5% Other	N = 15; 80% Caucasian, 7% Indian, 13% Asian	
Ethnicity	N = 30; 97% Non-Hispanic White, 3% Hispanic	N = 15; 93% Non-Hispanic 7% Hispanic	
Posterior insula Glx CSF corrected (mean ± SD AIU)	N = 39; 11.92 ± 1.57	10.97 ± 1.48	t = 2.45, p = 0.017
Posterior insula Glx ratio to total creatine (mean ± SD AIU)	N = 37; 1.62 ± 0.17	N = 25; 1.63 ± 0.21	t = 0.269, p = 0.789
Clinical Pain (VAS: mean ± SD)	4.88 ± 2.24		
Depression (HADS: mean ± SD)	N = 18; 5.11 ± 3.54		
Depression (CES-D: mean ± SD)	N = 12; 14.75 ± 7.55		

Table A.3. Participant Demographics. FM, fibromyalgia; HC, healthy control; SD, standard deviation; Glx, glutamate + glutamine; AIU, arbitrary institutional units; VAS, visual analog scale; HADS, Hospital Anxiety and Depression scale; CES-D, Center for Epidemiological Studies-Depression Scale

Table A.4: Current Medications in Fibromyalgia Patients

Medication	# Fibromyalgia Patients
Antidepressants (SSNRI, SSRI, NDRI, TCA)	9
Benzodiazepines	3
Pregabalin	2
Opioids/Narcotic Analgesics	5
Muscle Relaxants	8
NSAIDs	20
Marijuana	1

Table A.4. Current Medications in Fibromyalgia Patients. Data not collected in 9 FM participants, table above contains medication usage for remaining n=31 FM patients

Table A.5: Global Network Measures

Measure	FM(mean ± SD)	HC (mean ± SD)	Statistics
Global Efficiency	0.5740 ± 0.005	0.5733 ± 0.007	t=0.419, p=0.657
Clustering Coefficient	0.4730 ± 0.025	0.4739 ± 0.033	t=0.109, p=0.899
Average Path Length	2.01 ± 0.03	2.02 ± 0.05	t=0.694,p=0.490
Modularity	0.3349 ± 0.027	0.3406 ± 0.033	t=0.750, p=0.439

Table A.5. Global Network Measures. FM, fibromyalgia; HC, healthy control; SD, standard deviation

Table A.6: Hubs (Degree) in Fibromyalgia Patients and Healthy Controls

Hubs in Fibromyalgia Patients Brain Region (Node #)	Degree	Hubs in Healthy Controls Brain Region (Node #)	Degree
L Inferior Frontal Gyrus (242)	66.8	R Inferior Parietal Lobule (192)	66.5
Dorsal Anterior Cingulate (215)	67.2	L Superior Frontal Gyrus (218)	66.5
R Precuneus (156)	67.6	R Supplementary Motor Area (16)	66.5
L Mid Insula/Operculum (55)	67.8	R Precuneus (136)	66.6
R Superior Parietal (258)	68.1	R Primary/Secondary Visual Cortex (140)	66.8
L Primary Somatosensory Cortex (69)	68.2	L Superior Frontal Gyrus (50)	66.8
R Inferior Temporal Gyrus (179)	68.5	L Primary Somatosensory Cortex (23)	67.2
R Superior Temporal Gyrus (240)	68.5	L Primary Somatosensory Cortex (69)	67.2
R Mid Frontal Gyrus (189)	68.7	L Primary/Secondary Visual Cortex (154)	67.3
R Mid Cingulate (216)	68.8	R Visual Association Cortex (169)	67.5
L Mid Cingulate (94)	68.9	R Supplementary Motor Area (53)	67.5
L Precuneus (166)	69.1	L Inferior Frontal Gyrus (242)	67.7
R Mid Insula (60)	69.5	L Inferior Parietal Lobule (177)	67.7
R Inferior Frontal Gyrus (186)	69.5	R Angular Gyrus (96)	68.6
R Superior Temporal Gyrus (63)	69.7	R Supplementary Motor Area (54)	68.7
R Precuneus (136)	69.7	R Primary Motor Cortex (29)	68.8
L Primary Motor Cortex/Operculum (70)	69.8	R Superior Frontal Gyrus (219)	69.1
R Anterior Insula (209)	70.2	R Posterior Cingulate (203)	69.1
L Anterior Insula (208)	70.5	R Superior Temporal Gyrus (62)	69.3
R Primary Motor Cortex (29)	70.5	L Mid Temporal Gyrus (83)	69.4
R Supramarginal Gyrus (204)	70.7	L Superior Temporal Gyrus (58)	69.4
R Supplementary Motor Area (54)	70.8	R Mid Cingulate (216)	69.7
L Primary Somatosensory Cortex (65)	70.9	R Mid Insula (56)	70.4
R Posterior Cingulate (203)	71.4	L Mid Cingulate (59)	70.4
L Mid Cingulate (59)	71.9	R supramarginal gyrus (204)	70.9
L Inferior Parietal Lobule (235)	72.5	L Primary Somatosensory Cortex (65)	71.0
L Mid Cingulate (213)	72.8	R Primary Visual Cortex (141)	71.6
L Supplementary Motor Area (47)	74.1	R Secondary Visual Cortex (165)	72.6
R Superior Temporal Gyrus (62)	75.5	L Primary/Secondary Visual Cortex (172)	72.7
L Supplementary Motor Area (15)	76.4	R Visual Association Cortex (153)	72.7
R Mid Insula (56)	77.2	L Mid Cingulate (213)	72.8
L Superior Temporal Gyrus (58)	77.6	L Supplementary Motor Area (47)	73.3
		L Supplementary Motor Area (15)	74.3

Table A.6. Hubs (Degree) in Fibromyalgia Patients and Healthy Controls. L, left; R, right.

Table A.7: Hubs (Betweenness Centrality) in Fibromyalgia Patients and Healthy Controls

Hubs in Fibromyalgia Patients Brain Region (Node #)	Betweenness Centrality	Hubs in Healthy Controls Brain Region (Node #)	Betweenness Centrality
R Mid Insula (60)	328.8	R Primary Visual Cortex (141)	328.7
L Primary Motor/Operculum (70)	329.3	R Superior Temporal Gyrus (62)	329.1
R Superior Parietal (258)	330.3	R Superior Temporal Gyrus (63)	329.6
R Anterior Insula (211)	331.1	L Superior Frontal Gyrus (178)	335.1
R Inferior Frontal Gyrus (139)	332.6	L Superior Frontal Gyrus (220)	335.4
L Superior Temporal Gyrus (236)	333.2	R Precuneus (156)	337.8
L Inferior Frontal Gyrus (137)	333.6	R Inferior Frontal Gyrus (139)	339.1
R Mid Temporal Gyrus (119)	333.7	R Inferior Parietal Lobule (190)	339.3
R Precuneus (156)	338.8	R Mid Frontal Gyrus (189)	341.9
R Superior Temporal Gyrus (63)	341.1	L Superior Frontal Gyrus (103)	342.9
R Precuneus (251)	344.1	R Angular (96)	345.7
R Mid Frontal Gyrus (189)	345.4	L Inferior Parietal Lobule (177)	346.0
R Cuneus (159)	346.1	L Inferior Frontal Gyrus (176)	351.0
L Anterior Insula (208)	347.5	R Visual Association Cortex (153)	351.4
R Mid Cingulate (216)	347.8	R Inferior Parietal Lobule (192)	354.2
L Superior Frontal Gyrus (112)	349.8	L Mid Temporal Gyrus (120)	356.4
L Angular Gyrus (87)	351.4	R Primary Motor Cortex (29)	359.7
R Inferior Frontal Gyrus (186)	352.7	R Precuneus (163)	362.7
L Primary Somatosensory Cortex (65)	354.5	R Cuneus (159)	365.5
R Superior Temporal Gyrus (240)	355.9	L Precuneus (13)	367.3
L Inferior Frontal Gyrus (176)	356.6	L Mid Cingulate (59)	368.2
Dorsal Anterior Cingulate (215)	357.2	R Secondary Visual Cortex (165)	370.2
R Precuneus (136)	358.8	Dorsal Anterior Cingulate (215)	370.8
L Superior Frontal Gyrus (202)	372.2	L Secondary/Association Visual Cortex (172)	371.2
L Mid Cingulate (59)	377.6	L Mid Cingulate (94)	372.4
R Posterior Cingulate (203)	377.8	R Mid Cingulate (216)	372.9
R Inferior Temporal Gyrus (179)	377.9	L Supplementary Motor Area (47)	375.4
R Precuneus (163)	381.7	L Supplementary Motor Area (138)	376.3
R Inferior Parietal Lobule (235)	382.2	L Inferior Frontal Gyrus (242)	382.8
R Supramarginal Gyrus (204)	383.6	R Mid Insula (56)	388.7
L Supplementary Motor Area (47)	386.4	L Superior Temporal Gyrus (58)	390.7
L Mid Cingulate (213)	387.7	R Superior Frontal Gyrus (219)	393.1
R Primary Motor Cortex (29)	392.4	R Posterior Cingulate (203)	394.5
L Mid Cingulate (94)	399.5	L Medial Superior Frontal Gyrus (202)	397.6
R Superior Temporal Gyrus (62)	401.3	R Precuneus (136)	412.9
L Inferior Frontal Gyrus (242)	408.1	L Mid Cingulate (213)	419.2
L Superior Temporal Gyrus (58)	458.6	R Supramarginal (204)	424.6
L Supplementary Motor Area (15)	473.4	L Supplementary Motor Area (15)	438.0
R Mid Insula (56)	477.9		

Table A.7. Hubs (Betweenness Centrality) in Fibromyalgia Patients and Healthy Controls. L, left; R, right.

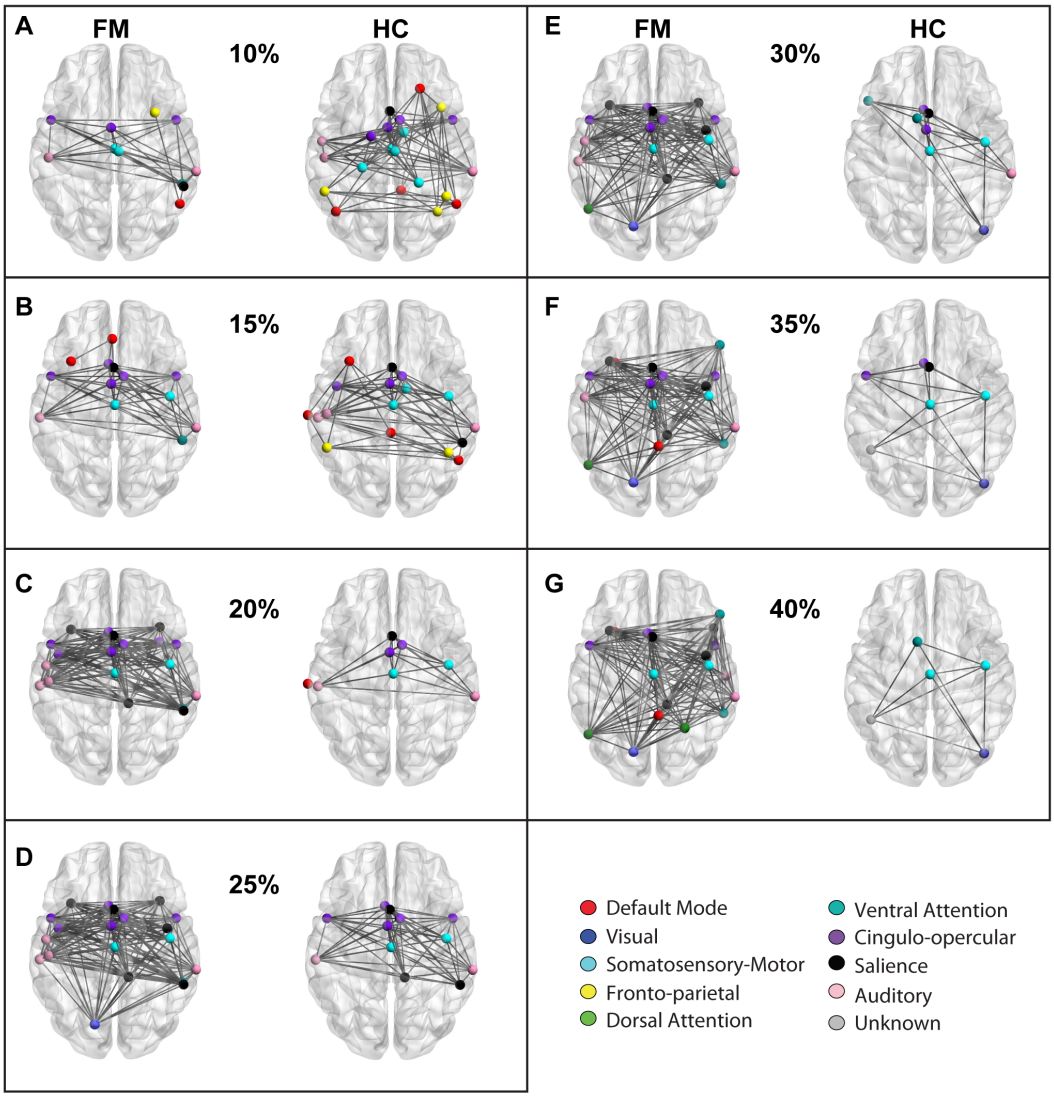

Figure A.2. Rich Club Membership across thresholds in FM and HC. Rich club membership is depicted for FM and HC at each of the thresholds examined, 10-40% (A-G). As described in the main text, we determined statistical significance of the rich club coefficient, ϕ (k), at each level of k with permutation testing using 1000 random networks with similar degree distribution and density. The range of k in which ϕ (k) is significantly different from ϕ_{random} (k), and where the ϕ_{norm} (k) is greater than one, is the rich-club regime. Differences between FM and HC in ϕ (k) at each level of k in the rich-club regime were tested in SPSS using independent samples t-tests. This was repeated for each threshold and a Bonferroni correction was applied. There were no significant differences in the rich club coefficient between FM and HC, however rich club membership was different between groups. The anterior insulae was a member of the rich club in FM patients for network densities between 20 and 40%. For visualization, the rich clubs are displayed at the highest level of k that was significantly different from random networks for each threshold and each group independently (10%: FM k= 47, HC k = 45; 15%: FM k = 64, HC k = 62; 20%: FM k = 78, HC k = 82; 25%: FM k = 92, HC k = 95; 30%: FM k = 106, HC k = 111; 35%: FM k = 121, HC k = 126; 40%: FM k = 133, HC k = 142).

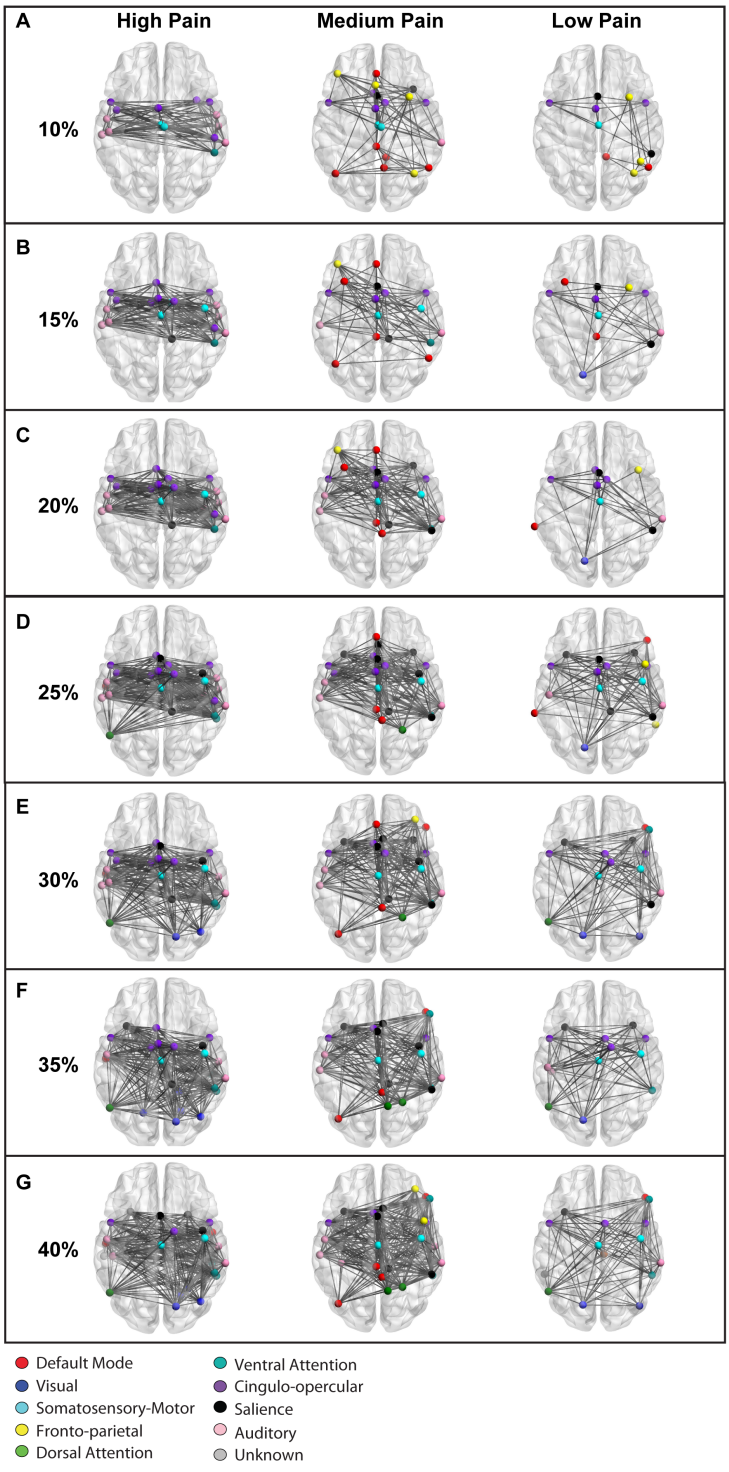

Figure A.3. Rich Club Hubs in FM Tertiles across thresholds. For high, medium and low pain FM tertiles, the rich club membership is depicted for all other network densities examined (10-40%, A-G). Differences in the rich club coefficient, ϕ (k), for each threshold were tested as described in the main text using one-way ANOVAs and Bonferroni corrections were applied. There were no significant differences between the tertiles in the rich club coefficient, however rich club membership varied across the tertiles and was consistent with results at 5% density described in the main text. For visualization, the rich clubs are displayed at the same level of k detailed for the FM group in Supplementary Fig 1.

Table A.8: Correlations Between Eigenvector Centrality and Clinical Pain in Fibromyalgia Patients

	Brain Region (Node #)	r-value	p-value
Positive Correlations	L Primary Somatosensory Cortex (20)	0.409	0.010
	R Primary Motor Cortex (21)	0.361	0.024
	L Primary Somatosensory Cortex (23)	0.323	0.045
	L Primary Motor Cortex (24)	0.358	0.025
	L Primary Motor Cortex (27)	0.363	0.023
	L Primary Somatosensory Cortex (30)	0.389	0.014
	R Supplementary Motor Area (31)	0.369	0.021
	R Primary Motor/Somatosensory Cortex (36)	0.468	0.003
	L Primary Motor Cortex (37)	0.383	0.016
	R Posterior Insula (43)	0.429	0.006
	L Primary Motor/Somatosensory Cortex (45)	0.366	0.022
	R Primary Motor/Somatosensory Cortex (46)	0.416	0.008
	R Supramarginal Gyrus (48)	0.398	0.012
	L Primary Motor Cortex/Operculum (55)	0.389	0.014
	R Superior Temporal Gyrus (62)	0.396	0.013
	R Superior Temporal Gyrus (63)	0.455	0.004
	R Posterior Insula (67)	0.344	0.032
	L Primary Motor Cortex/Operculum (70)	0.566	0.000
	R Primary Motor Cortex/Operculum (71)	0.368	0.021
	R Primary Motor/Somatosensory Cortex (72)	0.416	0.008
	R Superior Temporal Gyrus (238)	0.488	0.002
Negative Correlations	L Orbitofrontal Gyrus (78)	-0.347	0.031
	R Angular Gyrus (130)	-0.366	0.022
	L Superior Frontal Gyrus (138)	-0.355	0.027
	L Supplementary Motor Area (174)	-0.327	0.042
	R Mid Frontal Gyrus (196)	-0.387	0.015
	R Supramarginal Gyrus (204)	-0.332	0.039
	R Posterior Cingulate (221)	-0.331	0.039
	R Inferior Frontal Gyrus (241)	-0.387	0.015
	L Inferior Temporal Gyrus (262)	-0.435	0.006

Table A.8. Correlations Between Eigenvector Centrality and Clinical Pain in Fibromyalgia Patients. L, left; R, right.

Appendix B : Supplementary Figures and Tables

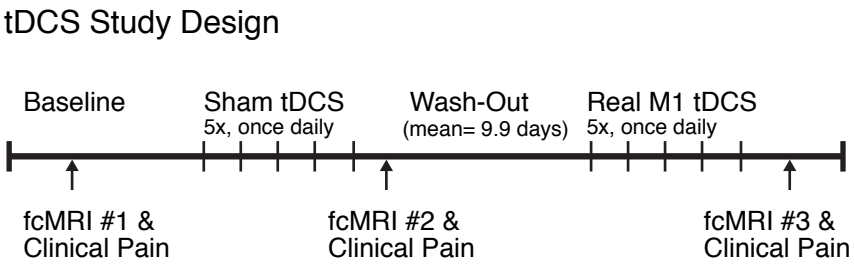

Figure B.1. Study Design. Our within-subjects crossover design had three phases: a baseline pain assessment and functional magnetic resonance imaging (fMRI) session #1, sham tDCS for five consecutive days followed by pain assessment and fMRI #2, and real tDCS for five consecutive days followed by pain assessment and fMRI #3. Sham and real tDCS phases were separated by a 7-11 day washout period (mean = 9.9 days).

Table B.1: Clinical Results

	Baseline (mean ± SD)	Sham (mean ± SD)	Real tDCS (mean ± SD)
Clinical Pain Intensity (VAS)	5.12 ± 2.30	4.08 ± 2.11	3.33 ± 2.84*
McGill Total Pain	24.09 ± 15.08	18.67 ± 12.47	19.33 ± 15.30
PANAS (Positive Affect)	19.78 ± 5.99	17.82 ± 5.47	16.09 ± 6.41
PANAS (Negative Affect)	14.33 ± 3.39	15.36 ± 5.46	12.73 ± 3.58*

*Table B.1. Clinical Results. * Significantly different from baseline at $p < 0.05$*

Table B.2: Patient Characteristics

ID	Age	VAS			McGill			PANAS					
								Positive			Negative		
		B	S	R	B	S	R	B	S	R	B	S	R
1	34	3	5	2	11	18	14	NA	NA	NA	NA	NA	NA
2	46	5	6	8	37	33	55	30	19	14	16	20	14
3	54	8	6	5	27	13	23	14	10	10	21	27	10
4	37	4	4	3	36	16	27	20	20	30	15	16	11
5	64	0	0	0	0	0	0	16	20	22	13	10	10
6	56	4	3	0	37	42	22	13	13	14	11	10	10
7	58	6.5	2	0	8	4	0	19	26	14	14	13	12
8	52	6	2	3	31	27	24	29	24	23	10	10	10
9	54	4	3	3	10	11	10	NA	10	10	NA	16	20
10	40	6	7	7	NA	12	27	NA	15	10	NA	18	18
11	45	7	5	2	21	16	4	19	16	13	12	10	10
12	52	8	6	7	47	32	26	18	23	17	17	19	15

Table B.2. Patient Characteristics. VAS, visual analog scale; PANAS, positive and negative affect scale; B, baseline; S, sham; R, real tDCS; NA, not available

Table B.3: Baseline FC Predicts Subsequent Analgesia

	Δ Clinical Pain (VAS) Sham - Baseline	Δ Clinical Pain (VAS) Real tDCS - Sham	Δ Clinical Pain (VAS) Real tDCS - Baseline
L M1 – L VL Baseline FC	r = -0.619 p = 0.042	r = -0.791 p = 0.004	r = -0.938 p = 0.001
L S1 – L anterior insula Baseline FC	r = -0.671 p = 0.024	r = -0.774 p = 0.005	r = -0.961 p = 0.001
L VL – PAG Baseline FC	r = -0.815 p = 0.002	r = -0.587 p = 0.057	r = -0.929 p = 0.001

Table B.3. Baseline FC Predicts Subsequent Analgesia. FC, functional connectivity; L, left; M1, primary motor cortex; VL, ventral lateral; S1, primary somatosensory cortex; PAG, periaqueductal gray

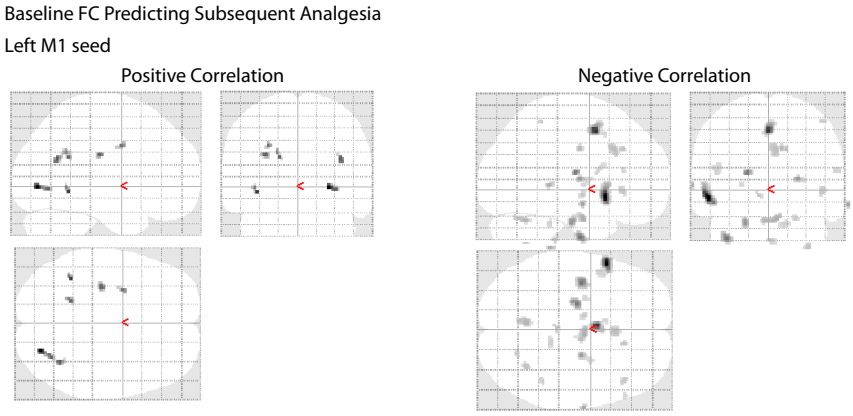

Figure B.2. Baseline FC Predicts Subsequent Analgesia. FM patients who had stronger FC at baseline between the left M1 seed and left VL thalamus, between left S1 and left anterior insula and between left VL thalamus and the PAG had greater improvement in clinical pain across sham and real tDCS. There were no regions that showed significant correlations between less FC at baseline and greater improvement in clinical pain. The glass brain results for the left M1 seed are depicted at a voxel threshold of p<0.001.

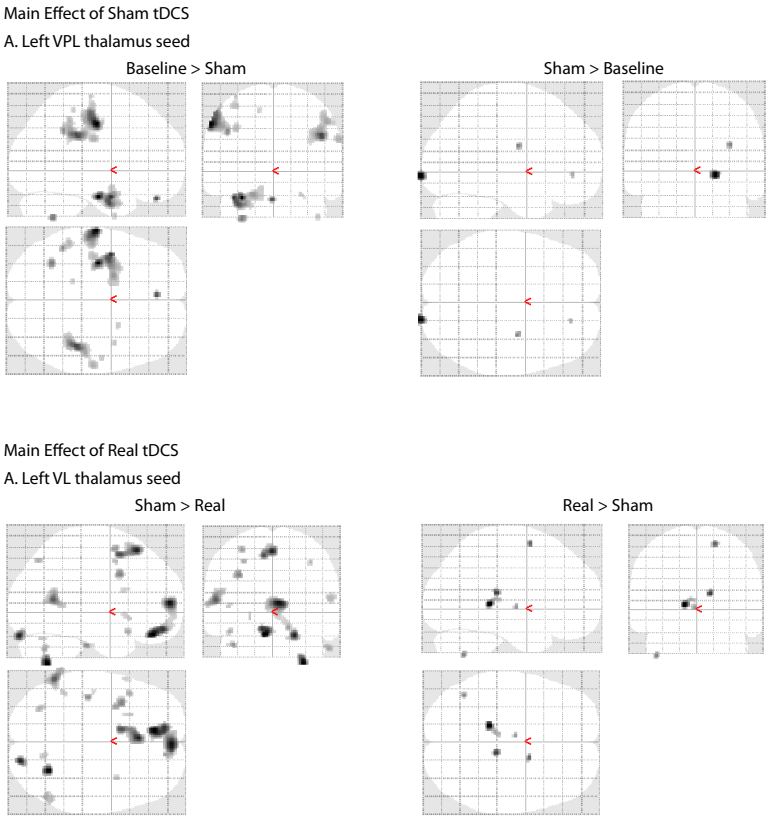

*Figure B.3. Main Effects of Sham and Real tDCS. **A,** The glass brain results for the left VPL thalamus seed are depicted at a voxel threshold of p<0.001 for the baseline > sham and sham > baseline contrasts. Significant results were only found for baseline > sham (see Table 3.2 main text). **B,** The glass brain results for the left VLL thalamus seed are depicted at a voxel threshold of p<0.001 for the sham > real tDCS and real tDCS > sham contrasts. Significant results were only found for sham > real tDCS (see Table 3.4 main text).*

Table B.4: Main effect of Real tDCS compared to Baseline

Seed FC Region	MNI coordinates (x y z)			T	Cluster size	Cluster p-value
Baseline > Real						
L VPL thalamus						
L IPL	-46	-50	34	5.40	239	0.041 FWE
PAG						
PCC	-12	-36	38	5.98	354	0.007 FWE
Baseline < Real						
N.S.						

Table B.4. Main effect of Real tDCS compared to Baseline. FC, functional connectivity; VAS, visual analog scale; L, left; R, right; VPL, ventral posterior lateral; IPL, inferior parietal lobule; PAG, periaqueductal gray; PCC, posterior cingulate; MNI, Montreal Neurological Institute

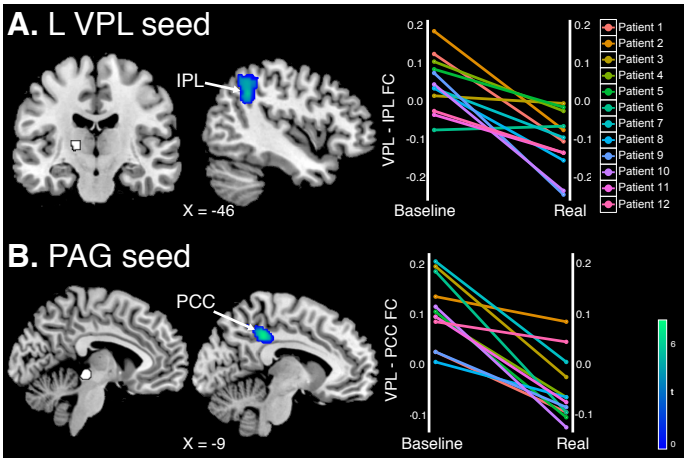

Figure B.4. Real tDCS decreases FC compared to baseline. ***A,*** *Decreased connectivity between the left VPL (seed in white) and IPL after real tDCS. Plots show changes in FC between baseline and real tDCS for each FM patient.* ***B,*** *Decreased connectivity between the PAG (seed in white) and PCC after real tDCS. VPL, ventral posterior lateral; IPL, inferior parietal lobule; PAG, periaqueductal gray; PCC, posterior cingulate; L, left; R, right; FC, functional connectivity (fisher transformed r-values).*

Table B.5: Correlations between change in FC and change in clinical pain (VAS) for baseline vs real

Seed FC Region	MNI coordinates (x y z)			T	Cluster size	Cluster p-value
L S1						
L SMA	-2	4	52	6.98	200	0.013 FWE

Table B.5. Correlations between change in FC and change in clinical pain (VAS) for baseline vs real. FC, functional connectivity; VAS, visual analog scale; L, left; R, right; S1, primary somatosensory cortex; SMA, supplementary motor area; MNI, Montreal Neurological Institute

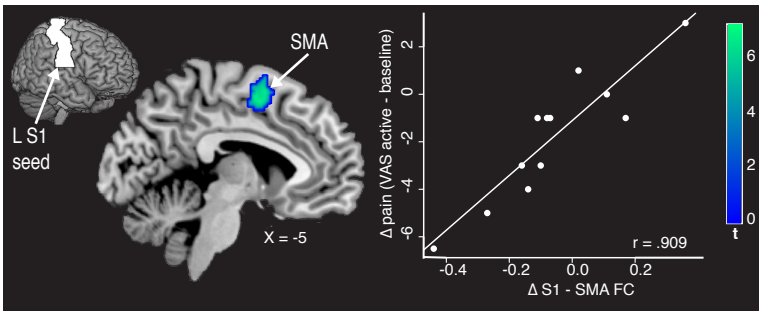

Figure B.5. Correlation between change in FC and change in clinical pain after real tDCS. Patients with reduced FC between the left S1 (seed in white) and left SMA had greater reductions in clinical pain after real tDCS compared to baseline. S1, primary somatosensory cortex; SMA, supplementary motor area; VAS, visual analog scale; L, left; R, right; FC, functional connectivity (fisher transformed r-values).

Table B.6: Correlations between change in FC and change in clinical pain (McGill) for real vs sham tDCS

	Δ McGill Clinical Pain Real tDCS - Sham
L VPL – R posterior insula Real - Sham FC	r = 0.752 p = 0.008
L VPL – M1/S1 Real - Sham FC	r = 0.602 p = 0.05
L VL – R posterior insula Real - Sham FC	r = 0.648 p = 0.031

Table B.6. Correlations between change in FC and change in clinical pain (McGill) for real vs sham tDCS. FC, functional connectivity; L, left; VPL, ventral posterior lateral; M1, primary motor cortex; S1, primary somatosensory cortex; VL, ventral lateral

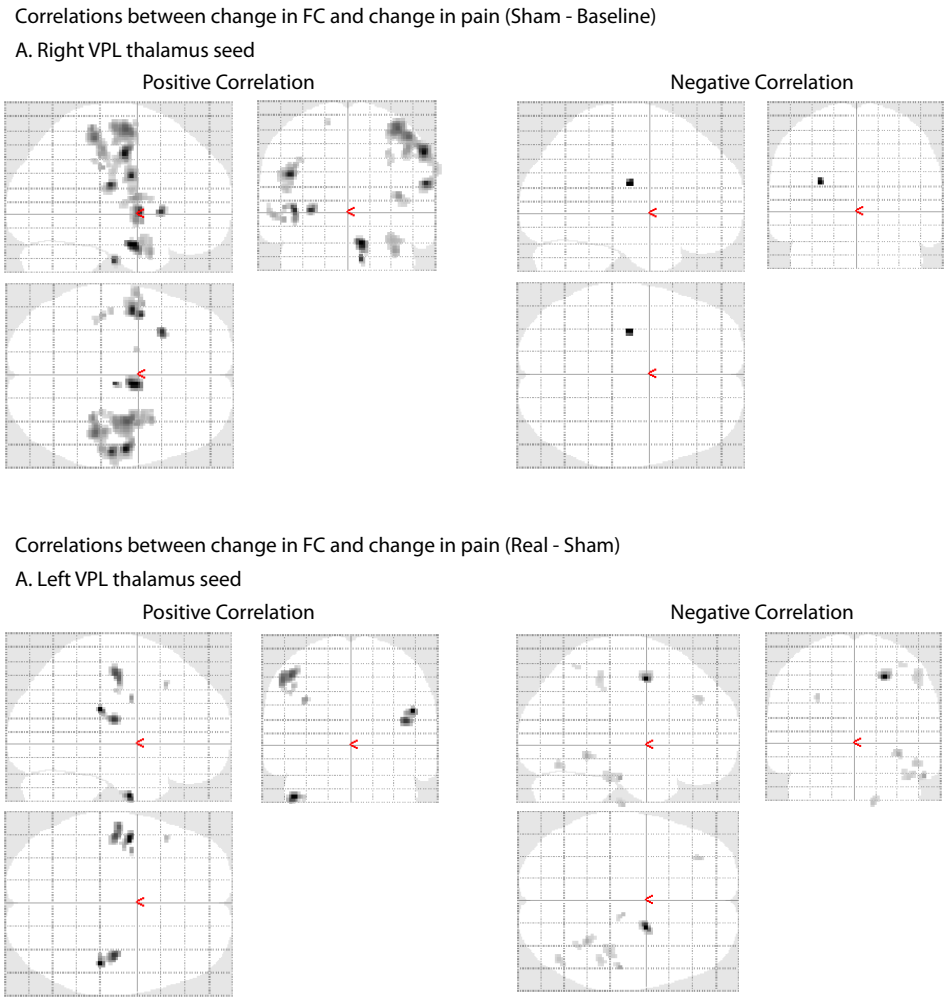

Figure B.6. Correlations between changes in functional connectivity and changes in pain. ***A,*** *The glass brain results for the right VPL thalamus seed are depicted at a voxel threshold of p<0.001. Significant results were only found for correlations between reductions in connectivity and reductions in clinical pain after sham tDCS (see Table 3.3). There were no significant correlations between increases in connectivity and reductions in clinical pain.* ***B,*** *The glass brain results for the left VPL thalamus seed are depicted at a voxel threshold of p<0.001. Significant results were only found for correlations between reductions in connectivity and reductions in clinical pain after real tDCS (see Table 3.5). There were no significant correlations between increases in connectivity and reductions in clinical pain.*